

INTERFACES IN SUPERSYMMETRIC FIELD THEORIES

by
DMITRII GALAKHOV

A dissertation submitted to the
Graduate School - New Brunswick
Rutgers, The State University of New Jersey
In partial fulfillment of the requirements
For the degree of
Doctor of Philosophy
Graduate Program in Physics and Astronomy

Written under the direction of
Professor Gregory W. Moore
And approved by

New Brunswick, New Jersey

OCTOBER, 2016

ABSTRACT OF THE DISSERTATION

Interfaces in Supersymmetric Field Theories

By **Dmitrii Galakhov**

Dissertation Director:

Professor Gregory W. Moore

Supersymmetry has proven to be a valuable tool in the study of non-perturbative dynamics in quantum field theory, gravity and string theory. In this thesis we consider supersymmetric interfaces. Interfaces are defects defined by spatially changing coupling constants. Interfaces can be used to probe the non-perturbative low energy dynamics of an underlying supersymmetric quantum field theory. We study interfaces in a set of four-dimensional quantum field theories with $\mathcal{N} = 2$ supersymmetry known as theories of class \mathcal{S} . Using these defects we probe the spin content of the spectrum of quantum states saturating the Bogomolnyi-Prasad-Sommerfeld bound. We also apply supersymmetric defects to the construction of knot and link invariants via quantum field theory. We associate to a knot - presented as a tangle - an interface defined by a spatially varying superpotential in a 2d supersymmetric Landau-Ginzburg model. We construct explicitly the Hilbert space of ground states on this interface as the cohomology of a nilpotent supercharge and prove that this Hilbert space is graded by $\mathbb{Z} \times \mathbb{Z}$ and is an invariant of the knot (or link). In explicit examples we show that the corresponding Poincaré polynomial coincides with the Poincaré polynomial of the renowned Khovanov homology that categorifies the Jones polynomial.

Acknowledgements

Working on this project was a great pleasure, although it would not be possible to complete it without help and wise advice of many extraordinary people.

Foremost I am deeply thankful to my advisor Gregory W. Moore for suggesting interesting and challenging projects, for his support and guidance through the graduate school. I have learned a lot from him and broadened significantly my scope to the theoretical physics.

I also had a great pleasure to collaborate with several brilliant physicists on number of projects. I am deeply grateful to my co-authors Pietro Longhi, Tom Mainiero, Dmitry Melnikov, Andrey Mironov, Alexei Morozov, Andrew Neitzke, Alexei Sleptsov.

I can not forget to mention and underestimate many useful conversations that helped a lot to collect many puzzle pieces. I gratefully thank Mina Aganagic, Semeon Arthamonov, Tudor Dimofte, Andrei Okounkov, Shamil Shakirov, Andrey Smirnov for helpful and stimulating discussions.

Finally, I would like to thank my family for their support and belief in me.

Dmitrii Galakhov

Rutgers University

May 2016

Table of Contents

Abstract	ii
Acknowledgements	iii
Table of Contents	iv
List of Figures	vii
1 Introduction & Preliminaries	1
1.1 Content and low energy effective action of 4d super Yang-Mills theory	3
1.2 BPS states in class \mathcal{S} theories	5
1.3 tt^* -geometry in supersymmetric Landau-Ginzburg theory	7
1.4 Interfaces in class \mathcal{S} theories	11
1.5 Knot theory review	13
1.5.1 Knot diagrams and Reidemeister moves	15
1.5.2 Kaufmann and Khovanov bracket	17
1.5.3 Vertex state model for Khovanov homology	19
2 BPS states in class \mathcal{S} theories	22
2.1 Spectral networks	24
2.2 Abstract Abelianization map	25
2.3 Flatness and sign rule	27
2.4 Projection to Fock-Goncharov coordinates	29
2.5 Wall-crossing	31
2.5.1 Line defects	31
2.5.2 Flip	33
2.5.3 MS-walls and wall-crossing formulae	34

2.6	BPS spectrum of Kronecker quiver theory families	36
2.6.1	Spectral networks for Kronecker quivers	36
2.6.2	Remarks on BPS dynamics	39
3	Application to knot homology	44
3.1	Homology origin in QFT: brief SUSY QM overview	44
3.2	Holomorphic reduction: Ward identities, Yang-Yang functional and conformal blocks	46
3.3	Spectral networks categorification	53
3.3.1	Solitons in a 'tHooft limit	53
3.3.2	Simpletons and categorified Abelianization map	58
3.3.3	Evolution, gluing and mutations	60
3.4	Braiding interfaces	62
3.4.1	Braiding as a parallel transport on the moduli space	62
3.4.2	\mathcal{R} -interfaces in the Heisenberg picture	65
3.4.3	Drinfeld R -matrix recovery, spins as filling number	67
3.4.4	Spin- $\frac{1}{2}$ \mathcal{R} -interface in the model of Wigner droplets	69
3.4.5	Spin- $\frac{1}{2}$ \mathcal{R} -interface in the model with symmetry breaking	71
3.4.6	Soliton spectrum of the model with symmetry breaking	74
3.5	Spin- $\frac{1}{2}$ knot(link) (co-)homology	76
3.5.1	Instantons in Landau-Ginzburg model	76
3.5.2	Why is $\mathbb{Q}_\zeta^2 = 0$?	81
3.5.3	Homotopy	84
3.5.3.1	Interface homotopy and complex quasi-isomorphism	84
3.5.3.2	Reidemeister move II	85
3.5.3.3	Reidemeister move III	87
3.5.3.4	Bulk vertices from wall-crossing formulae	90
3.5.4	Fusing/defusing interfaces	92
3.5.4.1	Quantum algebra heritage	92
3.5.4.2	Construction of fusing/defusing interfaces	95
3.5.4.3	Reidemeister move I	98
3.6	Summary of rules for MSW knot complex construction	100
3.7	Examples	103
3.7.1	Unknot	103

3.7.2	Hopf link	104
3.7.3	Trefoil	107
3.7.4	Figure-eight knot	108
3.8	Further remarks	112
3.8.1	Cabling and higher spin link (co-)homology	112
3.8.2	On skein relations, knot co-bordisms and equivalence to Khovanov homology	117
4	Discussion and outlook	120
Appendices		
A	Sign rule in Stokes coefficients	124
B	Solitons in $\mathbb{C}\mathbb{P}^\infty$ model	127
C	Homology calculus in Khovanov theory	130
C.1	Hopf link	130
C.2	Trefoil	132
D	Simplified tt^*-equations	136
E	Spectral curve for Knizhnik-Zamolodchikov connection	138
	References	140

List of Figures

1.1	Landau-Ginzburg theory on a cylinder.	11
1.2	Interface defect in 4d supersymmetric theory	12
1.3	Hopf link	18
2.1	Branching points and cuts	23
2.2	Examples of S-walls.	25
2.3	Regluing map	27
2.4	Spectral network joint	27
2.5	Lifts and detours	28
2.6	Auxiliary path	31
2.7	Flip	34
2.8	Wall-crossing	35
2.9	Kronecker quiver	36
2.10	Spectral network for a family of Kronecker quivers	38
3.1	Effective potential	55
3.2	Solitons between edges of Wigner droplets	61
3.3	Chern-Simons vs. Wess-Zumino-Witten	63
3.4	Deformed spectral curve for YY model and cycle choice on it.	66
3.5	Four mutations of \mathcal{R} -complex	68
3.6	Solitons in LG model with symmetry breaking.	73
3.7	Example of Bloch counterclockwise and clockwise solitons.	75
3.8	Soliton spectrum in the model with symmetry breaking	75
3.9	Phase transition in the model with symmetry breaking	76
3.10	Straight and curved instanton trajectories.	77

3.11 Bulk vertices	78
3.12 Instanton curved web for a simpleton.	80
3.13 Soliton central plot	86
3.14 Gluing field trajectories I.	92
3.15 Gluing field trajectories II.	92
3.16 Solitons \mathcal{X}_1 and \mathcal{X}_2	94
3.17 Path $p_2 \circ p_1^{-1} \circ p_2 \circ p_1^{-1}$	95
B.1 \mathbb{CP}^∞ critical network	129

Chapter 1

Introduction & Preliminaries

A universal physical phenomenon of great importance is a dependence of a physical system behavior on the energy scale. This dependence gives the whole variety of systems observed in nature despite different systems can behave quite differently, so ocean waves and deep inelastic scattering of quarks in nucleons are quite dissimilar, though they are both captured by different energy scales of the Standard Model Lagrangian. This concept has got a serious development during the last century and has a rigorous formulation in terms of the *renormalization group* (RG). With the change of the energy scale the system is modified with the renormalization group flow. The action is only a Wilsonian effective action that is valid up to some energy scale Λ . A physical system can even undergo a phase transition when some order parameter is developed. Unfortunately, modern computational tools are not enough to study this phenomenon in the full generality: so “running” of coupling constants in the quantum field theory at certain energy scales was described theoretically and is in agreement with the experiment, though, say, the problem of quark confinement and dynamical mass scale generation remains to be solved. Nevertheless there are simplified physical models where the problem of solving the RG flow equations may be attempted: given ultra-violet (UV) data one can describe the theory behavior in the infra-red (IR) limit, calculate effective coupling constants, degrees of freedom etc. Usually, a common feature of these models is to use relatively high amount of supersymmetries (SUSY) to suppress quantum field fluctuations.

We will concentrate on 4d $\mathcal{N} = 2$ supersymmetric theories, so called theories of class \mathcal{S} theories, and 2d $\mathcal{N} = (2, 2)$ supersymmetric Landau-Ginzburg theories. These theories have been attracting the interest of theorists for a while. And the reason is three-fold. First although the IR dynamics of these theories is simplified by supersymmetry it is still rather rich and is believed to be close to models appearing in nature. Moreover, these models happen to describe some low energy phenomena of

string/M-theory and supergravity. This gives particular insight into the non-perturbative behavior of these theories and their duality properties. And, finally, these models reveal reach mathematical structures governing their dynamics, that attracts, in turn, attention of a mathematical audience and helps in mutual development of both areas.

In this dissertation to study properties of these theories we will exploit a notion of interfaces: paths in the parameter space of the theory connecting different points. Physically interfaces are represented by operators or defects with spatially changing coupling constants or boundary conditions for fields interpolating between theories with different parameter setups. In supersymmetric theories interfaces turn out to be sensitive to the low energy effective spectra of states saturating the Bogomolnyi-Prasad-Sommerfeld (BPS) bound. On the other hand interface partition functions satisfy certain Ward identities reduced due to the supersymmetry to partial differential equations and their generalizations. This reveals a straight route to a tight interplay between IR dynamics of the quantum field theories and geometrical structures on their parameter spaces.

We will apply this setup to two problems: construction of the class \mathcal{S} theories BPS spectrum and construction of the knot(link) homology.

The structure of the dissertation is the following. In the rest of this introductory chapter we will introduce notions of class \mathcal{S} theories and supersymmetric Landau-Ginzburg theories, definition of interfaces in these theories, and, finally, a short review of knot theory basics we will use in what follows.

In chapter 2 we will apply the interface tool to the study of BPS spectra in class \mathcal{S} theories. We will determine Ward identities for an interface as a Hitchin system on the Riemann surface \mathcal{C} known as the UV curve. Thus we represent interfaces as a parallel transport on the moduli space of spectral (or Seiberg-Witten) curves. We explicitly deform (“refine”) the parallel transport to include information about the spin of BPS states and derive in some particular setups protected spin characters capturing BPS spectrum spin information.

In chapter 3 we will apply the interfaces in the supersymmetric Landau-Ginzburg (LG) theories to calculation of the knot(link) homologies. The braids will be represented as certain interfaces on the so called Yang-Yang LG theory parameter space. We will construct knots as braid closures. A braid homotopy is represented as an interface homotopy preserving the Hilbert space of non-perturbative ground states graded with the fermion number. We will construct closures of braids with the help of fusing/defusing interfaces. during this procedure we will encounter certain difficulties related to flavour charge of ground states, a way to overcome this obstacle will be proposed. We will construct explicitly this Hilbert space for a given knot diagram as a cohomology of the supercharge and show it

is invariant under the Reidemeister moves. In the explicit examples we show Poincaré polynomials coincide with Khovanov knot polynomials.

1.1 Content and low energy effective action of 4d super Yang-Mills theory

We start with a brief discussion of $\mathcal{N} = 2$ supersymmetry what is crucially relevant for the whole discussion and mention some its basic representations: vectormultiplet and hypermultiplet [4, 11, 12]. The first one is the $\mathcal{N} = 2$ vectormultiplet. It contains a gauge field A_μ , two Weyl fermions λ, ψ and a complex Higgs scalar ϕ , all are in the adjoint representation of the gauge group G . The hypermultiplet contains two Weyl fermions ψ_q and ψ_q^\dagger and complex bosons q and q^\dagger . We can arrange these fields into the following diagrams according to the action of the SUSY Clifford algebra:

$$\begin{array}{ccc}
 & A & \\
 a_1^\dagger \swarrow & & \searrow a_2^\dagger \\
 \lambda & & \psi \\
 a_2^\dagger \swarrow & & \searrow a_1^\dagger \\
 & \phi &
 \end{array}
 \qquad
 \begin{array}{ccc}
 & \psi_q & \\
 a_1^\dagger \swarrow & & \searrow a_2^\dagger \\
 q & & q^\dagger \\
 a_2^\dagger \swarrow & & \searrow a_1^\dagger \\
 & \psi_q^\dagger &
 \end{array}
 \tag{1.1}$$

One can construct Lagrangians in terms of the superfields making SUSY manifest:

$$\Psi = \Psi^{(1)}(\tilde{y}, \theta) + \sqrt{2}\tilde{\theta}^\alpha \Psi_\alpha^{(2)}(\tilde{y}, \theta) + \tilde{\theta}^2 \Psi_\alpha^{(3)}(\tilde{y}, \theta) \tag{1.2}$$

$$\Psi_\alpha^{(2)}(\tilde{y}, \theta) = W_\alpha(\tilde{y}, \theta), \quad \Psi^{(3)} = \int d^2\bar{\theta} \Phi^\dagger e^V \tag{1.3}$$

$$Q(y, \theta) = q(y) + \sqrt{2}\theta\psi_q(y) + \theta^2 F_q(y) \tag{1.4}$$

In these terms the $\mathcal{N} = 2$ super-Yang-Mills (SYM) Lagrangian reads

$$\begin{aligned}
 \mathcal{L} = & \frac{1}{4\pi} \Im \text{Tr} \int d^2\theta d^2\bar{\theta} \frac{\tau}{2} \Psi^2 + \\
 & + \sum_{i=1}^{N_f} \left[\int d^4\theta \left(Q_i^\dagger e^{-2V} Q_i + \tilde{Q}_i^\dagger e^{2V} \tilde{Q}_i \right) + \int d^2\theta \left(\sqrt{2}\tilde{Q}_i \Phi Q_i + m_i \tilde{Q}_i Q_i \right) + h.c. \right]
 \end{aligned}
 \tag{1.5}$$

We have constructed this Lagrangian in terms of a complex coupling constant $\tau = \frac{4\pi i}{g^2} + \frac{\theta}{2\pi}$, where g is a standard Yang-Mills coupling constant and θ defines a topological θ -term. Consider what happens physically when we start to flow down along the energy scale. It is important to notice first that after integration over auxiliary fields the Lagrangian acquires a potential term

$$V = -\frac{1}{2g^2} \text{Tr} \left([\phi^\dagger, \phi] \right)^2 \tag{1.6}$$

To define the vacuum of the theory one should minimize this potential by choosing the Higgs field to be aligned along the Cartan subalgebra \mathfrak{h} of the algebra of the initial Lie gauge group G . This vacuum brakes the initial gauge symmetry to the product $G \rightarrow U(1)^{\text{rank } G}$ via the Higgs mechanism, so that $\langle \phi \rangle = a_i H^i$, where H^i are Cartan algebra elements in corresponding representation, for example, for $SU(2)$ theory $\langle \phi \rangle = \text{diag}(a, -a)$. Still after the initial gauge symmetry is broken down the residual Weyl group symmetry remains. So to parameterize so called Coulomb branch of our theory we have to use Weyl invariants, for example, for the gauge group $SU(n)$ $u_k = \langle \frac{1}{k} \text{Tr } \phi^k \rangle$. These parameters change under the renormalization group flow and have some complicated relation to the scalar field expectation value $\langle \phi \rangle$ at low energies.

To proceed further one has to consider how the supersymmetry is affected by the renormalization group. The initial $SU(2)_R \otimes U(1)_R$ symmetry of the Lagrangian (1.5) suffers from anomalies [90]. The residual symmetry reads $(SU(2)_R \otimes \mathbb{Z}_{4N_c - 2N_f})/\mathbb{Z}_2$. So the low energy effective action should preserve this symmetry.

Thus we have all the ingredients to construct the low energy effective action explicitly. It contains Abelian $\mathcal{N} = 2$ vector multiplet flown down from the remained massless diagonal part of the high energy gauge field. The terms with at most two derivatives and not more than four fermions are constrained by $\mathcal{N} = 2$ supersymmetry [90]. They are all expressed in terms of a single holomorphic function \mathcal{F} called prepotential

$$\mathcal{L}_{\text{eff}} = \frac{1}{4\pi} \text{Im} \text{Tr} \int d^2\theta d^2\tilde{\theta} \mathcal{F}(\mathcal{A}) \quad (1.7)$$

The general form of the prepotential is prescribed by symmetries as well. For example, for pure $SU(2)$ theory

$$\mathcal{F}(a) = \frac{i}{2\pi} a^2 \log \frac{a^2}{\Lambda^2} + \sum_{k=1}^{\infty} c_k \left(\frac{\Lambda}{a} \right)^{4k} a^2 \quad (1.8)$$

The first term in this expansion comes from one-loop beta-function correction and higher corrections appear due to instanton contributions. The precise expression can be derived by integration over instanton moduli space [80], or by geometrical means, after one describes singularities of this function [90, 91]. The prepotential singularities have a deep physical meaning. They appear at those points of the moduli space where some excited states become massless and modify the low energy effective action so that considered description breaks down. So we follow to construction of excited states in the effective theory.

1.2 BPS states in class \mathcal{S} theories

A vast class of 4d $\mathcal{N} = 2$ supersymmetric theories can be engineered by a compactification of a stack of M5-branes on Riemann surfaces \mathcal{C} sometimes called UV curve [98, 38, 41, 67]. These are so called *class \mathcal{S} theories*. This class includes SYM theories, though it also includes theories not having a transparent weak coupling regime when its Lagrangian can be naively written in terms of local fields. Nevertheless, it is expected that in the low energy limit these theories are described by a Coulomb branch and a superpotential. These theories are generically parameterized by a punctured Riemann surface \mathcal{C} , certain boundary data D at punctures and a simply laced gauge algebra \mathfrak{g} , we will denote them as $\mathcal{S}(\mathcal{C}, D, \mathfrak{g})$.

A description of any composite state in the low energy limit is highly complicated, though the supersymmetry helps here as well. Since the supersymmetry is unbroken all the states in the theory fall into different representations. It is important to distinguish between so called short and long SUSY representations.

Additionally all the physical states satisfy the Bogomolny-Prasad-Sommerfeld (BPS) bound relating the mass of a state to topological characteristics of the gauge field at the spatial infinity.

The natural language for this kind of relations is the central extension of the SUSY algebra

$$\begin{aligned} \{Q_\alpha^I, \bar{Q}_{\dot{\alpha}J}\} &= 2\sigma_{\alpha\dot{\alpha}}^\mu P_\mu \delta_J^I, \\ \{Q_\alpha^I, Q_\beta^J\} &= 2\epsilon_{\alpha\beta} Z^{IJ}, \quad \alpha, \dot{\alpha} = 1, 2, \quad I = 1, \dots, \mathcal{N} \\ \{\bar{Q}_{\dot{\alpha}I}, \bar{Q}_{\dot{\beta}J}\} &= 2\epsilon_{\dot{\alpha}\dot{\beta}} Z_{IJ}^*, \end{aligned} \tag{1.9}$$

In the particular example of SYM theory[4, 11] the central charge reads:

$$Z = -\frac{1}{g^2} \int_{S_{R \rightarrow \infty}^2} \langle (-iF + *F)\phi \rangle \tag{1.10}$$

Where the integral is taken over a sphere at spatial infinity. This central charge can be simply expressed in terms of the “electric” and “magnetic” charges of a dyonic field configuration. In principle, we have a collection of central charges corresponding to different topological sectors spanning a lattice due to Dirac quantization condition

$$Z = a_i n_i + a_i^{(D)} m_i, \quad n, m \in \mathbb{Z} \tag{1.11}$$

Where a_i is a Higgs field expectation value and $a_i^{(D)}$ is its dual.

On the lattice we can consider a symplectic Dirac-Zwanziger-Schwinger (DZS) pairing given for two charges $\gamma_1 = (n_i^{(1)}, m_i^{(1)})$, $\gamma_2 = (n_j^{(2)}, m_j^{(2)})$ by the following expression:

$$\langle \gamma_1, \gamma_2 \rangle = \sum_i (n_i^{(1)} m_i^{(2)} - n_i^{(2)} m_i^{(1)}) \tag{1.12}$$

An important physical meaning of this pairing is that it corresponds to the classical angular momentum of the electro-magnetic field $J = \frac{1}{2} |\langle \gamma_1, \gamma_2 \rangle|$ generated by two dyons.

So all the effective physical states satisfy a BPS bound for its mass M :

$$M \geq |Z| \tag{1.13}$$

The states can be divided in two types of representations with respect to the action of the SUSY algebra $su(2)_R$ and the spatial rotation algebra $so(3)_R$

$$H_{\text{short}} = \rho \otimes h \tag{1.14}$$

$$H_{\text{long}} = \rho \otimes \rho \otimes h \tag{1.15}$$

The $\mathcal{N} = 2$ SUSY algebra representation can be considered as two copies of Clifford algebra representations ρ . So the long reps contain both copies, while on the short reps a half of SUSY generators is identically zero, thus the short reps contain only one copy. As a consequence they saturate the BPS bound, so the masses of such states are exactly known non-perturbatively.

Geometrical picture can be revealed from consideration of singularities and corresponding monodromies of the moduli space. These singularities arise due to that fact that some states become massless. In the simplest case of pure $SU(2)$ SYM theory such states are a monopole and a dyon [90, 91]. Such point of view allows one to complete the description of the low energy effective action by the geometric construction of the prepotential.

Starting with a punctured UV curve \mathcal{C} , having extra data D in punctures and assuming the gauge algebra to be \mathfrak{g} one constructs a complex IR curve Σ_u parameterized by the Coulomb branch coordinates u and endowed with a meromorphic form λ called a Seiberg-Witten differential [90, 91, 98]:

$$\Sigma_u : \quad \lambda^K + \sum_{r=2}^K \varphi_r \lambda^{K-r} = 0 \tag{1.16}$$

Where φ_r are meromorphic r -differentials on \mathcal{C} parameterized by the Coulomb branch parameters u_k and UV coupling constants (in the superconformal case) or by introduced cutoffs.

Then expectation values of the Higgs field can be calculated as period integrals of the Seiberg-Witten form:

$$a_i = \oint_{A_i} \lambda, \quad a_i^{(D)} = \oint_{B_i} \lambda \tag{1.17}$$

$$\tag{1.18}$$

In this context the symplectic form (1.12) on the charge lattice is inherited naturally from the intersection pairing of cycles on the Seiberg-Witten surface.

Traveling across the moduli space the masses of non-BPS states can vary and in some points it could happen that they saturate the BPS bound, while the BPS masses are restricted to saturate this bound everywhere. Thus to distinguish BPS states from non-BPS ones it is useful to introduce an index counting BPS states and equal to zero on non-BPS states. Such an index is called protected spin character (PSC) or refined BPS index, and it is defined as

$$\mathrm{Tr}_{H_{\mathrm{BPS}}}(2J_3)q^{2J_3}(-q)^{2I_3} = (q - q^{-1})\Omega(\gamma; u; q) \quad (1.19)$$

$$\Omega(\gamma; u; q) = \mathrm{Tr}_h q^{2J_3}(-q)^{2I_3} \quad (1.20)$$

where J_3 and I_3 are Cartan generators of unbroken spatial spin $so(3)$ and isospin $su(2)_R$ algebras correspondingly. Due to the presence of the second copy of the Clifford algebra representation Ω is identically zero on long reps and is non-trivial on short reps containing spin information as well:

- hypers: $\Omega(\text{hyper}) = 1$
- vectors: $\Omega(\text{vector}) = q + q^{-1}$

One can extract a simpler quantity representing just a weighted sum over BPS states representatives called a BPS index $\Omega_{\mathrm{BPS}}(u) = \Omega(u; -1)$.

This quantity is an index in that sense that it is piecewise constant while traveling across the moduli space jumping across so called walls of marginal stability.

As it was discovered in [19] it can happen that BPS particles form a new BPS boundstate. Thus it is a natural question if a composite BPS state can decay into more “fundamental” ones. This process to be possible one should satisfy energy and charge conservation conditions. Thus, for example, for a couple of BPS particles with charges Z_1 and Z_2 possibly forming a new bound we should satisfy

$$|Z_1 + Z_2| = |Z_1| + |Z_2| \quad (1.21)$$

What is possible only on the locus where $\arg Z_1 = \arg Z_2$, in other words charges have to be aligned on the complex plane. The special locus of the moduli space where some boundstates can become unstable and decay is called a wall of marginal stability. The walls of marginal stability separate the moduli space into chambers, inside a particular chamber BPS spectrum does not change.

1.3 tt^* -geometry in supersymmetric Landau-Ginzburg theory

Now let us review some basic properties of $\mathcal{N} = (2, 2)$ supersymmetric Landau-Ginzburg theories. We consider an N -dimensional Kähler manifold \mathcal{X} with a holomorphic superpotential $W : \mathcal{X} \rightarrow \mathbb{C}$.

The action in terms of chiral superfields Φ_i ($i = 1, \dots, N$) reads:

$$S = \int d^2x \left[\int d^4\theta K(\Phi_i, \bar{\Phi}_i) + \frac{1}{2} \left(\int d^2\theta W(\Phi_i) + \int d^2\bar{\theta} \bar{W}(\bar{\Phi}_i) \right) \right] \quad (1.22)$$

We can reexpress the Lagrangian in terms of component fields (world-sheet metric is $\text{diag}(-1, 1)$):

$$\begin{aligned} \mathcal{L} = & -g_{i\bar{j}} \partial^\mu \phi^i \partial_\mu \bar{\phi}^{\bar{j}} + \frac{i}{2} g_{i\bar{j}} \bar{\psi}_-^{\bar{j}} \left(\overleftrightarrow{\nabla}_0 + \overleftrightarrow{\nabla}_1 \right) \psi_-^i + \frac{i}{2} g_{i\bar{j}} \bar{\psi}_+^{\bar{j}} \left(\overleftrightarrow{\nabla}_0 - \overleftrightarrow{\nabla}_1 \right) \psi_+^i - \\ & - \frac{1}{4} g^{\bar{j}j} \partial_i \bar{W} \partial_j W - \frac{1}{2} (D_i \partial_j W) \psi_+^i \psi_-^j - \frac{1}{2} (D_{\bar{i}} \partial_{\bar{j}} \bar{W}) \bar{\psi}_-^{\bar{i}} \bar{\psi}_+^{\bar{j}} + R_{i\bar{j}k\bar{l}} \psi_+^i \psi_-^k \bar{\psi}_-^{\bar{j}} \bar{\psi}_+^{\bar{l}} \end{aligned} \quad (1.23)$$

Here we introduced Kähler metric $g_{i\bar{j}} = \partial_{i\bar{j}}^2 K(\phi^i, \bar{\phi}^{\bar{j}})$, Christoffel symbols $\Gamma_{jk}^i = g^{i\bar{l}} \partial_j g_{k\bar{l}}$, curvature tensor $R_{i\bar{j}k\bar{l}}$. Also we use the following notations:

$$\begin{aligned} \bar{\psi} \overleftrightarrow{\nabla}_\mu \chi &= \bar{\psi} \nabla_\mu \chi - (\nabla_\mu \bar{\psi}) \chi \\ \nabla_\mu \psi^i &= \partial_\mu \psi^i + \partial_\mu \phi^j \Gamma_{jk}^i \psi^k \\ D_i \partial_j W &= \partial_i \partial_j W - \Gamma_{ij}^k \partial_k W \end{aligned} \quad (1.24)$$

and the following Hermiticity conditions on fermions $\chi_\pm^\dagger = \bar{\chi}_\pm$, $(\bar{\psi} \chi)^\dagger = \bar{\chi} \psi$.

Implying the standard same time field commutators:

$$g_{i\bar{j}} \left[\phi^i(x_0, x_1), \partial_{x_0} \bar{\phi}^{\bar{j}}(x_0, x'_1) \right] = i\delta(x_1 - x'_1), \quad g_{i\bar{j}} \left\{ \psi_\alpha^i(x_0, x_1), \bar{\psi}_\beta^{\bar{j}}(x_0, x'_1) \right\} = \delta_{\alpha\beta} \delta(x_1 - x'_1) \quad (1.25)$$

We can construct supercharges in this model as the following expressions:

$$\begin{aligned} Q_\pm &= \int dx^1 \left[g_{i\bar{j}} (\partial_0 \pm \partial_1) \bar{\phi}^{\bar{j}} \psi_\pm^i \mp \frac{i}{2} \bar{\psi}_\mp^{\bar{i}} \partial_i \bar{W} \right] \\ \bar{Q}_\pm &= \int dx^1 \left[g_{i\bar{j}} \bar{\psi}_\pm^{\bar{i}} (\partial_0 \pm \partial_1) \phi^j \pm \frac{i}{2} \psi_\mp^i \partial_i W \right] \end{aligned} \quad (1.26)$$

They form a centrally extended algebra:

$$\begin{aligned} \{Q_+, Q_-\} &= 2i\bar{Z}, \quad \{\bar{Q}_+, \bar{Q}_-\} = -2iZ, \\ \{Q_\pm, \bar{Q}_\pm\} &= (\mathcal{H} \pm \mathcal{P}) \end{aligned} \quad (1.27)$$

Where central charge $Z = W(x \rightarrow +\infty) - W(x \rightarrow -\infty)$, and \mathcal{H} and \mathcal{P} are Hamiltonian and momentum operators correspondingly. Other anti-commutators are zero.

Now we can construct a family of nilpotent charges:

$$\mathbb{Q}_\zeta := Q_- - \zeta^{-1} \bar{Q}_+, \quad \bar{\mathbb{Q}}_\zeta := \bar{Q}_- - \zeta Q_+ \quad (1.28)$$

Moreover the Hamiltonian is almost \mathbb{Q}_ζ -exact:

$$\mathcal{H} = \frac{1}{2} \{ \mathbb{Q}_\zeta, \bar{\mathbb{Q}}_\zeta \} + 2\text{Re}(\zeta^{-1} Z) \quad (1.29)$$

Applying a usual logic we see that the theory admits imposing a BPS bound on eigenvalues of the Hamiltonian E :

$$E \geq 4|Z| \tag{1.30}$$

The role of BPS states saturating this bound in this theory is played by solitons. They are determined by solutions to a ζ -soliton equation

$$\partial_x \phi^i = \frac{i\zeta^{-1}}{2} \overline{\partial_{\phi^i} W} \tag{1.31}$$

We define a set $\mathfrak{S}_{\alpha\beta}(\zeta)$ of solutions to this equation with prescribed boundary conditions at spatial infinities α and β . Here α and β are critical points $\phi_{(*)}$ of the superpotential at spatial $\pm\infty$:

$$\partial_{\phi^i} W|_{\phi_{*(\alpha)}} = 0, \quad \partial_{\phi^i} W|_{\phi_{*(\beta)}} = 0 \tag{1.32}$$

Notice that $\mathfrak{S}_{\alpha\alpha}(\zeta)$ always contains a trivial solution $\phi^i(x) = \phi_{*(\alpha)}$ for arbitrary ζ .

Then actual perturbative BPS ground states are defined as small Gaussian fluctuations around soliton solutions and are annihilated by the supercharge \mathbb{Q}_ζ . Though on the quantum level these states can overlap through the instanton interpolation. And for two such quasi-classical states $|\chi\rangle$ and $|\chi'\rangle$ the following matrix element can be non-zero:

$$\langle \chi' | \mathbb{Q}_\zeta | \chi \rangle \neq 0 \tag{1.33}$$

This leads to the fact that some of the classical ground states are lifted. True quantum ground states are harmonic forms on the field space (the Hamiltonian in this case acts as a Laplacian). The space of the harmonic forms in this case is isomorphic to cohomologies of the supercharge \mathbb{Q}_ζ .

So one constructs a complex (Morse-Smale-Witten complex) [47, 96], where chains are these quasi-classical states, they are graded by their fermion numbers, the supercharge has degree 1 and acts as a differential on this complex.

The fermion number grading the chains in this complex is a pretty subtle quantity. A proper definition can be given in terms of so called η -invariant of the corresponding Dirac operator [7, 47], we postpone the definition of this fermion number. We will be able to derive an alternative definition from the Ward identities.

One of the basic definitions related to Landau-Ginzburg theories is so called chiral ring of operators. We define a chiral operator Φ_i as

$$[\mathbb{Q}_\zeta, \Phi_i] = 0 \tag{1.34}$$

We can define a \mathbb{Q}_ζ -closed class of chiral operators $[\Phi_i]$ equivalent up to \mathbb{Q}_ζ -exact piece

$$[\Phi_i] \sim [\Phi_i + \{\mathbb{Q}_\zeta, \rho\}] \quad (1.35)$$

Chiral operators form a ring [18]:

$$\Phi_i \Phi_j = C_{ij}^k \Phi_k + \{\mathbb{Q}_\zeta, \Lambda\} \quad (1.36)$$

Or for classes we get

$$[\Phi_i] [\Phi_j] = C_{ij}^k [\Phi_k] \quad (1.37)$$

Naively the chiral algebra depends on the choice of the supercharge, in particular, on the phase ζ . Nevertheless, structure constants C_{ij}^k are universal. One natural choice is to associate chiral fields to polynomials of superfields Φ_i representing supermultiplets containing scalar ϕ_i . Then the chiral ring is isomorphic to $\mathbb{C}[\phi_1, \dots, \phi_N]/\langle \partial_{\phi^i} W \rangle$.

Another natural way to define chiral operators is to consider them as marginal deformations of the superpotential

$$\delta W = \sum_i \delta t_i \Phi_i \quad (1.38)$$

Ground states in our theory form a representation. Indeed let us start with some ground state $|0\rangle$, then multiplied by a chiral field Φ_i a new state

$$|i\rangle := \Phi_i |0\rangle \quad (1.39)$$

is again a ground state. Then vacuum representation of the chiral algebra takes an explicit form

$$\Phi_i |j\rangle = C_{ij}^k |k\rangle = (C_i)_j^k |k\rangle \quad (1.40)$$

Analogously, we can define anti-chiral fields $[\bar{\mathbb{Q}}_\zeta, \bar{\Phi}_i]$ and states $|\bar{i}\rangle$. This is just another choice of a basis in the same space, hence there is a square matrix

$$G_{\bar{j}i} = \langle \bar{j} | i \rangle \quad (1.41)$$

defining Zamolodchikov metric $ds^2 = G_{\bar{j}i} d\bar{t}_j dt_i$ on the parameter space. Obviously the chiral ring structure depends on the parameters t_i , so the ground states do. Let us define a Berry connection $D_i = \partial_{t_i} + A_i$ on the quasi-classical vacuum bundle over the parameter space:

$$(A_i)_k^j := -G^{j\bar{l}} \partial_{t_i} G_{\bar{l}k} \quad (1.42)$$

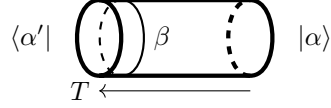


Figure 1.1: Landau-Ginzburg theory on a cylinder.

We construct supersymmetric interfaces in this theory by putting it on a cylinder. We consider a propagation along a cylinder of circumference β and put two ground states $|\alpha\rangle$ and $\langle\alpha' |$ corresponding to critical points (1.32) on its boundaries (see fig.1.1) also known as *Chan-Paton factors*.

We study a collection of partition functions as functions of marginal couplings t_i :

$$\mathcal{Z}_{\alpha\alpha'}[t] = \lim_{T \rightarrow \infty} \langle \alpha(t_0) | e^{-\int_0^T d\tau H(\tau)} | \alpha(t) \rangle \quad (1.43)$$

Let us substitute boundary critical points corresponding to ground states $\langle\alpha| \rightarrow \langle j|$, $|\alpha'\rangle \rightarrow |k\rangle$, and calculate how this partition function changed with t_i :

$$\partial_{t_i} \mathcal{Z}_{jk}[t] = \langle j(t_0) | e^{-\int_0^\infty d\tau H(\tau)} \underbrace{\partial_{t_i}}_{A_i} | k(t) \rangle + \langle j(t_0) | e^{-\int_0^\infty d\tau H(\tau)} (\beta\zeta^{-1} \underbrace{\partial_{t_i} W}_{\Phi_i}) | k(t) \rangle \quad (1.44)$$

Where the last term comes from the boundary term in the action. We can rewrite this equation as an action of a connection:

$$(\nabla_i)_k^l \mathcal{Z}_{jl}[t] = [\partial_{t_i} \delta_k^l + (A_i)_k^l - \beta\zeta^{-1} (C_i)_k^l] \mathcal{Z}_{jl}[t] = 0 \quad (1.45)$$

A similar connection takes place for conjugated parameters \bar{t}_i :

$$\bar{\nabla}_i = \partial_{\bar{t}_i} + \bar{A}_i - \beta\zeta \bar{C}_i, \quad \bar{\nabla} \mathcal{Z} = 0 \quad (1.46)$$

The Gauss-Manin connection $(\nabla_i, \bar{\nabla}_i)$ is flat or in components:

$$\begin{aligned} [D_i, \bar{D}_j] + \beta^2 [C_i, \bar{C}_j] &= 0 \\ [D_i, \bar{C}_j] &= [\bar{D}_i, C_j] = 0 \end{aligned} \quad (1.47)$$

These equations are usually referred to as tt^* -equations and they can be used to calculate Zamolodchikov metric [18] and it is usually far from being flat.

1.4 Interfaces in class \mathcal{S} theories

To put the discussions of 4d $\mathcal{N} = 2$ and 2d $\mathcal{N} = (2, 2)$ supersymmetric theories on a similar footing we consider a coupled 2d-4d system following [43].

Introduce a generalized Wilson-'tHooft surface defect in the 4d theory $\mathcal{S}^I(z)$. This defect is defined by a point z on the UV curve \mathcal{C} and choice of the vacuum I we will explain in what follows. This might be a Gukov-Witten type defect [56] represented by certain boundary conditions on the gauge field around a surface defect with axes aligned along time and x^3 axis in the 4d space. If we take a certain time slice this defect is represented by a 1d string, so it generalizes a usual notion of Dirac strings [28].

In the IR the coupled 2d-4d system can be considered as an effective theory in 2d. The preserved part of 4d supersymmetries by the defect can be seen as 2d superalgebra (see [43, Appendix A]). In particular, for a defect aligned along the x^3 -axis and preserving momentum components P_0 and P_3 one can choose the following identification:

$$Q_+ = -Q_{21}, \quad \bar{Q}_+ = \bar{Q}_{22}, \quad Q_- = \bar{Q}_{11}, \quad \bar{Q}_- = Q_{12} \quad (1.48)$$

In the IR we can also consider our defect as a defect in the IR effective Abelian theory. Then it is parameterized by two types of the parameters: monodromies α_i of the Abelian gauge fields in the 2d plane perpendicular to the defect and 2d theta angles η_i . Perturbatively these real parameters can be combined into complex ones (Gukov-Witten(GW) parameters):

$$t_i = \alpha_i + \tau_{ij}\eta_j \quad (1.49)$$

where τ_{ij} is an effective coupling constant ($\tau_{ij} = \frac{\partial^2}{\partial a_i \partial a_j} \mathcal{F}$). The defect generates in the IR a superpotential \mathcal{W} defining GW parameters:

$$t_i = \frac{\partial \mathcal{W}}{\partial a_i} \quad (1.50)$$

Then we introduce an interface along lines of sec.1.3 of certain phase ζ by varying the Gukov-Witten parameters along the spatial direction (see fig.1.2). So physically we have two possibly different vacua I and J on the opposite sides of the Dirac string and some dyonic field ‘‘blob’’ concentrated in the middle.

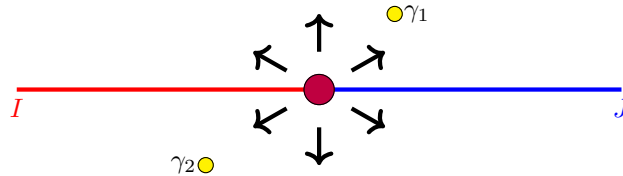


Figure 1.2: Interface defect in 4d supersymmetric theory

From the M-theory point of view it is natural to assign to surface defects M2-branes ending on M5-branes describing 4d theory over a two dimensional surface [3, 92, 39, 43]. To cover the world-

sheet of the surface defect this M2-brane is left with one extra dimension that is perpendicular to M5-brane, so M2-brane has a definite position z on the UV curve \mathcal{C} . Thus to an interface $\mathcal{I}_\zeta^{IJ}(\wp)$ interpolating between two surface defects $\mathcal{S}^I(z_1)$ and $\mathcal{S}^J(z_2)$ we associate a path on \mathcal{C} connecting points z_1 and z_2 . Let us reinterpret these spectral parameters z_i in terms of other observables.

Indeed, notice that the central charge of a state on the interface is not a single valued function of surface defects z_i , rather it has periods corresponding to contribution to the central charge from BPS dyons of the master class \mathcal{S} theory floating around (see fig.1.2):

$$Z_{IJ} = \mathcal{W}^I - \mathcal{W}^J + \sum_a \gamma_a \cdot \begin{pmatrix} \vec{a} \\ \vec{a}^{(D)} \end{pmatrix} \quad (1.51)$$

As we have seen in section 1.2 the vacuum expectation values a_i and $a_i^{(D)}$ appear as periods of Seiberg-Witten differential λ defined by the spectral cover Σ 1.16. So we expect that

$$\frac{\partial}{\partial z} \mathcal{W}^I = \frac{\partial}{\partial dz} \lambda^{(I)} \quad (1.52)$$

where $\lambda^{(I)}$ refers to the I -th root of eq.(1.16).

So we can consider z as a parameter of the theory, thus we have corresponding system of tt^* -equations for interfaces with changing z along them. This system is a Hitchin system on the Riemann surface \mathcal{C} with a gauge group $SU(K)$ since we have K vacua as the rank of the gauge group:

$$F_A + \beta^2 [C, \bar{C}] = 0, \quad D_A \bar{C} = \bar{D}_A C = 0 \quad (1.53)$$

This system implies a flatness of the Hitchin connection

$$\mathcal{A} = \left(\frac{\beta}{\zeta} C + A_z \right) dz + (\beta \zeta \bar{C} + A_{\bar{z}}) d\bar{z} \quad (1.54)$$

Partition functions of the interface for different vacua choices form flat sections of the Hitchin connection.

1.5 Knot theory review

It is a quite common problem in geometry to classify manifolds with possibly some extra structure modulo some equivalence relation. And a rather helpful tool on this route is some topological quantum field theory where this equivalence relation is a symmetry of a theory, so partition functions on these manifolds are invariants, depend only on the equivalence classes.

A particularly nice example of this geometry-QFT interplay are knot invariants derived from Chern-Simons theory [97].

Knots are embeddings $\gamma : S^1 \hookrightarrow M_3$, where M_3 is a 3d manifold, up to a regular homotopy (during this homotopy transform a tangent vector is never degenerate). Having this embedding we can construct an expectation value of a Wilson loop in the Chern-Simons theory as a path integral over gauge connections on M_3 :

$$P_R(q, a|\gamma) = \int [DA] \left(\text{Tr}_R \mathcal{P} \exp \oint_{\gamma} A \right) e^{i \frac{\kappa}{4\pi} \int_{M_3} \text{Ad}A + \frac{2}{3} A^3} \quad (1.55)$$

In the case of the gauge group $SU(N)$ and when the 3-manifold \mathcal{M}_3 is a sphere this expression is a rational function in variables

$$q = e^{\frac{2\pi i}{\kappa+N}}, \quad a = q^N \quad (1.56)$$

and it is known as Hoste-Ocneanu-Millett-Freyd-Lickorish-Yetter (HOMFLY) polynomial (if we substitute back $a = q^N$)[36], and this polynomial is an invariant (almost, there is an anomaly, but it is controllable and does not spoil everything) of a knot.

Returning back to the classification problem it is natural to ask if the HOMFLY polynomials **distinguish** knots, i.e. if two inequivalent knots have different HOMFLY polynomials. A generic answer is not known, though for symmetric reps R it is known that so called mutant knots are indistinguishable.

Nevertheless there are knot invariants (maps from knot regular homotopy classes to functions) with more refined structure.

For example, Khovanov polynomials [62] categorifying Jones polynomials (a case of HOMFLY polynomials for the gauge group $G = SU(2)$) are constructed in a somewhat different way, as Poincaré polynomials of certain complexes associated to a knot:

$$\mathcal{K}_{\square}(q, t|\gamma) = \sum_i t^i \text{qdim } H_i(\gamma) \quad (1.57)$$

Generalization to higher rank groups is known as Khovanov-Rozansky homology [64, 65], and correspondingly Khovanov-Rozansky polynomials $\mathcal{P}_{\square}(a, q, t)$. These polynomials refine the HOMFLY polynomials in the following sense: the Euler characteristic of the associated knot complex is the HOMFLY polynomial in the fundamental representation

$$\mathcal{P}_{\square}(q, a, -1|\gamma) = P_{\square}(q, a|\gamma) \quad (1.58)$$

And there is a common belief that one can construct superpolynomials $\mathcal{P}_R(q, a, t|\gamma)$ that are supposed to be generalization of the Khovanov-Rozansky polynomials on a generic representation R [31]. Though there is no explicit construction. So one of the major problems in this activity is to construct

some **refinement** of Chern-Simons theory capturing homological structure of knots and **define** superpolynomials.

And there are indication in the most recent literature that there is another deformation of knot polynomials possibly related to 5d super Yang-Mills theory [2, 6].

In this dissertation we will reformulate knot homology as a physical object arising in a quantum field theory problem.

Let us put this setup into an interfaces framework we have started with.

One can calculate alternatively the HOMFLY polynomial as a weighted monodromy trace of a conformal block in the Wess-Zumino-Witten (WZW) model [77, 73, 93]. In the WZW model on a 2d sphere one can define primary fields $\phi_i(z_i)$ depending on its position z_i on the sphere and falling into a representation of an algebra \mathfrak{g} of a compact Lie group G [35]. As functions of z_i conformal blocks of these primary fields are flat section of a flat Knizhnik-Zamolodchikov connection [69]:

$$\left(\partial_{z_i} + \frac{1}{\kappa + c_2(G)} \sum_{j \neq i} \frac{t_i^a \otimes t_j^a}{z_i - z_j} \right) \langle \phi_1(z_1) \dots \phi_n(z_n) \rangle = 0 \quad (1.59)$$

Here κ is a coupling constant as in the Chern-Simons path integral (1.55), c_2 is the second Casimir element, and t_i^a is an a -th generator of \mathfrak{g} acting on i -th primary field. The generators are subjected to a normalization condition $\text{Tr } t^a t^b = 2\delta^{ab}$.

To incorporate interfaces we will interpret the Knizhnik-Zamolodchikov connection as a reduction of tt^* -connection on a parameter space of so called Yang-Yang-Landau-Ginzburg model. Under this representation of knots(links) as interfaces the regular knot homotopy is translated to interface homotopy. The Hilbert space of true ground states on the interface is expected to be a homotopy invariant. In this dissertation we will construct this link interfaces explicitly, construct Hilbert spaces of ground states as cohomologies of the supercharge \mathbb{Q}_ζ and prove invariance of the corresponding Hilbert spaces under regular link homotopy. The corresponding Poincaré polynomials are shown to coincide with Khovanov polynomials in explicit examples.

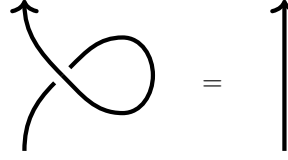
In the remaining part of the introduction we will remind some basic facts about knot theory necessary to proceed.

1.5.1 Knot diagrams and Reidemeister moves

Knots are usually depicted as knot diagrams on a 2d surface. The knot is projected to the 2d surface and in the intersections one keeps information about which strand is above, which one is below.

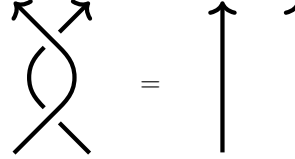
Two knot diagrams represent the same knots **iff** they can be related by a sequence of local moves called Reidemeister moves [86]:

Reidemeister move I:



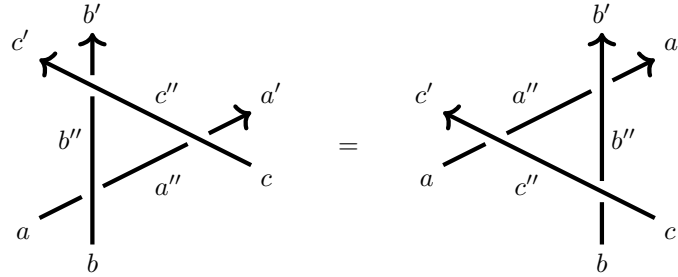
$$(1.60)$$

Reidemeister move II:



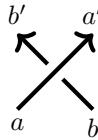
$$(1.61)$$

Reidemeister move III:



$$(1.62)$$

Define a local vertex:



$$\mathcal{R}_{a,b}^{a',b'} = (1.63)$$

The third Reidemeister move in this terms is called Yang-Baxter equation:

$$\boxed{\mathcal{R}_{a,b}^{a'',b''} \mathcal{R}_{a'',c}^{a',c''} \mathcal{R}_{b'',c''}^{b',c'} = \mathcal{R}_{b,c}^{b'',c''} \mathcal{R}_{a,c''}^{a'',c'} \mathcal{R}_{a'',b''}^{a',b'}} (1.64)$$

There is a long history of study of all these elements.

Here we just stress that a relation between Chern-Simons theory and Wess-Zumino-Witten model give a solution in terms of R -matrix for a quantum algebra $U_q(sl_n)$ [66]. The knot is considered as a time evolution of strands.

$U_q(sl_n)$ gives naturally three maps between representations and their tensor powers (R -matrix and q -Clebsch-Gordan coefficients) [68]:

$$R_{i,j}^{k,l} : \mathcal{A} \otimes \mathcal{A} \rightarrow \mathcal{A} \otimes \mathcal{A} (1.65)$$

$$C_{i,j}^k : \mathcal{A} \otimes \mathcal{A} \rightarrow \mathcal{A} (1.66)$$

$$C_k^{i,j} : \mathcal{A} \rightarrow \mathcal{A} \otimes \mathcal{A} (1.67)$$

Where \mathcal{A} is a representation of $U_q(sl_n)$, and we label vectors of these representations with indices i, j , and so on, \emptyset labels a trivial representation.

We associate these maps to braiding and (de)fusion elements:

$$\begin{array}{c} k \\ \diagdown \\ i \end{array} \begin{array}{c} l \\ \diagup \\ j \end{array} = R_{i,j}^{k,l}, \quad \begin{array}{c} i \\ \frown \\ j \end{array} = C_{\emptyset}^{i,j}, \quad \begin{array}{c} \frown \\ i \quad j \end{array} = C_{i,j}^{\emptyset} \quad (1.68)$$

Using these elements we can construct an expectation value for any knot, for example

$$\begin{array}{c} \text{Diagram of a knot with crossings labeled } l, m, n, p, q, r, s, t \text{ and strands labeled } i, j, k, l, m, n, p, q, r, s, t, u \end{array} \quad P = \sum_{i,j,\dots,u} (R^{-1})_{st}^{qr} (R^{-1})_{qr}^{np} R_{in}^{jl} R_{pu}^{mk} \times C_{\emptyset}^{is} C_{\emptyset}^{tu} C_{lm}^{\emptyset} C_{jk}^{\emptyset} \quad (1.69)$$

1.5.2 Kaufmann and Khovanov bracket

Here we follow reviews [8, 29]. One can construct a knot polynomial through so called Kaufmann bracket defined as:

$$\langle \emptyset \rangle = 1, \quad \langle \times \rangle = \langle \rangle \langle \rangle - q \langle \smile \rangle, \quad \langle \bigcirc \mathcal{L} \rangle = (q + q^{-1}) \langle \mathcal{L} \rangle \quad (1.70)$$

Thus we have for the Jones polynomial ($G = SU(2)$, $q = e^{\frac{2\pi i}{\kappa+2}}$):

$$J_q(\mathcal{K}) = \left\langle \text{Tr}_{\square} \mathcal{P} \exp \oint_{\mathcal{K}} A \right\rangle = \langle \mathcal{K} \rangle_{\text{Kaufmann}} \quad (1.71)$$

The Khovanov's setup starts with a homological refinement of the Kaufmann bracket:

$$\langle \emptyset \rangle = 1 \rightarrow \mathbb{Z} \rightarrow 1, \quad \langle \times \rangle = \left[0 \rightarrow \langle \rangle \langle \rangle \xrightarrow{d} q \langle \smile \rangle [1] \rightarrow 0 \right], \quad \langle \bigcirc \mathcal{L} \rangle = V \otimes \langle \mathcal{L} \rangle \quad (1.72)$$

Here q and $[1]$ are shifts in q -grading and homological grading. V is 2-dimensional q -graded vector space with

$$\text{qdeg } v_{\pm} = \pm 1 \quad (1.73)$$

So the diagram of the knot splits into a collection of free unlinked loops in different ways. The action of the differential splits or glues together loops.

For example, for the Hopf link (see fig.1.3) we have the following square of resolutions:

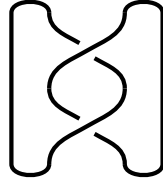


Figure 1.3: Hopf link

$$\begin{array}{ccccc}
 & 0 & & 0 & \\
 & \downarrow & & \downarrow & \\
 0 \longrightarrow & \text{[Two separate circles]} & \xrightarrow{m} & \text{[Hopf link]} & \longrightarrow 0 \\
 & (V \otimes V)[0] & & V[1] & \\
 & \downarrow m & & \downarrow \Delta & \\
 0 \longrightarrow & \text{[Two circles joined at a point]} & \xrightarrow{\Delta} & \text{[Hopf link with a central circle]} & \longrightarrow 0 \\
 & V[1] & & (V \otimes V)[2] & \\
 & \downarrow 0 & & \downarrow 0 & \\
 & 0 & & 0 &
 \end{array} \tag{1.74}$$

The differential implies an equivalence for gluing and splitting vector spaces accordingly:

$$0 \longrightarrow (V \otimes V)[0] \xrightarrow{d} V[1] \oplus V[1] \xrightarrow{d} (V \otimes V)[2] \longrightarrow 0 \tag{1.75}$$

Gluing vector spaces (multiplication):

$$\begin{array}{c}
 \text{[Two circles]} \rightarrow \text{[Two circles joined at a point]} , \\
 V \otimes V \xrightarrow{m} V, \quad m : \begin{cases} v_+ \otimes v_- \mapsto v_- \\ v_- \otimes v_+ \mapsto v_- \end{cases} \begin{cases} v_+ \otimes v_+ \mapsto v_+ \\ v_- \otimes v_- \mapsto 0 \end{cases}
 \end{array} \tag{1.76}$$

Splitting spaces (co-multiplication):

$$\begin{array}{c}
 \text{[Two circles joined at a point]} \rightarrow \text{[Two circles]} , \\
 V \xrightarrow{\Delta} V \otimes V, \quad \Delta : \begin{cases} v_+ \mapsto v_+ \otimes v_- + v_- \otimes v_+ \\ v_- \mapsto v_- \otimes v_- \end{cases}
 \end{array} \tag{1.77}$$

And the Khovanov polynomial is a Poincare polynomial of the resulting knot complex:

$$\mathcal{K}_{\square}(q, t|\gamma) = \sum_i t^i \text{qdim } H_i(\gamma) \quad (1.78)$$

A natural generalization of this quantity is expected to be a knot superpolynomial, a function $\mathcal{K}_R(q, a, t)$ depending on a group $SU(N)$ through the variable $a = q^N$, as well on representation R .

1.5.3 Vertex state model for Khovanov homology

In a particular case of a fundamental rep of $U_q(sl_2)$ R -matrix and cap/cup elements are known to reduce to the following vertex state model [100]:

$$\begin{array}{ccc} \begin{array}{c} + \quad + \\ \diagdown \quad / \\ / \quad \diagdown \\ + \quad + \end{array} = q^{\frac{1}{2}}, & \begin{array}{c} - \quad - \\ \diagdown \quad / \\ / \quad \diagdown \\ - \quad - \end{array} = q^{\frac{1}{2}}, & \begin{array}{c} - \quad + \\ \diagdown \quad / \\ / \quad \diagdown \\ + \quad - \end{array} = q^{-\frac{1}{2}} \\ \\ \begin{array}{c} + \quad - \\ \diagdown \quad / \\ / \quad \diagdown \\ - \quad + \end{array} = q^{-\frac{1}{2}}, & \begin{array}{c} + \quad - \\ \diagdown \quad / \\ / \quad \diagdown \\ + \quad - \end{array} = q^{\frac{1}{2}} - q^{-\frac{3}{2}}, & \begin{array}{c} - \quad + \\ \diagdown \quad / \\ / \quad \diagdown \\ - \quad + \end{array} = 0 \end{array} \quad (1.79)$$

And for the caps/cups:

$$\begin{array}{ccc} \begin{array}{c} + \quad - \\ \cup \end{array} = \begin{array}{c} \cup \\ + \quad - \end{array} = iq^{-\frac{1}{2}} \\ \\ \begin{array}{c} - \quad + \\ \cup \end{array} = \begin{array}{c} \cup \\ - \quad + \end{array} = -iq^{\frac{1}{2}} \end{array} \quad (1.80)$$

Let us rewrite Khovanov homology in a similar formulation.

This intersection formula can be reformulated as

$$\begin{array}{c} \diagdown \quad / \\ / \quad \diagdown \end{array} = q^{\frac{1}{2}} \left(\begin{array}{c} \cup \\ + \quad - \end{array} \oplus q^{-\frac{1}{2}} \begin{array}{c} \cup \\ - \quad + \end{array} \right) \quad (1.81)$$

We assign a weight t to homological degree, to get back Jones polynomials it is enough to switch to Euler characteristic, i.e. to substitute $t = -1$. The coefficients in (1.80) are consequently promoted to

$$\begin{array}{ccc} \begin{array}{c} + \quad - \\ \cup \end{array} = \begin{array}{c} \cup \\ + \quad - \end{array} = t^{\frac{1}{2}} q^{-\frac{1}{2}} \\ \\ \begin{array}{c} - \quad + \\ \cup \end{array} = \begin{array}{c} \cup \\ - \quad + \end{array} = t^{-\frac{1}{2}} q^{\frac{1}{2}} \end{array} \quad (1.82)$$

And the intersection has the same form. And for the opposite intersection we have

$$\begin{array}{c} \diagup \diagdown \\ \diagdown \diagup \end{array} = \begin{array}{c} \text{---} \\ \text{---} \\ \text{---} \\ \text{---} \end{array} = q^{-\frac{1}{2}} \left(\begin{array}{c} \text{---} \\ \text{---} \end{array} \oplus q^{\frac{1}{2}} \begin{array}{c} \text{---} \\ \text{---} \end{array} \right) \quad (1.83)$$

If we define 1d vector spaces spanned by v_+ and v_- as loops with certain spin projections on strands:

$$v_+ = \begin{array}{c} \text{---} \\ \text{---} \\ \text{---} \\ \text{---} \end{array}, \quad v_- = \begin{array}{c} \text{---} \\ \text{---} \\ \text{---} \\ \text{---} \end{array} \quad (1.84)$$

The multiplication law is analogous to the one in Khovanov's construction:

$$V \otimes V \xrightarrow{m} V, \quad m : \begin{cases} v_+ \otimes v_- \mapsto v_- \\ v_- \otimes v_+ \mapsto v_- \end{cases} \quad \begin{cases} v_+ \otimes v_+ \mapsto v_+ \\ v_- \otimes v_- \mapsto 0 \end{cases} \quad (1.85)$$

And the co-multiplication law also reads:

$$V \xrightarrow{\Delta} V \otimes V, \quad \Delta : \begin{cases} v_+ \mapsto v_+ \otimes v_- + v_- \otimes v_+ \\ v_- \mapsto v_- \otimes v_- \end{cases} \quad (1.86)$$

This construction also gives an invariant bi-graded homological group. The q -degree is weighted by the power of q variable in the expansion, the homological degree is weighted by the power of t variable correspondingly. The **framed** knot invariant is given by a bi-graded Poincaré polynomial:

$$\mathcal{P}_{\square}(q, t|\gamma) := \sum_{i,j} t^i q^j \dim H_{i,j}(\gamma) \quad (1.87)$$

For examples of a calculation in this setup see Appendix C.

To get a knot invariant we should take care that the framing enters as an overall monomial multiplier. It can be simply handled by a closer look to the first Reidemeister move. Indeed, it gives not equivalent polynomials, rather proportional ones, then we can rescale this proportionality coefficient back. So we define a knot invariant:

$$\hat{\mathcal{P}}_{\square}(q, t|\gamma) := (q^{-\frac{3}{2}} t)^{n_+ - n_-} \mathcal{P}_{\square}(q, t|\gamma) \quad (1.88)$$

where n_+ and n_- are numbers of positive and negative intersections defined as follows. Choose an orientation of the knot then we have two types of crossings, we assign to them signs $+$ and $-$ in the

following way:

$$n_- = \# \left(\begin{array}{c} \nearrow \nearrow \\ \searrow \searrow \end{array} \right), \quad n_+ = \# \left(\begin{array}{c} \nwarrow \nwarrow \\ \nearrow \nearrow \end{array} \right) \quad (1.89)$$

Notice that defined in this way the knot polynomial differs slightly from Khovanov's definition:

$$\mathcal{K}_{\square}(q, t|\gamma) = \mathcal{P}_{\square}(qt, t|\gamma). \quad (1.90)$$

Nevertheless, if we substitute $t = -1$ the resulting construction reduces to the physical vertex model. So we would use this setup as a goal for Chern-Simons homological refinement.

Chapter 2

BPS states in class \mathcal{S} theories

So as a background theory we have chosen a class $\mathcal{S}(\mathcal{C}, D, \mathfrak{g})$ theory.

As we have discussed in sec.1.4 a natural way to consider interfaces is to introduce their partition functions as flat sections of the Hitchin connection on the punctured Riemann surface \mathcal{C} :

$$F_A + \beta^2[C, \bar{C}] = 0, \quad D_A \bar{C} = \bar{D}_A C = 0 \quad (2.1)$$

All the fields here are in the adjoint representation of a simply laced algebra \mathfrak{g} . And boundary data at punctures D are certain boundary conditions for fields near the punctures.

The Hitchin system appears naturally in a compactification of a stack of M5-branes on the Riemann surface \mathcal{C} [42, 41].

For a family of interfaces $\mathcal{I}_\zeta^{IJ}(\wp)$ we construct a flat Hitchin connection:

$$\mathcal{A}(\zeta) = \left(\frac{\beta}{\zeta} C + A_z \right) dz + (\beta \zeta \bar{C} + A_{\bar{z}}) d\bar{z} \quad (2.2)$$

To an interface we associate a partition function Ψ being a flat section of this connection:

$$(d + \mathcal{A}(\zeta))\Psi = 0 \quad (2.3)$$

We follow [42, 41, 44, 43] and utilize the following trick. We analytically continue values of ζ from S^1 to the punctured Riemann sphere \mathbb{C}^\times . Then we can consider the limit $\zeta \rightarrow 0$. Then the analysis is quite similar to the study of asymptotic differential equation solutions due to G. Stokes, also known as a Wentzel-Kramers-Brillouin (WKB) method in physics (see e.g.[32]). We search for a solution in the following form:

$$\Psi(z) \sim e^{\zeta^{-1} \int x(t) dt} \quad (2.4)$$

So the first approximation reduces to an algebraic equation for the eikonal $x dz$:

$$\text{Det}(\mathbb{I} \cdot x(z) dz + C(z) dz) = 0 \quad (2.5)$$

This is an equation defining a complex curve Σ with a meromorphic differential $x dz$. To be binded to a physical theory one identifies this curve with the spectral curve Σ_u (1.16) and the meromorphic differential with the Seiberg-Witten differential $\lambda = x(z) dz$.

We choose some trivialization of the branched cover $\pi : \Sigma \rightarrow \mathcal{C}$: a collection of branching points and a collection of cuts (see fig.2.1). On a set $\mathcal{C}^c = \mathcal{C} \setminus \{\text{branch cuts}\}$ a global choice of the roots ordering can be made. Thus we have a well defined map $s : \Sigma \setminus \pi^{-1}\{\text{cuts}\} \rightarrow \mathbb{Z}$ that associates to each point on Σ not lying on the cut an order number of the cover sheet it is lying on. We continue the definition of the root ordering to the branching points and associate to each branch point and cut an element of the Galois group of the spectral cover (2.5) as a polynomial in x . In the case when \mathfrak{g} is of type A_{K-1} we have a K -fold cover, and in a generic position we can label the branching points by 2-cycles from the permutation group S_K (for a discussion of more generic situation see [74]).

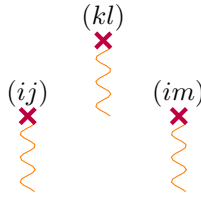


Figure 2.1: Branching points and cuts

Then we can write the asymptotic expansion in the following form:

$$\Psi(z) = \left(\sum_{i,j} \sum_{a \in \Gamma(z^{(i)}, z_0^{(j)})} \Omega(a) X_a \right) \Psi(z_0) \quad (2.6)$$

where $\Omega(a)$ are integer numbers, Stokes coefficients, $\Gamma(z^{(i)}, z_0^{(j)})$ is a set of relative homology classes of paths connecting i -th and j -th pre-images of points z and z_0 on the cover, and operators X_a are defined as

$$X_a = e^{\zeta^{-1} \int_a \lambda + O(\zeta^0)} E_a \quad (2.7)$$

where E_a is a square matrix with just one unit entry at position $(s(\partial_- a), s(\partial_+ a))$ where $\partial_{\pm} a$ are opposite ends of an oriented path a .

This decomposition is called *Abelianization map* since it represents a non-Abelian parallel transport with the \mathfrak{g} -valued connection along a Riemann surface \mathcal{C} in terms of an Abelian parallel transport on the cover Σ with a structure group being the Weyl subgroup of G .

Physically integer coefficients $\Omega(a)$ represent BPS indices (see discussion around eq.(1.20)) of bound 2d-4d states supported on the interface [43, 52]. The central charge of a state corresponding to the path a is defined as

$$Z_a = \int_a \lambda \tag{2.8}$$

For closed paths we can take a trace closure of the matrix valued function X_a to get scalar functions $X_\gamma(u)$ where moduli u parameterize the Seiberg-Witten curve and $\gamma \in H_1(\Sigma, \mathbb{Z})$. Functions $X_\gamma(u)$ define so called semi-flat coordinates [42] on the moduli space \mathcal{M} of solutions to the Hitchin system (2.1) modulo gauge transformations. These coordinates are closely related to classical Fock-Goncharov coordinates of the Teichmüller theory associated to ideal triangulations of the UV curve \mathcal{C} [34].

Integer valued functions $\Omega(a)$ are only piece-wise constants, indeed they depend on the point u on the moduli space of Seiberg-Witten curves and on the chosen phase ζ . In particular, when the phase of the interface ζ coincides with a phase ζ_0 of a dyonic BPS state, this BPS state can be captured by the interface or released [43] to form a new bound state. This changes BPS indices of the interface states in a certain way. So a knowledge of BPS indices of all interfaces for all the parameters allows one to calculate BPS indices of dyons in the class \mathcal{S} theory.

A promotion to the protected spin characters defined in (1.20) is less straightforward. Continuing analogy with the Fock-Goncharov coordinates one expects a deformation (“quantization”) of the Teichmüller space with a quantization parameter controlled by chemical potential q [44]. Consequently, we should introduce a deformation of the WKB method to incorporate this quantization and the spin information correspondingly. Thus we start with an abstract notion of the parallel transport and an Abelianization map, then we determine how the refining deformation and corresponding protected spin characters can be recovered.

2.1 Spectral networks

It is well-known that the WKB approximation fails to work near so called “turning points” (branching points in our terminology) since the exponentiated eikonal is near zero so the exponent can not be assumed to dominate. So the expansion (2.6) can not be a correct asymptotic of the flat section on the whole \mathcal{C} . Instead the coefficients $\Omega(a)$ jump discontinuously across anti-Stokes lines, or so called \mathcal{S} -walls. To define them we use the following principle: we will not notice a discontinuous behavior of coefficients in front of the exponentially small contributions. These exponentially small contributions

occur when the eikonal is purely real along the whole integration path. So we define (ij) -WKB lines (or anti-Stokes lines, or $\mathcal{S}_{(ij)}$ -walls) as real curves on \mathcal{C} satisfying the following equations:

$$\mathbf{i}_{\partial_t}(\lambda^{(i)} - \lambda^{(j)}) \in \mathbb{R}_{>0} \quad (2.9)$$

where ∂_t is a tangent vector to the \mathcal{S} -wall, $\lambda^{(i)}$ is the Seiberg-Witten differential on the i -th sheet and \mathbf{i} is a contraction map. There are two types of \mathcal{S} -walls: primary and descendent. Primary $\mathcal{S}_{(ij)}$ -walls are emanated from (ij) -branching point. Descendent $\mathcal{S}_{(ij)}$ are born or terminated in joints of $\mathcal{S}_{(ik)}$ and $\mathcal{S}_{(kj)}$ -walls (see fig.2.2)¹. So a generic pattern of \mathcal{S} -walls can be quite involved (see fig.2.10). We call the whole system of \mathcal{S} -walls a *spectral network* $SN(u, \zeta)$, by construction it depends on phase ζ and point u of the moduli space [45, 46].

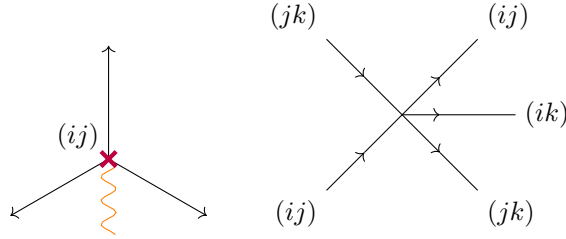


Figure 2.2: Examples of S-walls.

2.2 Abstract Abelianization map

In the previous section having a spectral cover Σ of a Riemann surface \mathcal{C} we have constructed a family of spectral networks $SN(u, \zeta)$. Now we present an abstract Abelianization of the parallel transport along the curve \mathcal{C} .

Following [52] we will apply the spectral networks machinery to associate the parallel transport \mathfrak{U} on a Riemann surface \mathcal{C} with a *non-Abelian* connection on it to a formal algebra \mathscr{Y} (these variables

¹We can describe branching points as zeroes of the discriminant of the spectral cover equation (2.5) with respect to the variable x . In the neighbourhood of the ramification point z_0 the discriminant can be expanded into Taylor series:

$$\text{Disc}(z) = \prod_{i < j} (x^{(i)} - x^{(j)})^2 = c(z - z_0) + O((z - z_0)^2)$$

In a generic setup coefficient c is non-zero, though if the spectral cover has some additional symmetries we might have to use higher orders in this expansion. So generically in the neighbourhood of the branching point $\lambda^{(i)} - \lambda^{(j)} \sim \alpha\sqrt{z - z_0}$ and we easily solve the \mathcal{S} -wall equation (2.9):

$$z(t) = z_0 + \left(\frac{3}{2}\zeta\alpha^{-1}\right)^{\frac{2}{3}} e^{\frac{2\pi i n}{3}t}, \quad t \geq 0, \quad n = 0, 1, 2$$

where t is a “time” along \mathcal{S} -wall trajectory. So generically one has *three* \mathcal{S} -walls emanated from each branching point. In the case when the branching point is of higher order (if it is a collision point of more than two sheets) we can perturb the parameters of the spectral cover, so that the branching point is resolved in a collection of close simple branching points.

are aimed to represent *Abelian* parallel transport along the cover) of paths on a covering surface Σ subjected to a minimal set of rules:

1. If two paths a and b are regular-homotopic² then

$$\mathcal{Y}_a = \mathcal{Y}_b \quad (2.10)$$

2. Concatenation rule

$$\mathcal{Y}_a \mathcal{Y}_b = \begin{cases} \mathcal{Y}_{a \circ b}, & \text{if a concatenation } a \circ b \text{ exists,} \\ 0, & \text{otherwise} \end{cases} \quad (2.11)$$

There are **no other natural a priori** rules for this algebra.

The spectral network $SN(u, \zeta)$ cuts the UV curve \mathcal{C} into charts $\mathcal{C} \setminus SN(u, \zeta) = \coprod_i U_i$. We define the parallel transport \mathfrak{U} along some path $\varphi \subset \mathcal{C}$ following these two *detour* rules:

1. If $\varphi \subset U_i$ we define the parallel transport just as a sum of parallel transports along all the sheets:

$$\mathfrak{U}_\varphi := \sum_{a \in \pi^{-1}(\varphi)} \mathcal{Y}_a \quad (2.12)$$

2. If the path φ intersects the spectral network along some $\mathcal{S}_{(ij)}$ -wall $\sigma \subset SN(u, \zeta)$ lying on the boundary of two charts U_+ and U_- , so that $\varphi \cap U_\pm = \varphi_\pm$ and $\sigma = \partial(U_+) \cup \partial(U_-)$ (see fig.2.3), the parallel transport is defined through a re-gluing map:

$$\mathfrak{U}_\varphi = \mathfrak{U}_{\varphi_+} (1 + \mathcal{T}_\sigma) \mathfrak{U}_{\varphi_-} \quad (2.13)$$

Where \mathcal{T}_σ is an element of the path algebra

$$\mathcal{T}_\sigma = \sum_{a \in D_\sigma} \mathcal{Y}_a \quad (2.14)$$

defined as a sum with multiplicities over all regular homotopy classes with endpoints located in lifts of the intersection point $z = \varphi \cap \sigma$ to i -th and j -th sheet correspondingly.

The element \mathcal{T}_σ change smoothly along the \mathcal{S} -wall σ , we just relocate endpoints of all the classes along corresponding lifts of σ . Though it changes discontinuously across branching points and joints of the spectral network.

²Let $I = [0, 1]$ be the unit interval parametrized by t , and consider an immersion $f : I \rightarrow X$ into a Riemann surface X , namely a smooth map such that $f : T_t I \rightarrow T_{f(t)} X$ is injective (i.e. the path never has zero velocity). A regular homotopy between two immersions is a homotopy through immersions.

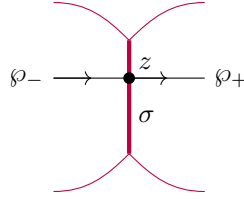
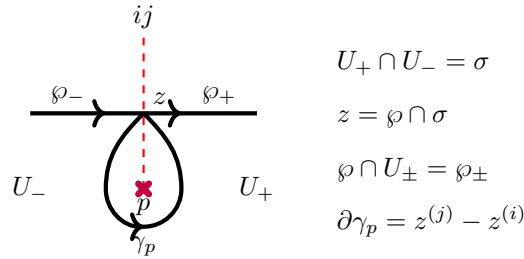


Figure 2.3: Regluing map

At branch points we impose *simpleton* boundary conditions:

$$\mathcal{T}_\sigma = \mathcal{Y}_{\gamma_p} \tag{2.15}$$

where $\gamma_p \subset \Sigma$ is a path starting from a lift of the intersection point $z = \wp \cap \sigma$ to i -th sheet and ending on a lift to the j -th sheet, encircling the branching point p :



Across joints (see fig.2.4) regluing elements change accordingly:

$$\mathcal{T}_{(ij)'} = \mathcal{T}_{(ij)}, \quad \mathcal{T}_{(jk)'} = \mathcal{T}_{(jk)}, \quad \mathcal{T}_{(ik)'} = \mathcal{T}_{(ik)} + \mathcal{T}_{(ij)}\mathcal{T}_{(jk)} \tag{2.16}$$

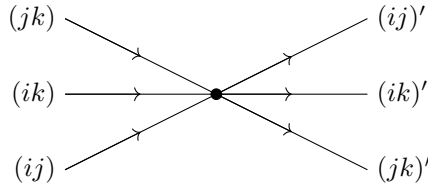


Figure 2.4: Spectral network joint

2.3 Flatness and sign rule

To show that abstract parallel transport presented in the previous section is flat indeed, i.e. for two regular homotopic paths \wp and \wp' on \mathcal{C}

$$\mathfrak{U}_\wp = \mathfrak{U}_{\wp'} \tag{2.17}$$

we start with the flatness across ramification points (see fig.2.5).

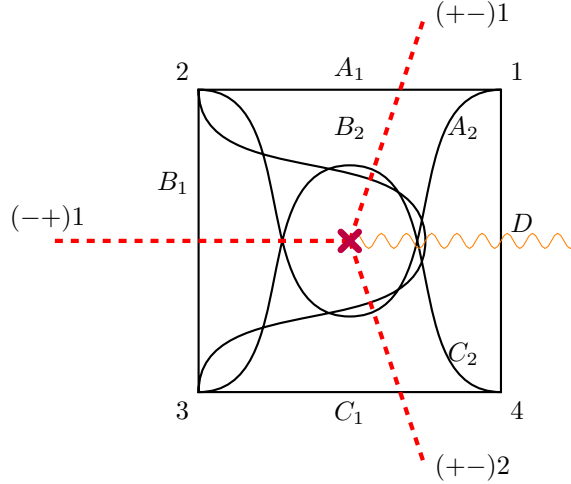


Figure 2.5: Lifts and detours

In a generic simple branching point two sheets are colliding, we denote them without loss of generality as a (+)-sheet and (-)-sheet, as we cross the cut we get an action of $(+-)$ -permutation. There are three \mathcal{S} -walls emanated from the branching point [52], those neighbour \mathcal{S} -walls that do not have a cut between them should be of opposite type, so we have chosen $(+-)$, $(-+)$ and $(+-)$ types as one goes counterclockwise.

The flatness condition requires that the parallel transports along path going through points 1, 2, 3, 4 and a path going directly from 1 to 4 through the cut are equal:

$$\mathfrak{U}_{1234} = \mathfrak{U}_{14} \quad (2.18)$$

Let us write both sides explicitly:

$$\begin{aligned} & \left(\mathcal{Y}[A_1^{++}] + \mathcal{Y}[A_1^{--}] + \mathcal{Y}[A_2^{+-}] \right) \left(\mathcal{Y}[B_1^{++}] + \mathcal{Y}[B_1^{--}] + \mathcal{Y}[B_2^{(-+)}] \right) \times \\ & \times \left(\mathcal{Y}[C_1^{++}] + \mathcal{Y}[C_1^{--}] + \mathcal{Y}[C_2^{+-}] \right) = \mathcal{Y}[D^{+-}] + \mathcal{Y}[D^{(-+)}] \end{aligned} \quad (2.19)$$

Here we have denoted explicit paths on the cover by labelling pre-images of end-points with sheets they are lying on. So path A_2^{+-} starts at preimage of point 1 on (+)-sheet and ends on the pre-image of point 2 on the (-)-sheet.

Thus we get the following equality:

$$\begin{aligned}
& \mathcal{Y} \left[\underbrace{A_1^{(++)} B_1^{(++)} C_1^{(++)}}_{a^{(++)}} \right] + \mathcal{Y} \left[\underbrace{A_1^{(--)} B_1^{(--)} C_1^{(--)}}_{a^{(--)}} \right] + \mathcal{Y} \left[\underbrace{A_1^{(++)} B_1^{(++)} C_2^{(+-)}}_{D^{(+-)}} \right] + \\
& + \mathcal{Y} \left[\underbrace{A_1^{(--)} B_2^{(-+)} C_1^{(++)}}_{D^{(-+)}} \right] + \mathcal{Y} \left[\underbrace{A_1^{(--)} B_2^{(-+)} C_2^{(+-)}}_{a'^{(--)}} \right] + \mathcal{Y} \left[\underbrace{A_2^{(+-)} B_1^{(--)} C_1^{(--)}}_{D^{(+-)}} \right] + \\
& + \mathcal{Y} \left[\underbrace{A_2^{(+-)} B_2^{(-+)} C_1^{(++)}}_{a'^{(++)}} \right] + \mathcal{Y} \left[\underbrace{A_2^{(+-)} B_2^{(-+)} C_2^{(+-)}}_{D^{(+-)} a'^{(--)}} \right] = \mathcal{Y}[D^{(+-)}] + \mathcal{Y}[D^{(-+)}]
\end{aligned} \tag{2.20}$$

Comparing the both sides of this equality we arrive to a condition on the path algebra. If we denote by a prime a difference between paths by a curl around the branching point, so

$$a = \text{blue loop with red cross and wavy line} , \quad a' = \text{blue loop with bubble, red cross and wavy line} \tag{2.21}$$

then the expansion of the flatness condition delivers a **new** equation for the path algebra:

$$\boxed{\mathcal{Y}_a + \mathcal{Y}_{a'} = 0} \tag{2.22}$$

We refer to this condition as a *sign rule*. Notice that a' has a little “bubble”. This bubble can not be eliminated since we are considering paths up to a regular homotopy.

The sign rule may be realised in different ways depending on a concrete representation of the path algebra. We will return to this discussion in sec.3.3.2 and Appendix A.

Other check of the homotopy invariance can be carried on, say, across joints or \mathcal{S} -walls, nevertheless the condition (2.22) is defining, so we can state a theorem.

Theorem 2.3.1. *Rules (2.12) and (2.13) define on a path algebra subjected to an extra condition (2.22) a flat parallel transport \mathfrak{U} , i.e. for two regularly homotopic paths $\wp_1 \sim \wp_2$ we have*

$$\mathfrak{U}_{\wp_1} = \mathfrak{U}_{\wp_2}$$

2.4 Projection to Fock-Goncharov coordinates

To determine a projection to quantum coordinates on the Hitchin moduli space analogous to quantum Fock-Goncharov coordinates on the Teichmüller space let us remind a desired quantization condition.

We consider dyonic operators X_γ labelled by dyonic charges $\gamma \in H_1(\Sigma, \mathbb{Z})$. Natural intersection pairing on the homology lattice $\langle \cdot, \cdot \rangle$ is identified with DSZ pairing (see section 1.2). We expect these generators to form a Heisenberg algebra:

$$X_\gamma X_{\gamma'} = q^{\langle \gamma, \gamma' \rangle} X_{\gamma+\gamma'} \tag{2.23}$$

where the parameter q is the chemical potential entering (1.20). This commutation relation can be argued from different points of view [44, 49, 61]. A brief physical explanation is the following. Consider a 3d BPS state as a multi-centered BPS molecule [76] of more elementary dyons. One can apply localization technique to this system and expects the system localizes to a critical configuration that is a fixed point of the spin generator J_3 . So the dyons should be located along the spatial x^3 -axis. Two dyons of charges γ and γ' respectively localized to the x^3 -axis create an electro-magnetic field with a classical axial momentum $J_3 = \frac{1}{2}\langle\gamma, \gamma'\rangle$ aligned along the x^3 -axis and contributing to the PSC as $q^{\langle\gamma, \gamma'\rangle}$.³

In the classical story we have identified the coordinates on the Hitchin moduli space with Abelian holonomies on the spectral cover. Here we expect that on closed paths γ the abstract path algebra acquires a representation:

$$\rho(\mathcal{A}_\gamma) = q^{f(\gamma)} X_{[\gamma]} \quad (2.24)$$

where $f(\gamma)$ is a scalar function of the path γ and $[\cdot]$ is a homology class of the corresponding regular homotopy class. If we implement a concatenation of closed cycles we can apply the representation map to the rule (2.11), this would imply the following equation for the function f :

$$“f(\gamma \circ \gamma') = f(\gamma) + f(\gamma') + \langle\gamma, \gamma'\rangle”$$

We have put it in quotation marks since we have not implemented a concatenation procedure for closed paths yet. Though this relation proposes to search for a function that behaves as a *quadratic refinement* of the intersection pairing, a nice candidate is the *writhe*.

Consider a path a as a map $a : [0, 1] \rightarrow \Sigma$. We denote as $\sigma(a)$ a set of self-intersection points of a . For each point $s \in \sigma(a)$ we can present two points $t_1, t_2 \in [0, 1]$, such that $t_1 < t_2$ and $a(t_1) = a(t_2)$. We define the writhe $\text{wr } a$ as a signed sum over self-intersections:

$$\text{wr } a = \sum_{s \in \sigma(a)} \text{sign} [d_{t_1(s)}\gamma \wedge d_{t_2(s)}\gamma] \quad (2.25)$$

where the sign of a form is defined as its orientation with respect to the surface area form. For example,

$$\text{wr} \left(\text{diagram} \right) = 3 \begin{matrix} \nearrow \\ \nwarrow \end{matrix} + 1 \begin{matrix} \nwarrow \\ \nearrow \end{matrix} = 2 \quad (2.26)$$

³There are other ways to derive this algebra. In the case of Liouville CFT it follows naturally from commutation relations of so called current operators, or check-operators [20, 49, 53]. In the case of the SYM theory in Ω -background these commutation relations can be read from [61].

To clarify the role of the writhe as of quadratic refinement for the intersection pairing consider two closed paths γ_1 and γ_2 possibly with self-intersections (see fig.2.6). Let us add an *auxiliary* path χ without self-intersections intersecting both γ_1 and γ_2 consequently. Intersection points divide χ in three pieces: χ_- , χ_0 and χ_+ . Now we can glue the auxiliary path with γ_i considering closed paths as open paths with the beginning and the end put in the intersection point. Thus we have:

$$\mathbf{wr}(\chi_- \circ \gamma_1 \circ \chi_0 \circ \gamma_2 \circ \chi_+) = \mathbf{wr}(\chi_- \circ \gamma_1 \circ \chi_0 \circ \chi_+) + \mathbf{wr}(\chi_- \circ \chi_0 \circ \gamma_2 \circ \chi_+) + \langle [\gamma_1], [\gamma_2] \rangle \quad (2.27)$$

where the last term comes from the mutual intersection of paths in question.

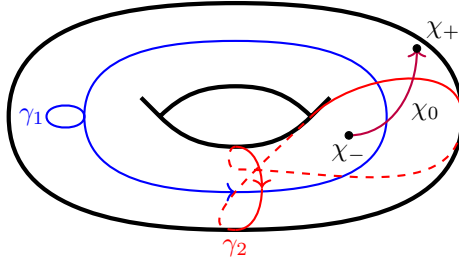


Figure 2.6: Auxiliary path

Still the function in the representation map (2.24) can have a piece linear in the path concatenation. To fix it we will use the sign rule (2.22). The paths different by a curl with a bubble should have opposite sign in this representation. We can easily calculate the number of curls as a number of branching points encircled by the path:

$$\mathbf{curl} \gamma := \frac{1}{\pi i} \int_{\gamma} d \log \lambda \quad (2.28)$$

When we compare curls of a and a' it is different by 1. Also notice that due to a small “bubble” in a definition of a' its writhe also differs by 1, so we should cancel q -powers due to this contribution. So, finally, our definition for a representation on closed curves reads

$$\rho[\mathcal{Z}_{\gamma}] = q^{\mathbf{wr} \gamma} (-q)^{\mathbf{curl} \gamma} X_{[\gamma]} \quad (2.29)$$

2.5 Wall-crossing

2.5.1 Line defects

An important class of defect operators preserving some supersymmetries allowed in class \mathcal{S} theories is called line defects [44, 43]. Line operators preserve a ζ -supersymmetry (see sec.1.4) analogous to interfaces. They can be considered as interfaces with identical surface defect boundary conditions

on its ends. So we can define partition functions of the line defects as *holonomy* traces of the Hitchin connection (2.2):

$$\langle L(\wp, \zeta) \rangle = \text{Tr Hol}_\wp (d + \mathcal{A}) \quad (2.30)$$

To include the chemical potential q for spin J_3 and isospin I_3 generators we define it as a representation map of the Abstract parallel transport holonomy:

$$\langle L(\wp, \zeta, q) \rangle = \rho[\mathfrak{A}_\wp] \quad (2.31)$$

The right hand side can be expanded over dyonic operators X_γ with coefficient in the polynomial ring $\mathbb{Z}[q, q^{-1}]$:

$$\langle L(\wp, \zeta, q) \rangle_u = \sum_{\gamma \in H_1(\Sigma, \mathbb{Z})} \bar{\Omega}_\gamma(q, u) X_\gamma \quad (2.32)$$

The coefficients $\bar{\Omega}_\gamma(q)$ have a meaning of the PSC of BPS states in a background with the line defect preserving supercharge \mathbb{Q}_ζ (so called *framed* BPS states) and in the electro-magnetic charge sector γ :

$$\bar{\Omega}_\gamma(q) = \text{Tr}_{\mathcal{H}_{BPS}} q^{2J_3} (-q)^{2I_3} \quad (2.33)$$

Relation (2.32) establishes the action of the RG flow since we have related a line defect given by UV data to low energy observables X_γ in the effective theory.

Definition (2.31) is not generic, indeed it depends on the choice of a marked point on the closed path \wp that enters the writhe, though this discrepancy can be controlled. In [52] it was proposed to consider a specific subclass of interfaces called *halo-saturated interfaces* and resulting holonomies. In [37] the definition was generalized further to be applicable to arbitrary line defects. The definition of the writhe of a closed path \wp that can be thought as a map $\wp : S^1 \rightarrow \Sigma$ was continued to a $U(1)$ Chern-Simons partition function of a Wilson loop $t \mapsto (\wp(t), t)$ in $\Sigma \times S^1$.

Functions $\Omega_\gamma(q, u)$ are only piecewise constant functions on the moduli space. This phenomenon is known as *wall-crossing*. The BPS spectrum of the theory jumps across certain loci on the moduli space, so PSC's do. On these loci BPS states can decay into each other, conservation laws for these decays impose a real one dimensional condition on the loci, so generically they are represented by codimension-1 hypersurfaces in the moduli space dividing it into chambers where functions $\Omega_\gamma(q, u)$ are constants.

There are several hierarchical orders of wall-crossing. So one distinguishes:

- **\mathcal{S} -walls.** We have already encountered \mathcal{S} -walls, they are responsible for appearance of soliton BPS states in the spectrum of effective 2d theory on the interface. Detour rule (2.13) assigns to solitons their topological and flavour charges. And the central charge of a soliton configuration is calculated according to the rule (2.8). We will return to discussion of the connection between detours and solitons in sec.3.3.1.
- **\mathcal{K} -walls.** \mathcal{K} -walls appear in the framed BPS wall-crossing. Physically, in the low energy limit the framed BPS state can be thought of as a dyonic heavy core of electro-magnetic charge γ_c and a halo of bound 3d BPS particles of charge γ_h (possibly different species of different charges) floating around (see fig.1.2). An effective size of the halo cloud is given by Denef's formula [23]

$$r_{\text{halo}} = \frac{\langle \gamma_h, \gamma_c \rangle}{2\text{Im} [\zeta^{-1} Z_{\gamma_h}(u)]} \quad (2.34)$$

This size diverges on co-dimension 1 hypersurfaces in the extended moduli space (u, ζ) called \mathcal{K} -walls. Across \mathcal{K} -walls framed BPS degeneracies entering (2.32) jump.

- **MS-walls.** Marginal stability walls (or MS-walls) are defined as codimension 1 hypersurfaces in the moduli space where the very 3d BPS states in class \mathcal{S} theory without any defect inclusion become stable or unstable.

2.5.2 Flip

So far we have discussed \mathcal{S} -walls. Now we use our construction of line defects to study \mathcal{K} -walls, this would give us information about BPS spectrum of the class \mathcal{S} theories and then we will be able to collect information about MS-walls.

The framed PSC's in (2.32) are determined by spectral network topology. So discontinuity in framed PSC's is related to discontinuity in spectral network topology.

Let us consider a simplest case of two close branching points of the same (ij) -type (see fig.2.7).

Suppose we start to vary the phase $\zeta = e^{i\vartheta}$, the topology of the spectral network undergoes a discontinuous transition through a *critical* network at some phase ϑ_c . This transition is also known as a *flip* of triangulation or cluster *mutation* in the Fock-Goncharov picture [34]. In the critical network some \mathcal{S} -walls instead of flowing to a puncture connect two branching points (actually it could be the same branching point). A lift of the finite \mathcal{S} -wall is a closed path γ_c on Σ , then from (2.9) we define easily the critical phase:

$$\vartheta_c = \text{Arg } Z_{\gamma_c} \quad (2.35)$$

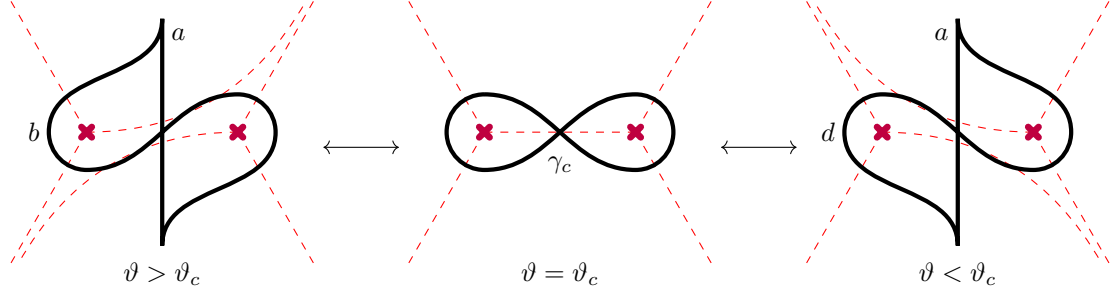


Figure 2.7: Flip

Let us calculate the parallel transport along the path a before and after the flip:

$$\begin{aligned} \mathfrak{U}_a^{(\vartheta > \vartheta_c)} &= \mathcal{Y}_{\tilde{a}^{(i)}} + \mathcal{Y}_{\tilde{b}^{(i)}} + \mathcal{Y}_{\tilde{a}^{(j)}} \\ \mathfrak{U}_a^{(\vartheta < \vartheta_c)} &= \mathcal{Y}_{\tilde{a}^{(i)}} + \mathcal{Y}_{\tilde{a}^{(j)}} + \mathcal{Y}_{\tilde{d}^{(j)}} \end{aligned} \quad (2.36)$$

Here $\tilde{a}^{(i)}$ is a lift of path a to sheet (i) and correspondingly for other paths and lifts.

Suppose a is continued somehow to a closed path, then we consider the same equations in the representation ρ to get expectation values of line defects:

$$\begin{aligned} \langle L(\vartheta > \vartheta_c) \rangle &= X_\gamma (1 + qX_{\gamma_c}) + X_\gamma^{-1} \\ \langle L(\vartheta < \vartheta_c) \rangle &= X_\gamma + X_\gamma^{-1} (1 + q^{-1}X_{\gamma_c}) \end{aligned} \quad (2.37)$$

One can represent the transition through this \mathcal{K} -wall as an action of \mathcal{K} -morphism on Fock-Goncharov coordinates:

$$\mathcal{K} : X_\gamma \mapsto X_\gamma (1 + qX_{\gamma_c}) \quad (2.38)$$

Comparing this factor to a factor from a gas of free BPS dyons (see for example [76, sec. 2.3]) one observes that under the flip a hypermultiplet of charge γ_c is bound to the line defect.

In a generic case when a halo of BPS particles of charge γ_h is bound to the line defect the corresponding \mathcal{K} -morphism reads:

$$\mathcal{K}_{\gamma_h}^{\Omega_{\gamma_h}(q)} : X_\gamma \mapsto X_\gamma \left[\prod_{m \in \mathbb{Z}} \prod_{m'=1-|\langle \gamma, \gamma_h \rangle|}^{|\langle \gamma, \gamma_h \rangle|-1} (1 + (-q)^m q^{m' - \langle \gamma, \gamma_h \rangle} X_{\gamma_h})^{a_m(\gamma_h)} \right]^{\text{sign} \langle \gamma, \gamma_h \rangle} \quad (2.39)$$

where powers $a_m(\gamma_h)$ are defined by the PSC of the BPS halo particle:

$$\Omega_{\gamma_h}(q) =: \sum_{m \in \mathbb{Z}} a_m(\gamma_h) (-q)^m \quad (2.40)$$

2.5.3 MS-walls and wall-crossing formulae

To describe MS-walls consider a collection of intersecting \mathcal{K} -walls on the extended moduli space (u, ζ) . For example assume we have two \mathcal{K} -walls corresponding to BPS particles of charges γ and γ'

(see fig.2.8), as we will see in a moment if intersection pairing for these charges reads $\langle \gamma, \gamma' \rangle = 1$ a new bound state of charge $\gamma + \gamma'$ appears in the joint. Projecting intersection locus to the moduli space we will get a MS-wall.

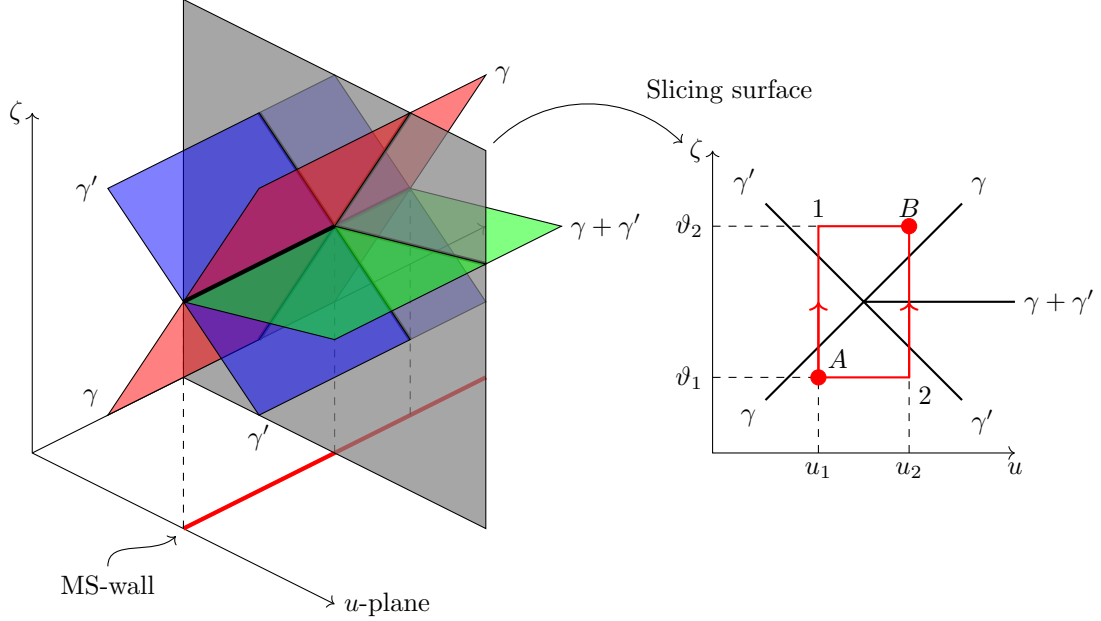


Figure 2.8: Wall-crossing

Let us choose some 1d path intersecting the MS-wall, considering different values of ζ we will get a slicing surface. We consider two points A and B , and two homotopic paths. Consider spaces \mathcal{X}_A and \mathcal{X}_B of *all* the line defects in points A and B correspondingly. We can go from point A to point B either along path 1 or along path 2, these two possibilities induce two distinguished composite morphisms:

$$\begin{array}{ccc}
 & \mathbf{S}(u_1; \vartheta_1, \vartheta_2) & \\
 \mathcal{X}_A & \begin{array}{c} \curvearrowright \\ \curvearrowleft \end{array} & \mathcal{X}_B \\
 & \mathbf{S}(u_2; \vartheta_1, \vartheta_2) &
 \end{array} \tag{2.41}$$

Since these morphisms are common for all the generators in the ring of IR dyonic operators we conclude:

$$\mathbf{S}(u_1; \vartheta_1, \vartheta_2) = \mathbf{S}(u_2; \vartheta_1, \vartheta_2) \tag{2.42}$$

These morphisms are also known as *spectrum generators* and can be written as composition of

elementary \mathcal{K} -wall morphisms:

$$\mathbf{S}(u; \vartheta_1, \vartheta_2) = \prod_{\vartheta_1 < \text{Arg } Z_{\gamma_c} < \vartheta_2} \mathcal{K}_{\gamma_c}^{\Omega_{\gamma_c}(a)} \quad (2.43)$$

where product goes over all the charges of BPS particles γ_c , and \mathcal{K} -morphisms are ordered in the product according to phases $\text{Arg } Z_{\gamma_c}$. So generically if none of BPS particle charge phase crosses either ϑ_1 or ϑ_2 the morphism $\mathbf{S}(u; \vartheta_1, \vartheta_2)$ is constant on the moduli space.

Equation (2.42) was first derived by Kontsevich and Soibelman [70, 71] in application to a construction of Donaldson-Thomas invariants for Calabi-Yau 3-folds.

As we see the \mathcal{K} -morphisms provide a flat parallel transport on the moduli space. We will exploit this fact in what follows when we consider knot invariants.

2.6 BPS spectrum of Kronecker quiver theory families

2.6.1 Spectral networks for Kronecker quivers

In addition to spectral networks, one alternative route to the BPS spectrum is the dual description in terms of quiver quantum mechanics [23, 76]. The problem of counting BPS states gets mapped into that of counting cohomology classes of moduli spaces of quiver representations. Quiver quantum mechanics arises as an effective theory on the BPS state world-line. The corresponding partition function representing PSC can be calculated by introducing Ω -background and following application of the localization technique [81]. Quivers are nicely encoding matter content of $\mathcal{N} = 4$ supersymmetric matrix quantum mechanics: quiver dimension vector $\gamma = \{n_i\}_{k=1}^N$ encodes gauge symmetry of the theory $\bigotimes_{k=1}^N U(n_i)$, vertices of the quiver represent vector multiplets of the gauge field, and, finally, each arrow between nodes i and j is assigned to chiral matter fields in representation $(\square, \bar{\square})$ of $U(n_i) \times U(n_j)$.

In this section we will provide results of calculating the PSC's in theories associated to a Kronecker quiver (see fig.2.10): these are quivers consisting of two nodes with p arrows directed from one node to the other.

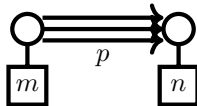


Figure 2.9: Kronecker quiver

This quiver with dimension vector (m, n) describes PSC's of BPS molecules consisting of m and

n “elementary dyons” with charges γ_1 and γ_2 with DZS pairing $\langle \gamma_1, \gamma_2 \rangle = p$. It is well-known that this system has just one MS-wall defined by a difference $\text{Arg } Z_{\gamma_1} - \text{Arg } Z_{\gamma_2}$. If this difference is less than 0 then only elementary BPS particles are presented, in the other chamber states of arbitrarily high spin are presented, moreover corresponding central charges form a dense cone on the complex plane [55]. So we expect the following wall-crossing formula:

$$\mathcal{K}_{\gamma_1} \mathcal{K}_{\gamma_2} = \mathcal{K}_{\gamma_2} \left[\prod_{(a,b) \in \mathbb{Z}^2} \mathcal{K}_{a\gamma_1 + b\gamma_2}^{\Omega_{a\gamma_1 + b\gamma_2}(q)} \right] \mathcal{K}_{\gamma_1} \quad (2.44)$$

where all products are taken in order of increasing central charge phase (when read from left to right).

A critical spectral network at certain phase $\zeta_c = e^{i\vartheta_c}$ gives a description of all \mathcal{K}_γ -walls such that $\text{Arg } Z_{\gamma_c} = \vartheta_c$, so we will describe simultaneously a ray of charges $n\gamma_c$, $n \in \mathbb{N}$. Let us adopt a useful notation for this problem, a morphism corresponding to all the morphisms on the concrete charge ray is defined as:

$$\mathfrak{R}_{\zeta_c} := \prod_{n \in \mathbb{N}} \mathcal{K}_{n\gamma_c}^{\Omega_{n\gamma_c}(q)} \quad (2.45)$$

The algebra of Fock-Goncharov variables (2.23) implies $X_{n\gamma} = X_\gamma^n$, so the ray morphism is still represented by some function $Q(X_\gamma)$ of one variable X_γ , in particular,

$$Q_{\zeta_c}(x) = \prod_{n \in \mathbb{N}} \prod_{m \in \mathbb{Z}} (1 + (-q)^m x^{mn})^{a_m(n\gamma)} \quad (2.46)$$

$$\mathfrak{R}_{\zeta_c} : X_\gamma \mapsto X_\gamma \prod_{m=1-|\langle \gamma, \gamma_c \rangle|}^{|\langle \gamma, \gamma_c \rangle|-1} Q_{\zeta_c}(q^{m-\langle \gamma, \gamma_c \rangle} X_{\gamma_c})^{\text{sign } \langle \gamma, \gamma_c \rangle}$$

A typical example of a Kronecker quiver MS-wall appears already in the super-Yang-Mills theory with gauge group pure $SU(3)$ and without chiral matter [51]. The corresponding UV curve \mathcal{C} is represented by a cylinder, the IR Seiberg-Witten curve Σ is a 3-fold cover of \mathcal{C} with four branching points. One can construct a family of critical spectral networks describing \mathfrak{R}_{ζ_c} -walls for the p -Kronecker quiver setup [52], see fig.2.10, we have depicted only critical \mathcal{S} -walls of finite length on this scheme. The critical spectral network is represented by p connected blocks. For a charge ray $(\alpha m, \alpha n)$, where α is integer and m and n are co-prime, the block consists of $m \times n$ cells. Each cell consists of a bunch of \mathcal{S} -walls squeezed to a single line in the critical phase, in a generic case there is an infinite number of \mathcal{S} -walls encrypted in this diagram. Blocks are glued to each other in one diagonal, as well they are glued around the cylinder according to marks A_i , B_i , so the critical \mathcal{S} -walls are winding around the cylinder p times. \mathcal{S} -walls of different types are denoted by different colors: (ij) and (ji) – blue, (jk) and (kj) – red, (ik) and (ki) – purple.

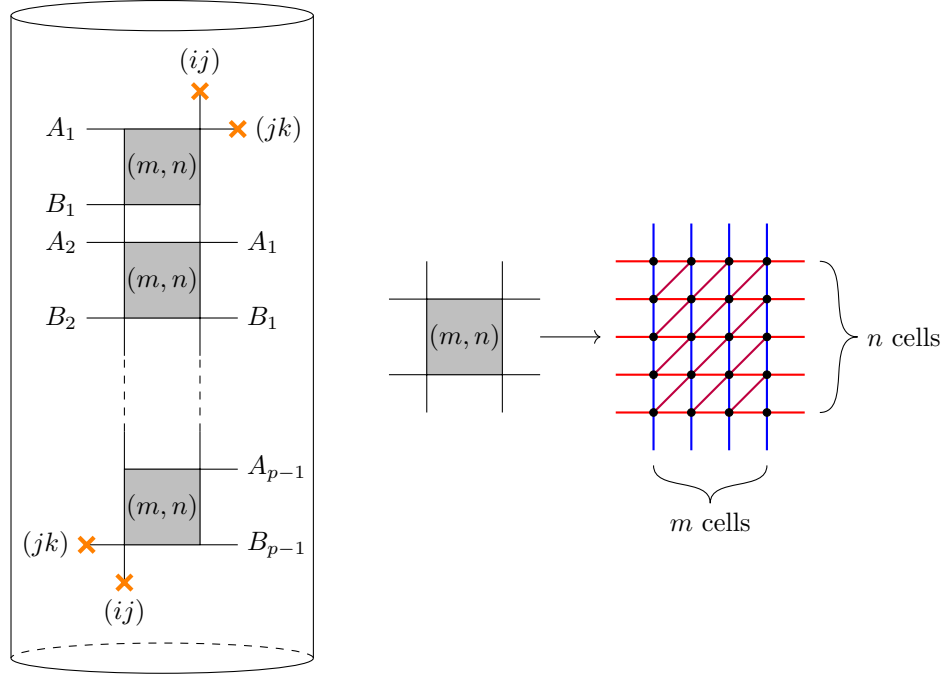


Figure 2.10: Spectral network for a family of Kronecker quivers

The spectral network technique allows one to calculate the \mathfrak{R}_{ζ_c} -morphism explicitly in terms of solutions to certain higher order functional equations. In the simplest case of a charge ray (α, α) this construction reads [52]:

$$Q(x, q) = \prod_{s=-\frac{p-1}{2}}^{\frac{p-1}{2}} P(xq^{2s}, q) \quad (2.47)$$

where function P is a solution of a functional equation:

$$P(x, q) = 1 + x \prod_{s=-(p-2)}^{p-2} P(xq^{2s}, q)^{p-1-|s|} \quad (2.48)$$

Boundary condition for this equation can be easily derived from the form of factors (2.39), indeed if we assume that all the variables X_γ tend to 0, then all these factors reduce to a factor 1, so we conclude:

$$P(0, q) = 1 \quad (2.49)$$

Let us consider solutions to this equation in some elementary cases.

$p = 1$. In this case the critical network is just a saddle. The functional equation is algebraic actually and can be solved explicitly:

$$P(x, q) = 1 + x \tag{2.50}$$

$$Q(x, q) = 1 + x$$

Comparing this expression to expansion (2.46) we see that this morphism is just a flip morphism we have encountered before. So this \mathcal{K} -wall corresponds to presence of a hypermultiplet in the BPS spectrum.

$p = 2$. In this case we get again an algebraic equation for P :

$$P(x, q) = (1 - x) \tag{2.51}$$

$$Q(x, q) = (1 - xq)(1 - xq^{-1}) \tag{2.52}$$

We conclude $\Omega(q) = q + q^{-1}$, and this means a vectormultiplet presented in the spectrum.

$p \geq 3$. Equation is no more purely algebraic. We can attempt to solve it perturbatively expanding the function P as Taylor series in variable x . Up to the second order the solution reads:

$$P(x, q) = 1 + x + \frac{q^{2(p-1)} + q^{-2(p-1)} - 2}{(q + q^{-1})^2 - 4} x^2 + O(x^3) \tag{2.53}$$

One can use this expansion to a very high order to confirm all the predicted PSC's coincide with ones derived by other methods [52]. For example, for charge $(1, 1)$ and generic p the PSC reads:

$$\Omega_p(q) = \frac{q^p - q^{-p}}{q - q^{-1}} \tag{2.54}$$

This quantity is also known as quantum number $[p]_q$ or a quantum dimension. This result can be simply reproduced in the multi-centered model of BPS states [23, 76]. In this case the configuration is represented by a ‘‘Hall atom’’: a pair of two dyons with DZS pairing p , or just an electron and a monopole of magnetic charge p . Ground states in this system are given by $p + 1$ Landau levels on a sphere, due to interaction of the electron spin with magnetic field of the monopole levels are lifted, so there are p ground states that fall nicely into a representation of spin $SU(2)$ and give a quantum dimension of this representation as PSC [23].

2.6.2 Remarks on BPS dynamics

We can suppress the chemical potential substituting $q = -1$ and returning BPS index instead of PSC, then equation (2.48) becomes algebraic:

$$P(x) = 1 + xP(x)^{(p-1)^2} \tag{2.55}$$

This equation had been identified previously by Kontsevich and Soibelman [70] and by Gross and Pandharipande [55], as the one governing the generating function of BPS degeneracies. A surprising physical conclusion appears when one considers asymptotic behavior of the BPS index with the charge growing [94]:

$$\Omega_{(n,n)} \sim e^{c_p n}, \quad c_p = (p-1)^2 \log(p-1)^2 - (p-2) \log(p-2) \quad (2.56)$$

On the other hand we can estimate the entropy, a logarithm of a number of degrees of freedom stored in a box of volume V and in the momentum space below energy level E in a generic asymptotically free theory:

$$S = \kappa V^{\frac{1}{4}} E^{\frac{3}{4}} \quad (2.57)$$

where κ is a non-universal constant depending on the theory. The BPS index is a signed sum over distinguished degrees of freedom, it can not exceed the whole number of degrees of freedom. Implying that the central charge grows linearly with the electro-magnetic charge one gets an apparent paradox:

$$\Omega \sim e^{\kappa n} \lesssim e^S \sim e^{\tilde{\kappa} n^{\frac{3}{4}}} \quad (2.58)$$

The resolution of this paradox comes from taking into account the fact that our bound applies only to the theory in a finite volume. If the size of BPS states becomes large enough and they do not fit into the box of finite volume, then they do not contribute to the naive counting of degrees of freedom.

Using the multi-centered model of BPS molecules one can make a simple estimate of an effective size of a these molecules. Suppose it consists of “elementary” BPS particles of charges γ_1 and γ_2 , then the size of the molecule is constrained from below:

$$r_{\text{molecule}} \geq \frac{\langle \gamma_1, \gamma_2 \rangle}{2\text{Im}(Z_{\gamma_1} \bar{Z}_{\gamma_2})} |Z_{\gamma}| \quad (2.59)$$

where Z_{γ} is a total central charge of the molecule. For a molecule given by a dimension vector (n, n) $Z_{\gamma} = n(Z_{\gamma_1} + Z_{\gamma_2})$. So the volume of the box suitable to include a molecule scales as $V \sim V_0 n^3$. Eventually, we have to revise the entropy bound:

$$S(n) \sim e^{\tilde{\kappa} n^{\frac{3}{2}}} \quad (2.60)$$

And this revised bound resolves the paradox.

The BPS particles preserve massive little subgroup of the Lorentz group of space-time transformations. So PSC of a physical state naturally decomposes over characters of spin $SU(2)$. This

implies the PSC's are invariant under the change $q \leftrightarrow q^{-1}$ of the chemical potential. Spin $SU(2)$ can be associated to Lefschetz $SU(2)$ acting on quiver representation cohomology [23]. Generically, we associate the PSC to a Poincaré polynomial⁴ of this cohomological group:

$$\Omega_\gamma(q) = q^{-2J_{\max}(\gamma)} \chi_\gamma(q) \quad (2.61)$$

where J_{\max} is the highest admissible spin of the corresponding quiver variety, a charge-dependent bound on this quantity is known as Kac's theorem (see [88]).

Quiver Poincaré polynomials reveal a specific pattern first noticed by Reineke [87]. With growing charge the polynomial tails start to stabilize, for example, for $p = 3$:

$$\begin{aligned} \chi_{(4,3)}(q) &= 1 + q^2 + 3q^4 + 5q^6 + 8q^8 + 10q^{10} + 12q^{12} + 12q^{14} + O(q^{16}) \\ \chi_{(7,6)}(q) &= 1 + q^2 + 3q^4 + 5q^6 + 10q^8 + 16q^{10} + 29q^{12} + 43q^{14} + O(q^{16}) \\ \chi_{(8,6)}(q) &= 1 + q^2 + 3q^4 + 5q^6 + 10q^8 + 16q^{10} + 29q^{12} + 45q^{14} + O(q^{16}) \\ \chi_{(8,7)}(q) &= 1 + q^2 + 3q^4 + 5q^6 + 10q^8 + 16q^{10} + 29q^{12} + 45q^{14} + O(q^{16}) \end{aligned} \quad (2.62)$$

The limiting polynomial this sequence converges to is expected to be a Poincaré polynomial of the classifying space $B(GL_n \times GL_n/\mathbb{C}^*)$ where \mathbb{C}^* is a subgroup of elements $(\lambda\mathbb{I}, \lambda^{-1}\mathbb{I})$ [30].

We will reproduce Kac's theorem bound and the limiting polynomial from the functional equation (2.48) following [52].

Let us search for a solution to (2.48) in terms of a Taylor expansion

$$P^{(p)}(x, q) = \sum_{n=0} \omega_n^{(p)}(q) x^n \quad (2.63)$$

The contribution to a particular Taylor coefficient in front of z can be represented as a sum over partitions $t_{s,j}$. We label non-negative integers $t_{s,j}$ by a pair of integers (s, j) ; s corresponds to a contribution of a term with a shift controlled by s in (2.48), while j distinguishes formally between the terms with the same s gathered into powers in (2.48). We sum over all possible values of $t_{s,j}$ inserting a Kronecker symbol, so that only a few contribute. The recursion relation reads

$$\omega_k^{(p)}(q) = \sum_{t_{s,j}=0}^{\infty} q^{2 \sum_{s,j} s t_{s,j}} \left(\prod_{s=-(p-2)}^{p-2} \prod_{j=1}^{p-1-|s|} \omega_{t_{s,j}}^{(p)}(q) \right) \delta_{k-1, \sum_{s,j} t_{s,j}} \quad (2.64)$$

The highest power of q is contributed by $t_{p-2,1} = k-1$ with all the others t 's set to zero, therefore we may recast the above as a recursion relation for the the maximal power α_k for q in $\omega_k^{(p)}(q)$, together with a boundary condition:

$$\alpha_k = \alpha_{k-1} + 2(p-2)(k-1), \quad \alpha_1 = 0 \quad (2.65)$$

⁴ It would be more precise to call this quantity a χ_y -genus, though if the moduli space is smooth it can be identified with the Poincaré polynomial (see the discussion in [22, section 2.5]).

which is solved by

$$\alpha_k = (p-2)k(k-1). \quad (2.66)$$

Since Q is related to P by (2.47), the highest power of q in the coefficient of z^k is $\alpha_k + (p-1)k$.

Hence, finally, the highest spin for the (n, n) state reads

$$2J_{\max}(n) + n - 1 = \alpha_n + (p-1)n \quad (2.67)$$

This entails a beautiful agreement of our formula (2.48) with previously known results from quiver representation theory

$$2J_{\max}(n) = (p-2)n^2 + 1 \quad (2.68)$$

Now we switch to calculation of the limiting polynomial. As a preliminary remark, notice that the expansion of the products in the generating function allows one to relate coefficients in the formal series to the PSC

$$\omega_n^{(p)}(q) = q^{\alpha_n - 2J_{\max}(n)} \frac{1 - q^{2n}}{1 - q^2} \Omega^{(p)}(q, n\gamma_c) \left(1 + O(q^{(p-1)n})\right) \quad (2.69)$$

and by $O(q^p)$ we denote a formal series in q , starting with a term of degree p .

Introducing the series

$$\tilde{\chi}_n^{(p)}(y) := y^{-(p-2)n(n-1)} \omega_n^{(p)}(y) \quad (2.70)$$

we can focus on its stabilization since (assuming $|q| < 1$)

$$\begin{aligned} \lim_{n \rightarrow \infty} \tilde{\chi}_n^{(p)}(q) &= (1 - q^2)^{-1} \chi_{\infty(1,1)}^{(p)}(y), \\ \lim_{p \rightarrow \infty} \tilde{\chi}_n^{(p)}(q) &= \frac{1 - q^{2n}}{1 - q^2} \chi_{(n,n)}^{(\infty)}(q). \end{aligned} \quad (2.71)$$

Performing the substitution $\omega_n^{(p)}(q) \mapsto \tilde{\chi}_n^{(p)}(q)q^{(p-2)n(n-1)}$, $s \mapsto s - (p-2)$ into (2.64) we arrive at the following recursion relation

$$\begin{aligned} \tilde{\chi}_k^{(p)}(q) &= \sum_{t_{s,j}=0}^{\infty} q^{2 \sum_{s,j} s t_{s,j} + (p-2) \sum_{(s,j) \neq (s',j')} t_{s,j} t_{s',j'}} \times \\ &\times \left(\prod_{s=0}^{2(p-2)} \prod_{j=1}^{p-1-|s-(p-2)|} \tilde{\chi}_{t_{s,j}}^{(p)}(q) \right) \delta_{k-1, \sum_{s,j} t_{s,j}} \end{aligned} \quad (2.72)$$

where the second summation in the power of q goes over different pairs of indices. In the limit $p \rightarrow \infty$, precisely that summation causes a *localization* (assuming $|q| < 1$ and noticing that the power is non-negative) on partitions of $k-1$ satisfying $\sum_{(s,j) \neq (s',j')} t_{s,j} t_{s',j'} = 0$, these are partitions

consisting of just one $t_{s,j} = k - 1$ with all the others being zero. Thus we are eventually left with a summation over positions (s, j)

$$\tilde{\chi}_k^{(\infty)}(q) = \sum_{s=0}^{\infty} (1+s) q^{2s(k-1)} \tilde{\chi}_{k-1}^{(\infty)}(q). \quad (2.73)$$

This reproduces the result known from quiver representation theory, the corresponding limiting Poincaré series read

$$\chi(q) = \frac{1 - q^2}{\prod_{j=1}^{\infty} (1 - q^{2j})^2} \quad (2.74)$$

Chapter 3

Application to knot homology

3.1 Homology origin in QFT: brief SUSY QM overview

We make a brief review of the origin of the cohomology in supersymmetric quantum mechanics following [96] (see also reviews in [47, 59]).

We consider the supersymmetric quantum mechanics of a particle moving in a Riemann manifold \mathcal{M} of dimension n with Euclidean metric g .

The Lagrangian of this system is given by

$$L = \frac{1}{2}g_{ij}\dot{x}^i\dot{x}^j + \frac{i}{2}g_{ij}(\bar{\psi}^i\nabla_t\psi^j - \nabla_t\bar{\psi}^i\psi^j) - \frac{1}{2}R_{ijkl}\psi^i\bar{\psi}^j\psi^k\bar{\psi}^l - \frac{1}{2}g_{ij}\partial_i h\partial_j h - \nabla_i\partial_j h\bar{\psi}^i\psi^j \quad (3.1)$$

where

$$\nabla_t\psi^i = \partial_t\psi^i + \Gamma_{jk}^i\dot{x}^j\psi^k, \quad \nabla_i\partial_j h = \partial_i\partial_j h - \Gamma_{ij}^k\partial_k h, \quad (3.2)$$

and R_{ijkl} and Γ_{ij}^k are the Riemann tensor and the Cristoffel symbols correspondingly on the manifold \mathcal{M} . And the function of coordinates h is recognized as a Morse height function with a non-degenerate Hessian in extrema points.

The supersymmetric quantum mechanics action is invariant under infinitesimal SUSY transformations:

$$\begin{aligned} \delta\phi^i &= \epsilon\bar{\psi}^i - \bar{\epsilon}\psi^i \\ \delta\psi^i &= \epsilon(i\dot{x}^i - \Gamma_{jk}^i\bar{\psi}^j\psi^k + g^{ij}\partial_j h) \\ \delta\bar{\psi}^i &= \bar{\epsilon}(-i\dot{x}^i - \Gamma_{jk}^i\bar{\psi}^j\psi^k + g^{ij}\partial_j h) \end{aligned} \quad (3.3)$$

One can calculate supercharges as corresponding Noether currents:

$$Q = e^{-h}\bar{\psi}^i\frac{\partial}{\partial x^i}e^h, \quad \bar{Q} = e^h\psi^i\frac{\partial}{\partial x^i}e^{-h} \quad (3.4)$$

Identifying fields ψ^i with 1-forms dx^i on the manifold \mathcal{M} we see that supercharges behave as conjugated differentials:

$$Q = e^{-h} d e^h =: d_h, \quad \bar{Q} = e^h d^\dagger e^{-h} =: d_h^\dagger \quad (3.5)$$

The Hamiltonian in this system is a conjugated Laplace operator:

$$\mathcal{H} = \frac{1}{4} \left(d_h d_h^\dagger + d_h^\dagger d_h \right) \quad (3.6)$$

The Hilbert space of ground states is identified with the space of harmonic forms on \mathcal{M} with respect to Laplacian \mathcal{H} . The Hodge decomposition theorem (see e.g.[54]) implies the space of harmonic forms is isomorphic to the cohomology $H^\bullet(\mathcal{M}, d_h)$. Though the conjugation e^h can be considered as an invertible chain-map (we will return to its role in sec.3.5.3) preserving cohomology

$$H^\bullet(\mathcal{M}, d_h) \cong H^\bullet(\mathcal{M}, d_{h'}) \quad (3.7)$$

so cohomology of the supercharge Q coincides with the deRahm cohomology of \mathcal{M} .

If we consider an opposite limit when the height function scales as $h \rightarrow \lambda h$, $\lambda \rightarrow \infty$ the ground states are localized near critical points of h where the potential term $g_{ij} \partial_i h \partial_j h$ vanishes. Near a critical point x_* choose coordinates x^I , s.t.

$$h = h(x_*) + \sum_I c_I (x^I)^2 + O(|y|^3) \quad (3.8)$$

c_I are eigen values of the Hessian of h in point x_* , they are non-zero in our setup.

In this coordinates the Hamiltonian in the neighbourhood of the critical point x_* can be decomposed as

$$H = \frac{1}{2} \sum_I [p_I^2 + \lambda^2 c_I (x^I)^2 + \lambda c_I [\bar{\psi}^I, \psi^I]] \quad (3.9)$$

If we denote by $|0\rangle$ a vector annihilated by all ψ^I we can determine the ground states up to the leading order in the perturbation theory in the following way:

$$\Psi_{x_*}^{(0)} = e^{-\lambda \sum_I |c_I| (x^I)^2} \prod_{J: c_J < 0} \bar{\psi}^J |0\rangle \quad (3.10)$$

Non-perturbative corrections due to instantons deform Q -matrix elements to be generically non-zero. So one defines a Morse-Smale-Witten (MSW) complex as a vector space spanned by perturbative ground state wave functions¹:

$$\mathbb{M} = \bigoplus_{x_*} \mathbb{C} \left[\Psi_{x_*}^{(0)} \right] \quad (3.11)$$

¹Here we used as an underlying ring the complex field \mathbb{C} since the complex structure is naturally inherited from the complex structure of the Hilbert space. See also footnote 7 on page 102.

Its cohomology $H^\bullet(\mathbb{M}, Q)$ is isomorphic to $H^\bullet(\mathcal{M}, d_h)$, so to the deRahm cohomology.

We can use $H^\bullet(\mathbb{M}, Q)$ as a homotopy invariant of functions h . And we will exploit this point of view in what follows. To put Landau-Ginzburg theory on a similar footing one considers the target space of the SLG model \mathcal{X} as a real space [47] parameterized by real coordinates u^a . The height function on LG fields reads:

$$h = - \int_D dx \left[\lambda_a \frac{du^a}{dx} - \frac{1}{2} \text{Re}(\zeta^{-1} W) \right] \quad (3.12)$$

where $\lambda = \lambda_a du^a$ is a locally defined form $d\lambda = \frac{i}{2} g_{i\bar{j}} d\phi^i \wedge d\bar{\phi}^{\bar{j}}$.

We will be able to associate knot(link) embeddings to interfaces in so called supersymmetric Yang-Yang-Landau-Ginzburg theory, therefore knot homotopy will be translated to homotopy of the interface and the height function h . Derived in this way a Hilbert space of true interface ground states is expected to be a knot (link) invariant.

3.2 Holomorphic reduction: Ward identities, Yang-Yang functional and conformal blocks

Similarly to the discussed model of supersymmetric quantum mechanics the supersymmetric Landau-Ginzburg theory also can be approached in two limits.

The Euclideanized Landau-Ginzburg action is almost \mathbb{Q}_ζ -exact:

$$S = \{\mathbb{Q}_\zeta, \mathcal{V}\} + 2\beta \text{Re}(\zeta^{-1} Z) \quad (3.13)$$

So we rewrite the partition function as a generalized path integral in this model on a cylinder (see fig.1.1):

$$\mathcal{Z}_{\alpha'\alpha}[u] = \int_{\substack{\phi(T=-\infty)=\varphi_\alpha \\ \phi(T=\infty)=\varphi_{\alpha'}}} [\mathcal{D}\phi][\mathcal{D}\psi] e^{u\{\mathbb{Q}_\zeta, \mathcal{V}\} + 2\beta \text{Re}(\zeta^{-1} Z)} \quad (3.14)$$

Here ϕ_α and $\phi_{\alpha'}^*$ are quasi-classical solutions corresponding to ground states $|\alpha\rangle$ and $\langle\alpha'|$ on a cylinder. According to the usual localization philosophy the generalized partition function is independent of u and coincides with expression (1.43). Therefore we consider two natural limits:

- Quasi-classical limit $u \rightarrow \infty$. In this limit quasi-classical solutions giving minimum to the action contribute, and quantum fluctuations around these solutions are suppressed, so the partition function reduces to a sum over all the quasi-classical trajectories weighted with the

action and one-loop determinant:

$$\mathcal{Z}_{\alpha'\alpha} = \sum_{s \in \mathfrak{S}_{\alpha'\alpha}(-i\zeta)} e^{\beta\zeta^{-1}Z_s + \beta\zeta\bar{Z}_s} \Delta_s \quad (3.15)$$

Notice in this case the classical equation of motion coincides with the soliton equation (1.31) up to a rotated phase ζ , so we used a set of soliton solutions $\mathfrak{S}_{\alpha'\alpha}(-i\zeta)$. The contribution of one-loop determinants is captured by Δ_s .

- Alternative limit $u \rightarrow 0$ “kills” all the dynamics and leads to just an integral over boundary field values:

$$Z_{\alpha'\alpha} = \int \Omega_{\alpha'} \wedge \Omega_{\alpha} e^{2\beta \operatorname{Re}(\zeta^{-1}\Delta W)} \quad (3.16)$$

Here Ω 's are middle-dimensional forms on the Kähler manifold \mathcal{X} corresponding to vacuum states [60]. Generically vacuum state functions are difficult to define. We will not use their explicit form, so we do not specify them.

These expressions might seem too trivial to be real partition functions of a physical model. In the first expansion (3.15) complications come from the determinant Δ_s , in the case when α and α' are the same vacuum and no soliton jumps are presented this determinant should coincide with a diagonal component of so called Zamolodchikov metric that is far from being flat, and even in the simplest case of cubic superpotential W it is represented by Painlevé transcendents (see [18]). On the other hand complications in expansion (3.16) are represented by choice of specific forms Ω as we have mentioned.

Here we will apply a *holomorphic reduction trick* we have already encountered in the beginning of chapter 2 in the Hitchin system consideration. Initially ζ was a complex phase confined to a unit circle. Now let us continue analytically ζ to $\zeta \in \mathbb{C}^\times$. Thus we define two complex variables $\lambda = \beta\zeta^{-1}$ and $\tilde{\lambda} = \beta\zeta$ (let us remind that β is a circumference of a compactified dimension so it is positive real). In this way we rewrite tt^* -connection (1.45) and (1.46):

$$\nabla_i = \partial_{t_i} + A_i - \lambda C_i \quad (3.17)$$

$$\bar{\nabla}_i = \partial_{\bar{t}_i} + \bar{A}_i - \tilde{\lambda} \bar{C}_i \quad (3.18)$$

as well as its flat section – partition function – in two ways:

- A sum over solitons (3.15):

$$\mathcal{Z}_{\alpha\alpha'} = \sum_{s \in \mathfrak{S}_{\alpha\alpha'}(-i\lambda)} e^{\lambda Z_s + \tilde{\lambda} \bar{Z}_s} \Delta_s \quad (3.19)$$

It is important to notice that the set $\mathfrak{S}_{\alpha\alpha'}(x)$ depends only on the phase of x , rather than on its absolute value.

- An integral (3.16):

$$\mathcal{Z}_{\alpha\alpha'} = \int \Omega_{\alpha} \wedge \Omega_{\alpha'} e^{\lambda\Delta W + \bar{\lambda}\Delta\bar{W}} \quad (3.20)$$

From now on we will consider a **holomorphic** limit:

$$\beta, \zeta \rightarrow 0, \quad \tilde{\lambda} \rightarrow 0, \quad \lambda \sim \text{const} \quad (3.21)$$

In this limit the Berry curvature on the vacuum bundle vanishes, so we can choose the connection to be just flat. In this case the partition function can be considered as a flat section of just tt^* -connection holomorphic part (we will call it holomorphically reduced tt^* -connection):

$$(\partial_{t_i} + \lambda C_i)\mathcal{Z}[t] = 0 \quad (3.22)$$

Following [60] form Ω becomes just purely holomorphic form. Indeed an integral (called brane amplitude)

$$\Pi = \int D\phi e^{\lambda W(\phi)} \quad (3.23)$$

where we used a simple measure $D\phi = \prod_i d\phi_i$ satisfies (3.22) as we will see further.

As well a simplification appears in the sum over solitons. In the limit $\beta \rightarrow 0$ only zero frequency modes around the soliton background (1.31) contribute. This contribution can be reexpressed in terms of a fermion number f_s :

$$\Delta_s = e^{\pi i f_s + O(\beta)} \quad (3.24)$$

If we substitute the expression for the sum over solitons into tt^* -equations and again consider the holomorphic limit, we will get equations for the soliton action:

$$\text{Det}(\partial_{t_i} Z_s \mathbf{1} - C_i) = 0 \quad (3.25)$$

This equation implies existence of a zero eigen vector $\Lambda_s[t_i]$ (in a generic position (away from branching points) all the eigenvalues are distinct so there is just one zero eigenvalue, therefore just one dimensional null-space):

$$(\partial_{t_i} Z_s \mathbf{1} - C_i)\Lambda_s[t_i] = 0 \quad (3.26)$$

Then we can determine the fermion number through a scalar product:

$$\partial_{t_i}(\pi i f_s) = -\frac{\Lambda_s^\dagger \partial_{t_i} \Lambda_s}{\Lambda_s^\dagger \Lambda_s} \quad (3.27)$$

Thus we expect the following asymptotic behavior in the limit $\lambda \rightarrow \infty$ from the solution to (3.22):

$$\mathcal{Z}_{\alpha\alpha'} = \sum_{s \in \mathfrak{S}_{\alpha\alpha'}(-i\lambda)} e^{\lambda Z_s[t_i] + \pi i f_s[t_i] + O(\lambda^{-1})} \quad (3.28)$$

Indeed, substituting this asymptotics into (3.22) and expanding we return to equations (3.26) and (3.27).

Notice that we can get different vacuum amplitudes by acting with chiral fields Φ_i as well we can choose different integration contours \mathcal{L}_J in the boundary amplitude (3.23). So consider a generic brane amplitude:

$$\Pi_i^J[t] := \int_{\mathcal{L}_J} D\phi \Phi_i(\phi) e^{\lambda W(\phi)} \quad (3.29)$$

Let \mathcal{L}_J be a Lefschetz thimble defined in a generic position as an integration path going through the J -th critical point of the function W along the steepest descend path given by the soliton equation (1.31) and going away on its ends to singularities where the exponent starts to diverge (this might be the same singularity, say, ∞).² The basis of the chiral ring is expected to have the same dimensionality as the number of quasi-classical vacua: the number of W -critical points. The same is the number of independent Lefschetz thimbles \mathcal{L}_J . Therefore linearly independent flat sections (3.29) form a non-degenerate **square** matrix Π_i^J . Having this matrix we can reconstruct holomorphically reduced tt^* -connection as a Berry connection:

$$\nabla_i = \partial_{t_i} - (\partial_{t_i} \Pi) \Pi^{-1} \quad (3.30)$$

Now let us explain briefly why (3.29) is a generic flat section of holomorphically reduced tt^* -connection. We suppress the index J assuming Π to be a column with arbitrary choice of the Lefschetz thimble.

We can calculate

$$\partial_{t_i} \Pi_j[t] = \lambda \int_{\mathcal{L}} D\phi \Phi_i(\phi) \Phi_j(\phi) e^{\lambda W(\phi)} \quad (3.31)$$

The equivalence of the chiral ring to $\mathbb{C}[\phi_1, \dots, \phi_n] / \langle \partial_{\phi_i} W \rangle$ implies in turn

$$\Phi_i(\phi) \Phi_j(\phi) = C_{ij}^k \Phi_k(\phi) + \sum_p h_p \partial_{\phi_p} W(\phi) \quad (3.32)$$

²One distinguishes left and right Lefschetz thimbles different by imposing a condition on the trajectory to approach critical value either at spatial $-\infty$, or $+\infty$ correspondingly. For distinctness we choose left Lefschetz thimbles.

Where h_p are some constants independent of ϕ . Substituting it back we notice that the terms proportional to h_p cancel out due to the Stokes theorem, so the wave function Π_i satisfies

$$\boxed{\partial_{t_i} \Pi_j[t] = \lambda C_{ij}^k \Pi_k[t]} \quad (3.33)$$

Generally tt^* -connection is also called Lax tt^* -connection implying relation to integrable models. The very representation (3.16) implies a presence of a hierarchy of differential equations like flat section condition (1.45) derived via Ward identities or so called Schwinger-Dyson equations when we use invariance of the integral with respect to change of integration variables. Let us see how it works in the case of holomorphically reduced tt^* -connection.

Indeed, notice the integrals (3.29) are invariant under change of variables $\phi_i \rightarrow \phi_i + \epsilon f(\phi_i)$ where f is an arbitrary function and ϵ is a small parameter. Expanding them in ϵ we derive an infinite hierarchy of Ward identities:

$$\sum_i \int_{\mathcal{L}} D\phi (f'(\phi_i) \Phi_k(\phi) + f(\phi_i) [\lambda \partial_{\phi_i} W \Phi_k(\phi) + \partial_{\phi_i} \Phi_k(\phi)]) e^{\lambda W(\phi)} = 0 \quad (3.34)$$

Now we can expand the integrand over chiral fields:

$$\begin{aligned} & \sum_i (f'(\phi_i) \Phi_k(\phi) + f(\phi_i) [\lambda \partial_{\phi_i} W + \partial_{\phi_i} \Phi_k(\phi)]) = \\ & = D_0(t) + \sum_i D_i(t) \Phi_i(\phi) + \sum_p m_p(t) \partial_{\phi_p} O_p(t, \phi) \end{aligned} \quad (3.35)$$

here $D_i(t)$ are coefficients of this expansion, some combinations of chiral ring structure constants. The last term drops out by Stokes, while the remaining ones give a collection of differential equations:

$$\left(D_0(t) + \sum_i D_i(t) \partial_{t_i} \right) \Pi[t] = 0 \quad (3.36)$$

These equations give a holomorphic connection on the same space of wave functions $\Pi_i[t]$ so we conclude:

$$\boxed{\text{reduced } tt^* \text{-equations are } \mathbf{equivalent} \text{ to Ward identities}}$$

Example. Let us illustrate this simple statement by a simple example: the Airy function. Consider the following superpotential

$$W = \frac{1}{3} \phi^3 - z\phi \quad (3.37)$$

In this case the chiral ring reads:

$$\frac{\mathbb{C}[\phi]}{\langle \phi^2 = z \rangle} \simeq \mathbb{C}[1] \oplus \mathbb{C}[\phi] \quad (3.38)$$

The chiral ring is generated by two chiral fields $\mathbf{1}$ and ϕ with the following structure constants:

$$\mathbf{1} \circ \mathbf{1} = \mathbf{1}, \quad \mathbf{1} \circ \phi = \phi \circ \mathbf{1} = \phi, \quad \phi \circ \phi = z \mathbf{1} \quad (3.39)$$

In this case it is simple to construct holomorphically reduced tt^* -connection. We choose the following column of the partition functions:

$$\Pi(z) = \begin{pmatrix} \langle \psi | \mathbf{1} \rangle \\ \langle \psi | \phi \rangle \end{pmatrix} \quad (3.40)$$

Just substituting the corresponding values of of structure constants we get the following tt^* -connection:

$$\partial_z Z(z) = -\lambda \begin{pmatrix} 0 & 1 \\ z & 0 \end{pmatrix} Z(z) \quad (3.41)$$

Notice this equation is equivalent to the Airy equation:

$$[\lambda^{-2} \partial_z^2 - z] \langle \psi | \mathbf{1} \rangle = 0 \quad (3.42)$$

Airy equation can be easily derived through the Ward identities for the Airy integral, indeed,

$$\text{Ai}(z) = \int_{\mathcal{L}} d\phi e^{\lambda \left(\frac{\phi^3}{3} - z\phi \right)} \quad (3.43)$$

Where \mathcal{L} is one of Lefschetz thimbles, it does not matter which one we choose since integrals with both choices satisfy the same differential equation, nevertheless different choices of the integration cycle would give some linear combination of two Airy functions $\text{Ai}(z)$ and $\text{Bi}(z)$. Making substitution $\phi \rightarrow \phi + \epsilon$ and expanding in ϵ we get

$$\int_{\mathcal{L}} d\phi (\phi^2 - z) e^{\lambda \left(\frac{\phi^3}{3} - z\phi \right)} = 0 \quad (3.44)$$

The term ϕ^2 can be mimicked by an action of the second derivative, so we arrive to the Airy equation:

$$[\lambda^{-2} \partial_z^2 - z] \text{Ai}(z) = 0 \quad (3.45)$$

Let us consider the following family of superpotentials

$$W = - \sum_{i=1}^N \log(z - \phi_i) + 2 \sum_{1 \leq i < j \leq N} \log(\phi_i - \phi_j) + \sum_{i=1}^N V(\phi_i, q_a) \quad (3.46)$$

Here we have N Landau-Ginzburg *indistinguishable* fields and put them into a common holomorphic potential $V(\phi, q_a)$ with parameters q_a and experiencing 2d Coulomb interaction. Actually this choice is related to an integrability of 2d Coulomb gas model.

Following our logic instead of explicit calculation of structure constants and holomorphically reduced tt^* -connection let us consider differential equations arising from Ward identities on the integral representation. In the particular case of the Coulomb-gas-like potential (3.46) we have the following Ward identities:

$$\left[\lambda^{-1} \partial_z^2 - V'(z) \partial_z + \sum_a D^a(z, q) \partial_{q_a} \right] Z(z, q) = 0 \quad (3.47)$$

Where D^a are meromorphic functions of z , q_a depending on explicit form of the potential V . Here we do not specify boundary vacua for the partition function since as we expect the same differential equation for all the vacua choices. A detailed derivation of this equation is postponed to Appendix D. This equation can be easily reformulated as a connection component ∇_z on the parameter space. So will refer to it as **holomorphically reduced tt^* -connection** for this family of Landau-Ginzburg models.

To proceed to the knot theory we would like to choose a concrete family of Yang-Yang potentials:

$$V(\phi, q_a) = - \sum_a k_a \log(\phi - q_a) \quad (3.48)$$

And eventually in the Yang-Yang case we arrive to the following partial differential equation:

$$\left[\lambda^{-1} \partial_z^2 + \left(\sum_a \frac{k_a}{z - q_a} \right) \partial_z - \sum_a \frac{1}{z - q_a} \partial_{q_a} \right] \Pi_0(z, q) = 0 \quad (3.49)$$

Making a new substitution

$$\Pi_0(z, q) =: \left(\prod_{a < b} (q_a - q_b)^{-\frac{k_a k_b}{2}} \right) \left(\prod_a (z - q_a)^{-\frac{\lambda}{2} k_a} \right) \Xi(z, q) \quad (3.50)$$

We derive for the wave function Ξ the following equation:

$$\left[\lambda^{-1} \partial_z^2 - \sum_a \left(\frac{1}{2} \frac{k_a(k_a + 1)}{(z - q_a)^2} + \frac{1}{z - q_a} \partial_{q_a} \right) \right] \Xi(z, q) = 0 \quad (3.51)$$

Thus the chiral part of the partition function takes values in the space of Liouville conformal blocks in CFT with central charge $c = 1 - 6(\lambda^{1/2} - \lambda^{-1/2})^2$ [10, 101].

$$\Xi(z, q) = \left\langle \Phi_{(2,1)}(z) \prod_a V_{\Delta_a}(q_a) \right\rangle, \quad \Delta_a = \frac{k_a(k_a + 1)}{2} \quad (3.52)$$

In sec.3.4 we will explain how we use this connection to construct knot invariants.

Now let us use the Ward identities corresponding to the holomorphically reduced tt^* -connection in the models of class (3.46) to extract information about solitons in these models. Indeed the expansion over soliton solutions (3.28) should give an alternative representation of the brane amplitude:

$$\Pi[z, q_a] = \sum_{\mathfrak{s} \in \mathfrak{S}} c_{\mathfrak{s}} e^{\lambda W_{\mathfrak{s}}[z, q_a] + \pi i f_{\mathfrak{s}}[z, q_a] + O(\lambda^{-1})} \quad (3.53)$$

In this expansion we do not know the space of solutions \mathfrak{S} , neither expansion constants c_s . Nevertheless we can substitute this expansion into (3.47) and derive following equations for exponent argument in the limit $\lambda \rightarrow \infty$:

$$(\partial_z \Delta W_s)^2 - V' \partial_z \Delta W_s + \sum_a D^a \partial_{q_a} \Delta W_s = 0 \quad (3.54)$$

$$(2\partial_z \Delta W_s - V') \partial_z (\pi i f_s) + \partial_z^2 \Delta W_s + \sum_a D^a(z, q_a) \partial_{q_a} (\pi i f_s) = 0 \quad (3.55)$$

So to determine what soliton solutions are presented in the spectrum and do contribute to the partition function we should solve the first equation. The corresponding solution would give a central charge of the corresponding soliton. And the fermion number of the found soliton can be calculated from the second equation.

At this stage these equations are not very illuminating since they are still partial differential equations and to determine their solution we have to impose boundary conditions on a complex co-dimension 1 surface in the parameter space unless we can simplify it or we know an exact solution to the initial equation like in RCFTs. In what follows we will consider a specific limit simplifying these equations.

3.3 Spectral networks categorification

Before going to description of the categorification process let us remind what an inverse process, *decategorification*, should do. Decategorification suppresses notion of the Poincaré polynomial to the Euler characteristic of a complex, so we forget about underlying vector spaces and take into account only their dimensions. Notice that the partition function of an interface (1.43) depends on Chan-Paton factors, so it is represented by a Chan-Paton matrix. Analogously to an interface one associates a Chan-Paton matrix of complexes [47]. We will consider an interface complex as formal sum of all Chan-Paton complexes. So applying Euler characteristic map χ to a complex generically we will get a matrix of Euler characteristics, or a linear operator. So as a check we can consider Euler characteristics of any expression in our discussion in this section and derive a corresponding expression from chapter 2.

3.3.1 Solitons in a 'tHooft limit

Now let us consider the following scaling of the potential (3.46):

$$W = -\sum_{i=1}^N \log(z - \phi_i) + 2 \sum_{1 \leq i < j \leq N} \log(\phi_i - \phi_j) + \frac{1}{g} \sum_{i=1}^N V(\phi_i, q_r) \quad (3.56)$$

Now we take a limit $g \rightarrow 0$ while the number of fields $N \rightarrow \infty$ so that

$$gN \sim \text{const} \quad (3.57)$$

We will explain why this simultaneous 'tHooft limit is necessary in the consideration of the Yang-Yang potential in what follows, the chosen scaling can be interpreted as a consideration of large coefficients $k_a \sim \frac{1}{g}$ in (3.48).

We expect the following phenomena:

- In the vacuum equation the potential term is dominant

$$\partial_{\phi_i} W \sim \frac{1}{g} V'(\phi_i) = 0 \quad (3.58)$$

Thus all the stationary points for N fields ϕ_i are localized near the extrema of the potential p_a : $V'(p_a) = 0$. Thus we can choose a tuple of filling numbers $\{N_a\}$, so that $\sum_a N_a = N$. In this picture N_a fields ϕ^i are put in the vacuum p_a . “Renormalized” filling numbers $c_a = gN_a$ are finite in this limit. A generic approximate ground state wave function reads:

$$\Psi(\phi) = \sum_{\substack{\text{tuples} \\ \{N_a\}}} c_{\{N_a\}} \prod_{i_1=1}^{N_1} \delta(\phi^{i_1} - p_1) \prod_{i_2=1}^{N_2} \delta(\phi^{i_2} - p_2) \dots \quad (3.59)$$

- The second term in (3.56) is a repulsive 2d Coulomb potential. It does not allow to put all the particles in one minimum. Rather they form “droplets” of finite thickness when the c_a are small. Indeed let us estimate the position deviation $\delta\phi_a$ of some particle from the vacuum p_a by a mean field approximation:

$$\frac{1}{g} V''(p_a) \delta\phi_a - \frac{N_a}{\delta\phi_a} = 0, \quad \delta\phi_a \sim \sqrt{\frac{c_a}{V''(p_a)}} \quad (3.60)$$

The approximation $c_a \ll 1$ is known as a Dijkgraaf-Vafa (DV) phase [25, 26, 24] (see also [78] and references therein) in a theory of matrix models. In this phase the vacua concentrate near extrema of the potential in “Wigner droplets”. While these droplets are small they do not affect each other, so probability distributions of the particles are approximately given by Wigner semicircle distributions:

$$\Psi_{\text{thick}}(\phi) = \sum_{\substack{\text{tuples} \\ \{N_a\}}} c_{\{N_a\}} \prod_{i_1=1}^{N_1} w_{-V''(p_1)/c_1}^{\frac{1}{2}}(\phi^{i_1} - p_1) \prod_{i_2=1}^{N_2} w_{-V''(p_2)/c_2}^{\frac{1}{2}}(\phi^{i_2} - p_2) \dots \quad (3.61)$$

where

$$w_{\kappa}(z) = \frac{\sqrt{\kappa}}{2\pi} \sqrt{4 - \kappa z^2}$$

Let us estimate contributions of different terms into superpotential (3.56). Single sum over index gives a factor of order N . Thus we have

$$\begin{aligned} -\sum_i \log(z - \phi_i) &\sim N \sim \frac{1}{g} \\ 2 \sum_{i < j} \log(\phi_i - \phi_j) &\sim N^2 \sim \frac{1}{g^2} \\ \frac{1}{g} \sum_i V(\phi_i, q_a) &\sim \frac{N}{g} \sim \frac{1}{g^2} \end{aligned} \quad (3.62)$$

So we expect the following asymptotic behavior of the potential difference for solitons:

$$\Delta W_s =: \frac{1}{g^2} \mathbf{F}(q_a) + \frac{1}{g} \mathbf{W}(z, q_a) + \mathcal{O}(g^0) \quad (3.63)$$

Notice the term of order g^{-2} depends only on parameters q_a while the term of order g^{-1} depends on both q_a and z .

Now let us depict an effective potential for fields ϕ^i following from mean field analysis. See fig.3.1.

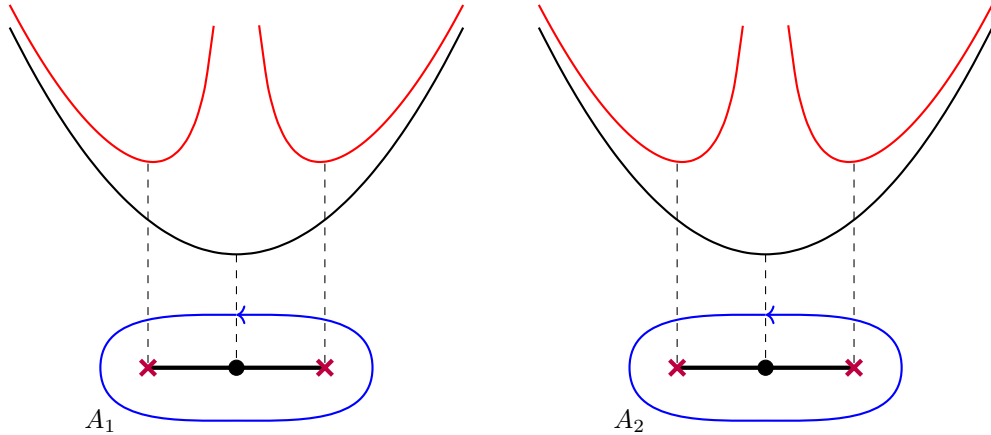


Figure 3.1: Effective potential

First we have an external potential $V(p)$ drawn by the black color that has extrema (we have drawn two separate minima). The droplets of fields ϕ^i collected in these extrema create extra repulsive (attractive) “hills” (drawn by the red color). So a particle ϕ^i in this picture “sees” an effective potential, where all the extrema of the potential $V(p)$ are doubled. This is a generic picture, though in the DV phase ($c_a \ll 1$) this doubling resolution is small and we can denote new effective vacua $p_a^{(\pm)}$.

So we expect **solitons** hopping from $p_a^{(\pm)}$ to $p_b^{(\pm)}$, or $p_a^{(+)}$ to $p_a^{(-)}$ or vice versa. Though these solitons do not contribute to the partition function **unless** their phases are not aligned with ζ not to break \mathbb{Q}_ζ .

If we add rescaling to the equation (3.54) it would look like

$$(\partial_z \Delta W_{\mathfrak{s}})^2 - \frac{1}{g} V' \partial_z \Delta W_{\mathfrak{s}} + \sum_r D^r \partial_{q_r} \Delta W_{\mathfrak{s}} = 0 \quad (3.64)$$

Up to higher g -corrections, the equation simplifies, instead of being PDE it becomes a first order ODE:

$$(\partial_z \mathbf{W})^2 - V'(z) (\partial_z \mathbf{W}) + \sum_r D_r u_r = 0 \quad (3.65)$$

This equation is known as a spectral cover $\Sigma \rightarrow \mathcal{C}$, and

$$u_r := \partial_{q_r} \mathbf{F}(q) \quad (3.66)$$

are moduli.

The solution to this equation has branches

$$\partial_z \mathbf{W} = \frac{1}{2} V'(z) \pm \frac{1}{2} \sqrt{(V'(z))^2 - 4 \sum_r D_r u_r} \quad (3.67)$$

The branching points in the case of DV phase ($c_a, u_r \ll 1$) are slightly resolving the minima of the potential p_a , moreover, as we will see later they are exactly positions $p_a^{(\pm)}$ of effective vacua as it is depicted at fig.3.1.

Now consider integrals of $d\mathbf{W}$ over periods of the spectral cover. A -periods are simple

$$\oint_{A_a} d\mathbf{W} = g \oint_{A_a} dz \left\langle \sum_i \frac{1}{z - \phi^i} \right\rangle_{\text{SLG}} = 2\pi i g N_a = 2\pi i c_a \quad (3.68)$$

B -periods are less trivial. Though we can estimate them using a well-known formula from electrostatics for the potential difference $\Delta_{ab}\varphi$

$$\Delta_{ab}\varphi = \frac{\partial E_{ab}}{\partial q} \quad (3.69)$$

where E_{ab} is an energy, and q is a charge. The integral of $d\mathbf{W}$ over B -cycle encircling p_a and p_b corresponds to the potential change of charge moved from p_a vacuum to p_b vacuum. the role of the energy is played by the free energy \mathbf{F} , and the charge we have already determined to be c_a . Thus we have

$$\oint_{B_a} d\mathbf{W} = \frac{\partial \mathbf{F}}{\partial c_a} \quad (3.70)$$

Thus we may think of $d\mathbf{W}$ as of a Seiberg-Witten differential of an effective theory given by a spectral curve (2.5), and of \mathbf{F} as of a corresponding prepotential. Indeed the spectral curve corresponds to a theory of class \mathcal{S} type A_1 on $\mathcal{C} = \mathbb{P}^1 \setminus \{\text{punctures}\}$ with simple punctures z and q_a

and mass parameters on the punctures given by k_a 's. Notice that at least when $V(p)$ is a polynomial the relevant chiral operators can be produced through deformation of the coefficients. There are as many relevant deformations as the order of $V'(p)$, so the number of the A -cycles and the number of moduli coincide.³

Now let us draw more information about solitons from the asymptotic analysis. So generically we expect the following asymptotic behavior of holomorphically reduced tt^* -connection flat section:

$$Z(z, q) = \sum_{p \in \mathfrak{D}_\zeta} d_p \exp \left(\lambda \left(\frac{1}{g^2} \mathbf{F} + \frac{1}{g} \int_p d\mathbf{W} \right) + \mathcal{O}(g^0, \zeta^0) \right) \quad (3.71)$$

Here we have used a set of detours \mathfrak{D}_ζ of paths on the IR curve Σ (defined by (2.5)) that emerges in the consideration due to the Stokes phenomenon, and d_p are Stokes parameters counting degeneracies of detour appearance with signs. We have already discussed construction of the detour paths in chapter 2, let us just remind that this set can be defined purely by consideration of tt^* -section equation asymptotic behavior, no extra field theory data are needed. Now we make two important remarks allowing one actually to count solitons in the presented 'tHooft limit:

- Comparing expansions (3.71) and (3.28) we conclude that soliton elementary partition functions contributing in saddle points of the Landau-Ginzburg action are in one-to-one correspondence with detours. So having calculated the expansion (3.71) and actual set \mathfrak{D}_ζ we expect to calculate the set $\mathfrak{S}(\zeta)$ from eq.(3.28) through this correspondence:

$$\boxed{\sigma : \mathfrak{D}_\zeta \rightarrow \mathfrak{S}(\zeta)} \quad (3.72)$$

- Using this correspondence we can also define fermion numbers of solitons. Eq.(3.55) simplifies in the 'tHooft limit as well and can be explicitly solved. Actually, we are not so interested in the value of a fermion number of a state as in the difference of fermion numbers of two states

³ It is important to notice that we are able to present a set of equivalent observables, while even IR dynamics of the class \mathcal{S} theory and Landau-Ginzburg theory under consideration are different. This can be easily seen by counting quasi-classical vacuum states. The number of IR vacua on a surface defect in the class \mathcal{S} theory is given by the order of the spectral cover (see [43, Sec. 3.4] for example), while the number of vacua in the Landau-Ginzburg theory is given by a number of Bethe roots for N LG particles. Moreover, in what follows we will associate mutations to solitons in the Landau-Ginzburg theory carrying topological charge, while the same mutations in class \mathcal{S} theories are associated to a 4d BPS particle presence in the IR theory spectrum, and 4d BPS particles have only a flavour charge in the effective surface defect theory, no topological charge.

to define grading difference in the MSW complex. So for two solitons s and s' we have ⁴:

$$f_s - f_{s'} = -\frac{1}{2\pi i} \int_{\sigma^{-1}(s) - \sigma^{-1}(s')} d \log \left(\mathbf{W}' - \frac{1}{2} V' \right) - \frac{1}{4\pi i} \int_{\sigma^{-1}(s) - \sigma^{-1}(s')} \frac{dV'}{\mathbf{W}' - \frac{1}{2} V'} \quad (3.73)$$

Here we have used a map $\sigma^{-1} : \mathfrak{S}(\zeta) \rightarrow \mathfrak{D}_\zeta$. One might expect higher order g -corrections to this solution. However we expect that the result of this difference is an integer number for topologically equivalent solitons, so it can not depend on free parameter g , hence higher order g -corrections should be cancelled out in this difference.

3.3.2 Simpletons and categorified Abelianization map

Now we would like to apply ideas of the spectral networks we have discussed in chapter 2 to flat connections on the spaces of the ground states in the supersymmetric Landau-Ginzburg model generated by marginal coupling deformations. This makes us to associate certain parallel transports in the marginal coupling space to interfaces. For the general theory of interfaces we refer to [47].

Rules summarized in sec.2.2 allow one to represent parallel transport problem (3.71) in abstract terms. To an interface \mathfrak{U}_φ transporting a Coulomb probe parameter z (see eq.3.46) along a path φ we associate an asymptotic expansion over detours $\mathfrak{D}_\zeta(\varphi)$ depending on the phase ζ and on the path φ of the interface:

$$\mathfrak{U}_\varphi = \sum_{p \in \mathfrak{D}_\zeta(\varphi)} \mathscr{Y}_p \quad (3.74)$$

Having a path variable \mathscr{Y}_p we can take the corresponding path element p in $\mathfrak{D}_\zeta(\varphi)$ and associate to it corresponding approximate solution $\sigma(p)$ of the forced soliton equation (1.31), to this solution we associate a perturbative wave function $\Psi[\mathscr{Y}_p]$ analogous to (3.10).

We define the corresponding MSW complex for the interface \mathfrak{U}_φ as a vector space:

$$\mathbb{M}(\mathfrak{U}_\varphi) = \bigoplus_{p \in \mathfrak{D}_\zeta(\varphi)} \mathbb{C}[\Psi[\mathscr{Y}_p]] \quad (3.75)$$

Let us argue that this complex is a regular homotopy invariant of φ , to do so we should implement the sign rule (2.22).

Depending on a concrete morphism of path categories the condition (2.22) can be realized in different ways. We should realize it in terms of complexes and the reasonable realization is that

⁴This formula can be compared to a naive formula for the fermion number counting number of Dirac operator eigenvalues crossed zero value

$$f = \frac{1}{2\pi i} \int d \log \text{Det}_{i,j} \left\langle \frac{\partial^2 W}{\partial \phi^i \partial \phi^j} \right\rangle$$

It is well known that this formula has a restricted range of applicability. So we will be careful and apply our expression only to solitons represented by path of the same homology class. To define fermion numbers for solitons appearing in the \mathcal{R} -complex we consider explicitly fusion of Liouville fields.

a direct sum of complexes associated with \mathcal{Y}_a and $\mathcal{Y}_{a'}$ (see (2.21)) is quasi-isomorphic to the zero complex. In other words $\mathbb{C}[\Psi[\mathcal{Y}_a]]$ and $\mathbb{C}[\Psi[\mathcal{Y}_{a'}]]$ form an exact sequence under the action of the differential:

$$\boxed{0 \rightarrow \mathbb{C}[\Psi[\mathcal{Y}_a]] \xrightarrow{\mathbb{Q}_\zeta} \mathbb{C}[\Psi[\mathcal{Y}_{a'}]] \rightarrow 0} \quad (3.76)$$

Or, vice versa

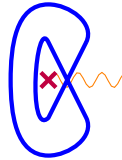
$$0 \rightarrow \mathbb{C}[\Psi[\mathcal{Y}_{a'}]] \xrightarrow{\mathbb{Q}_\zeta} \mathbb{C}[\Psi[\mathcal{Y}_a]] \rightarrow 0 \quad (3.77)$$

Or, returning to solitons we write:

$$\langle \Psi_{s(a')} | \mathbb{Q}_\zeta | \Psi_{s(a)} \rangle = \pm 1 \quad (3.78)$$

Where we have used a map $s : \mathfrak{D}_\zeta \rightarrow \mathfrak{S}(\zeta)$ relating paths to soliton solutions.

Indeed if we calculate the fermion number difference for these two states according to our formula in the 'tHooft limit (3.73) as an integral around square root singularity:



$$\Delta f = f_a - f_{a'} = \frac{1}{2\pi i} \int_0^{\pm 4\pi} d \log \sqrt{e^{i\theta}} = \pm 1 \quad (3.79)$$

Let us construct these states explicitly.

Suppose we have some generic superpotential $W(\phi, z)$ depending on fields ϕ and parameters z . Now suppose at some critical value of the parameter z_* two vacuum field values collide

$$\phi_{*1}(z_*) = \phi_{*2}(z_*) = \phi_*$$

We can introduce new variables in the neighbourhood of the critical point z_* (ramification point of the spectral cover)

$$\delta\phi = \phi - \phi_*, \quad \delta z = z - z_*$$

Then the superpotential near this point can be expanded as

$$W = A \delta\phi^3 + B \delta\phi \delta z + \text{higher terms} \quad (3.80)$$

Thus without loss of generality we can parameterize the theory in the neighbourhood of ramification points by a cubic potential:

$$W(\phi, z) = \frac{1}{3}\phi^3 - \phi z \quad (3.81)$$

One can easily calculate corresponding critical points:

$$\phi_{*\pm} = \pm z^{\frac{1}{2}}, \quad \Delta W = -\frac{4}{3} z^{\frac{3}{2}} \quad (3.82)$$

And as we see there are three values $z = e^{\frac{2\pi i}{3}n}$ when soliton jumps are admissible, these are our three \mathcal{S} -walls (compare to sec.2.1).

We will construct an explicit field configuration contributing to the matrix element (3.78) in sec.3.5.1 in terms of curved webs.

3.3.3 Evolution, gluing and mutations

One can introduce a natural composition operation on interfaces. For this purpose we will adopt a notation \boxtimes analogous to [47]. We define \boxtimes as bilinear operation with respect to direct sum \oplus , so it is enough to define it on generators. The interface Hilbert space of ground states is a subspace of the Hilbert space of perturbative ground states being quantum fluctuations around quasi-classical trajectories in the field space $\phi_*^i(x)$, let us denote a classical trajectory by p and the corresponding state by Ψ_p ⁵. Suppose two trajectories p and p' can be concatenated, we denote their concatenation as $p' \circ p$, then we define the gluing composition of complexes as of vector spaces (compare to the path algebra form sec.2.2):

$$\mathbb{C}[\Psi_p] \boxtimes \mathbb{C}[\Psi_{p'}] = \begin{cases} \mathbb{C}[\Psi_{p' \circ p}], & \text{if } p \text{ and } p' \text{ can be concatenated,} \\ \emptyset, & \text{otherwise} \end{cases} \quad (3.83)$$

Let us discuss a connection between the Coulomb probe interface when we change its parameter z and interfaces in the master theory when we change moduli or phase ζ (see superpotential (3.46)). Suppose we construct a MSW complex $\mathbb{M}_\gamma^{\tilde{u}}$ for an interface corresponding to change of parameter z of the Coulomb probe along path γ while phase ζ and other parameters \tilde{u} are fixed. Now suppose z is fixed and \tilde{u} changes to a new point \tilde{u}' . An interface \mathcal{I}_U interpolating between points \tilde{u} and \tilde{u}' along some path in the parameter space connects two models and its Euler characteristic may be represented as a shift operator (a matrix of Euler characteristics of Chan-Paton complexes) acting on the partition function space, indeed, the reduction to the Euler characteristic χ returns us to representation of parallel transports in terms of coordinates on the moduli space of flat connections (see sec.2.5.1). The interface \mathcal{I}_U transports an interface $\mathbb{M}_\gamma^{\tilde{u}}$ to $\mathbb{M}_\gamma^{\tilde{u}'}$, this evolution in the Heisenberg picture gives the following relation for Euler characteristics of these interfaces:

$$\chi(\mathbb{M}_\gamma^{\tilde{u}'}) = \chi(\mathcal{I}_U) \chi(\mathbb{M}_\gamma^{\tilde{u}}) \chi(\mathcal{I}_U)^{-1} \quad (3.84)$$

⁵In comparison to [47, eq.(17.7)] we have suppressed boundary condition indices i and j' assuming this information is stored in the solution p

This relation is lifted to a quasi-isomorphism of complexes:

$$\mathbb{M}_\gamma^{\bar{u}'} \boxtimes \mathcal{I}_U \sim \mathcal{I}_U \boxtimes \mathbb{M}_\gamma^{\bar{u}} \quad (3.85)$$

If different families of complexes $\mathbb{M}_\gamma^{\bar{u}}$ and $\mathbb{M}_\gamma^{\bar{u}'}$ for different γ are known equation (3.85) can be used to derive interface \mathcal{I}_U .

As an example let us consider an interface performing the simplest flip mutation (2.38). Classically, we can represent the flip as evolution:

$$\mathcal{K}_{\gamma'}(X_\gamma) = \phi_{\gamma'} X_\gamma \phi_{\gamma'}^{-1} \quad (3.86)$$

where the function ϕ_γ is quantum dilogarithm function (see [33] and also [44, sec.3.4.1]) defined as:

$$\phi_\gamma = \prod_{k=0}^{\infty} (1 + q^{2k+1} X_\gamma) \quad (3.87)$$

The action of quantum dilogarithm is going to be mimicked by corresponding interface Φ_γ satisfying evolution equation (see fig.2.7)

$$(\mathbb{C}[\Psi[\mathcal{A}_{\bar{a}(1)}]] \oplus \mathbb{C}[\Psi[\mathcal{B}_{\bar{b}(1)}]]) \boxtimes \Phi_{\gamma_c} \sim \Phi_{\gamma_c} \boxtimes \mathbb{C}[\Psi[\mathcal{A}_{\bar{a}(1)}]] \quad (3.88)$$

The Euler characteristics of Φ_γ we already know, it is given by the quantum dilogarithm. So we expect

$$\Phi_{\gamma_c} = (\mathbb{C} \oplus \mathbb{C}[\mathcal{X}_0]) \boxtimes (\mathbb{C} \oplus \mathbb{C}[\mathcal{X}_1]) \boxtimes (\mathbb{C} \oplus \mathbb{C}[\mathcal{X}_2]) \boxtimes \dots \quad (3.89)$$

where \mathcal{X}_k is a soliton wave function with corresponding Euler characteristics $\chi(\mathcal{X}_k) = q^{2k+1} X_{\gamma_c}$. It is easy to construct those solitons (see fig.3.2). Indeed the interface is represented by a “shower”

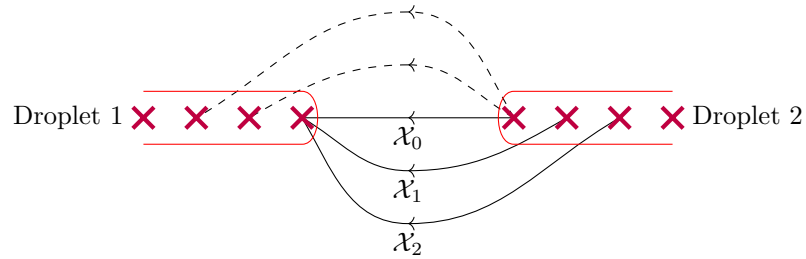


Figure 3.2: Solitons between edges of Wigner droplets

of solitons interpolating from all the vacua at one edge of Wigner droplet neighbour by neighbour to the very tip of another edge. Actually, there are two types of solitons depicted by solid lines and dashed ones satisfying condition $\chi(\mathcal{X}_k) = q^{2k+1} X_{\gamma_c}$, however in the spectrum just one shower is presented, another shower appears after phase transition across a stability wall. An example of

a similar transition is presented in sec.3.4.6. We do not expect contributions of other solitons, say, from a center of a Wigner droplet to the center of another one since these solutions are suppressed by their energy. As we will see an asymptotic solution in the limit $q \rightarrow 0$ we have presented captures actually an exact solution in the non-categorified case, i.e. we can reproduce Drinfeld R -matrices, key elements of a Jones polynomial construction, from these flip interfaces in their asymptotic form (3.87). So we hope that (3.89) captures enough information to reproduce a correct \mathcal{R} -interfaces (see sec.3.4.4) and knot cohomologies.

3.4 Braiding interfaces

3.4.1 Braiding as a parallel transport on the moduli space

As we have discussed in section 1.5 the physical approach to knot(link) invariants treats these invariants as knotted Wilson loop observables in the Chern-Simons theory. n -component link described by a collection of maps $\gamma_i : S^1 \rightarrow \mathcal{M}_3$ gives rise to the following average:

$$\int [DA] \prod_i \left(\text{Tr}_{R_i} \mathcal{P} \exp \oint_{\gamma_i} A \right) e^{i \frac{\kappa}{4\pi} \int_{M_3} \text{Ad}A + \frac{2}{3} A^3} \quad (3.90)$$

We can associate its own representation R_i to each component of the link. Here κ is an integer valued constant know as Chern-Simons level, we assume that the gauge group is $SU(N)$.

One of the popular ways to calculate this average is to use the relation between Chern-Simons theory and the Wess-Zumino-Witten (WZW) model. Suppose our 3-manifold \mathcal{M} is a product of a time interval I and some Riemann surface \mathcal{C} . And suppose we have embedded some link into $\mathcal{M} = \mathcal{C} \times I$. The path integral (3.90) can be interpreted as an evolution of quantum states assigned to each time slice. Let us choose some time slice t , the link intersects \mathcal{C} at this time in points q_i (see fig.3.3). To each point q_i we associate a representation R_i coinciding with the representation of the Wilson loop puncturing \mathcal{C} at this point if a tangent vector to the Wilson line has a positive angle with the surface or with complex conjugated one to the representation of the Wilson loop if the angle is negative. The corresponding space of states depends on the surface \mathcal{C} and puncture data (q_i, R_i) .

This space of states coincides with the space of conformal blocks in the WZW model [97, 77]. In the case \mathcal{C} is a Riemann sphere we can present $\left(\bigotimes_i R_i \right)$ -valued wave functions Ψ of punctures q_i spanning this space. These wave functions satisfy the Knizhnik-Zamolodchikov equations [69]:

$$\left(\partial_{q_i} + \frac{1}{\kappa + N} \sum_{j \neq i} \frac{T_i^a \otimes T_j^a}{q_i - q_j} \right) \Psi(q_i) = 0 \quad (3.91)$$

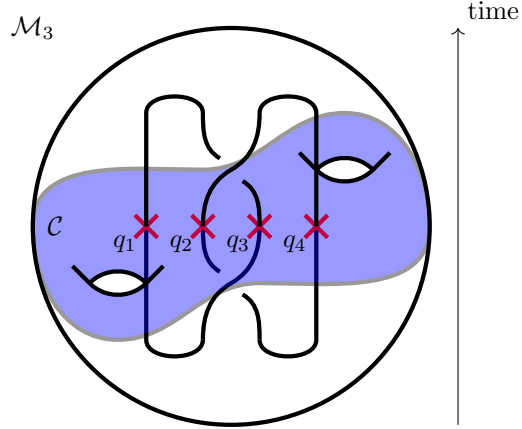


Figure 3.3: Chern-Simons vs. Wess-Zumino-Witten

where T_i^a are generators of the algebra $\mathfrak{su}(N)$ acting on R_i .

These equations can be thought of as a Schrödinger evolution equation in quantum mechanics.

Having an element \mathcal{B} of a braid group we associate to it a trajectory representative: trajectories of punctures $q_i : [0, T] \rightarrow \mathcal{C}$ as functions of time t . An evolution operator

$$\mathfrak{U}(T) = \mathcal{P} \exp \int_0^T dt \sum_{i \neq j} \frac{1}{\kappa + N} \frac{T_i^a \otimes T_j^a}{q_j(t) - q_i(t)} \dot{q}_i(t) \quad (3.92)$$

is invariant under regular homotopic transformations of trajectories $q_i(t)$, so it is an invariant of braid group element \mathcal{B} .

In what follows we will be interested in the gauge group $SU(2)$, so we do not distinguish representations and their conjugates, all the representations are labelled by spin J .

To connect this setup to spectral networks we have discussed in chapter 2 let us consider Heisenberg evolution picture where operators \mathcal{O} are changing with time:

$$\mathcal{O}(T) = \mathfrak{U}(T) \mathcal{O}(0) \mathfrak{U}(T)^{-1} \quad (3.93)$$

As a set of operators consider Wilson loops in the fundamental representation lying on the time slice \mathcal{C} . They can be described by introducing an additional strand with coordinate z :

$$\left[\partial_z + \frac{1}{\kappa + 2} \sum_i \frac{\sigma^a \otimes T_i^a}{z - q_i} \right] \Psi(z; q_i) = 0 \quad (3.94)$$

where σ^a are Pauli matrices. Consider an asymptotic expansion when spins associated to strands are large $J_i \sim h_i/(2g)$, $g \rightarrow 0$, we expect the following behavior (compare to sec.3.3.1):

$$\Psi(z|q_i) \sim -\frac{(\kappa+2)^{-1}}{g^2} \mathbf{F}(q_i) - \frac{(\kappa+2)^{-1}}{g} \int^z d\mathbf{W}(z, q_i) \quad (3.95)$$

The resulting equation for the exponent argument coincides with the spectral cover equation (3.65) (see derivation of this equation in Appendix E):

$$(d\mathbf{W})^2 = \sum_i \left(\frac{h_i^2}{(z - q_i)} + \frac{\partial_{q_i} \mathbf{F}}{z - q_i} \right) dz^2 \quad (3.96)$$

The spectral cover appearing in this setup is similar to one encountered in class \mathcal{S} theory consideration, in Liouville CFT and Yang-Yang-Landau-Ginzburg theory. So we can discuss all these examples on a similar footing [50]. Wilson loops \mathcal{O} correspond to holonomies of connection (3.94), thus their asymptotic behavior is analogous to line defect behavior we have discussed in sec.2.5.1.

Asymptotic expansion coefficients of line defects are piece-wise constants on the moduli space, i.e. as functions of q_i . As we follow braid element \mathcal{B} along the parameter space we cross some \mathcal{K} -walls, so to the evolution operator we associate an ordered set of \mathcal{K} -morphisms:

$$\mathfrak{U}(T) \rightsquigarrow \prod_a \mathcal{K}_a \quad (3.97)$$

Wall-crossing formulae ensure that the resulting morphism is a braid invariant. A similar construction is widely known in the literature (see e.g.[58, 27]) in a slightly different fashion. The flips of triangulations in the Teichmüller theory corresponding to simple \mathcal{K} -morphisms in our picture are represented by tetrahedron gluing. The adjoint action of \mathcal{K} -morphism is associated to a Chern-Simons partition function on a tetrahedron.

In a way similar to the WZW conformal block on the time slice of \mathcal{M}_3 description one can consider analogous Liouville (Toda) conformal blocks with degenerate vertex operators. A collection of null-vector equations for all vertex operators entering the conformal block is a self-consistent system of partial differential equations, one can treat them again as connections on the configuration space of vertex operator positions and proceed to an evolution operator (open Verlinde operator [40]) in this system that is a braid invariant. Remarkably, it is possible to prove an equivalence of quantum algebra $U_q(sl_2)$ and Liouville algebra as braided tensor categories [84, 83].

Finally, we can think of braid representatives and associated evolution as parallel transport and interfaces in the Yang-Yang-Landau-Ginzburg (YYLG) theory. We expect that homotopically equivalent braids give homotopically equivalent interfaces, therefore Hilbert spaces of true ground states isomorphic to each other as graded vector spaces. Thus we expect a well-defined map from the braid group to isomorphism classes of YYLG ground state Hilbert spaces (corresponding Poincaré polynomials).

To arrive actually to knot (link) invariants one should introduce fusing/defusing operators or a trace operation. We will see that there are certain obstacles on this route. So in what follows we will

present a calculation of an interface representation for the braid group generators (in analogy to R -matrices we will call them \mathcal{R} -twists) in two ways: using Heisenberg evolution picture in the 'tHooft limit and in a model with symmetry breaking of [48], and we will observe an agreement between these calculations. For computational reasons the second model is simpler, so we will proceed with it in the rest of this chapter. We will show explicitly that the resulting model describes braid invariants. Afterwards we will describe an obstacle with fusing/defusing interfaces construction and propose a resolution (reduction) that will allow us to construct knot invariants.

3.4.2 \mathcal{R} -interfaces in the Heisenberg picture

In the topological field theory two following braids are identical:

The diagram shows two equivalent braiding configurations in a Heisenberg picture. The vertical axis is labeled q_a and the horizontal axis is labeled x . On the left, a vertical interface I is on the left, followed by a \mathcal{R} -twist (a crossing of two strands), and then another vertical interface I on the right. On the right, a vertical interface I' is on the right, preceded by a \mathcal{R} -twist, and then another vertical interface I' on the left. The two diagrams are separated by an equals sign, indicating they represent the same complex.

This is a diagrammatic representation of the following relation (compare to (3.85)):

$$\boxed{I \boxtimes \mathcal{R} \sim \mathcal{R} \boxtimes I'} \quad (3.99)$$

where \boxtimes is a consequent gluing of interfaces (see sec.3.3.3) and \sim implies quasi-isomorphism of complexes.

This equation is enough to define \mathcal{R} -matrix as a differential operator acting on a space of partition functions (3.47) [58, 57]. We will use it to define \mathcal{R} -interface in the same fashion.

As we discussed we can construct solitons corresponding to the Verlinde interface using the spectral cover $\Sigma(3.65)$. In the particular case of YYLG model it is given by (3.96). Here Hamiltonians h_a are renormalized weights ($k_a = h_a/g$) of representations sitting on the strands and $u_a = \partial_{q_a} \mathbf{F}$ are moduli. The q -deformation procedure as in chapter 2 performs indeed a canonical quantization of the parameter space: unified space of the puncture positions and Coulomb branch.

In a generic case, moduli u_a are not independent due to conformal invariance, indeed, in the case of superconformal $SU(2)$ SYM theory with $N_f = 4$ the only parameter is the bare coupling constant τ and the conjugated modulus is a Higgs vev.

Though the calculation becomes much more convenient if we use a wider class of spectral curves including (3.96):

$$d\mathbf{W}^2 = \frac{\prod_{j=1}^{2n+2} (z - p_j)}{\prod_{a=1}^n (z - q_a)^2} dz^2 \quad (3.100)$$

Here q_a are strands positions, and p_j are new moduli that will be ramification points. We put these parameters on the complex plane in such a way that q_a lie on the real line and each q_a is accompanied by two branching points p_{2a-1} and p_{2a} , two remaining b.p.'s p_{2n+1} and p_{2n+2} we put in such a way they have large positive (negative) imaginary part. Then we take the following choice of basic cycles as depicted in fig.3.4.

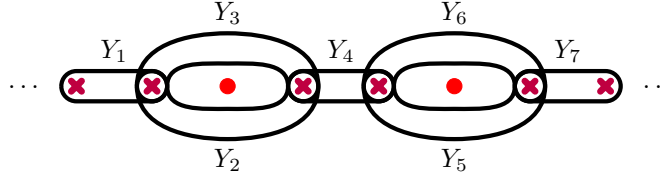


Figure 3.4: Deformed spectral curve for YY model and cycle choice on it.

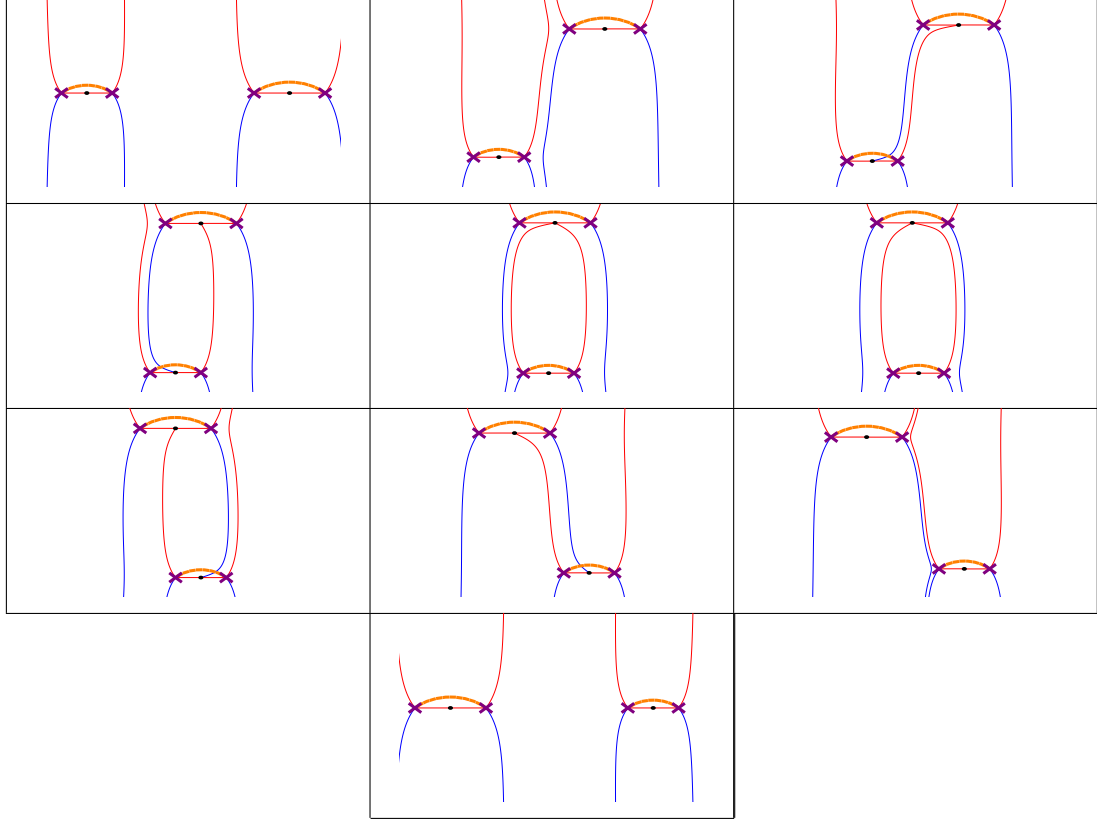
As before we associate to the chosen cycles soliton complexes \mathcal{Y}_i , though in the non-refined case ($t = -1$) those are just differential operators Y_i acting on the Yang-Yang partition function. They represent quantized Fock-Goncharov coordinates on the Teichmüller space associated to triangulations of \mathcal{C} (see sec.2.4) and satisfy a Heisenberg algebra

$$Y_i Y_j = q^{2b_{ji}} Y_j Y_i \quad (3.101)$$

where the matrix $B = (b_{ij})$ is the matrix of intersection form on cycles. For this chosen system of cycles this matrix reads

$$B = \begin{pmatrix} 0 & 1 & -1 & 0 & 0 & 0 & 0 \\ -1 & 0 & 0 & 1 & 0 & 0 & 0 \\ 1 & 0 & 0 & -1 & 0 & 0 & 0 \\ 0 & -1 & 1 & 0 & 1 & -1 & 0 \\ 0 & 0 & 0 & -1 & 0 & 0 & 1 \\ 0 & 0 & 0 & 1 & 0 & 0 & -1 \\ 0 & 0 & 0 & 0 & -1 & 1 & 0 \end{pmatrix} \quad (3.102)$$

As we move parameters q_a and Wigner droplets according to \mathcal{R} -twist the spectral network goes through the following film “frames”:



On these frames the choice of cuts is given by orange color, purple crosses denote branching points. Black dots are two singularities we are permuting. Lines of the spectral network are drawn either red or blue depending on if it is of type $(+-)$ or $(-+)$ correspondingly.

As we can see the topology of spectral networks changes four times, this corresponds to four consequent mutations. Thus we construct our \mathcal{R} -interface as:

$$\boxed{\mathcal{R} = S \boxtimes \Phi_4 \boxtimes \Phi_3 \boxtimes \Phi_2 \boxtimes \Phi_1} \quad (3.103)$$

Where Φ_i are mutations corresponding to edge-to-edge solitons we discussed in sec.3.3.3. (see fig.3.5). And S is a classical soliton-less contribution from permutation of the Wigner droplets as wholes, indeed there is a mean field effective potential between Wigner droplets depending logarithmically on their positions on \mathcal{C} , and this potential gives a $2\pi i$ shift when braiding.

3.4.3 Drinfeld R -matrix recovery, spins as filling number

We can easily recover Drinfeld R -matrix from (3.103) by substituting soliton contribution by operators Y_i .

We can choose a “polarization”: say, the wave function representing distribution of the LG fields

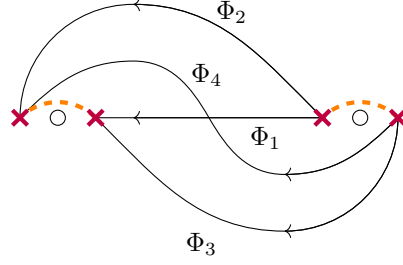


Figure 3.5: Four mutations of \mathcal{R} -complex

among Wigner droplets is an eigenfunction of Y_3 and Y_6 :

$$Y_3 \Xi = q^{2N_3} \Xi, \quad Y_6 \Xi = q^{2N_6} \Xi \quad (3.104)$$

Where $q = e^{\pi i \lambda}$, and N_3 and N_6 are filling numbers of corresponding Wigner droplets encircled by these cycles. Then a soliton interpolating between different Wigner droplets acts as a shift operator:

$$Y_4 = e^{\partial_{N_6} - \partial_{N_3}} \quad (3.105)$$

Substituting corresponding classical expressions for mutation contributions and expanding (3.103) we get an expression for the Drinfeld universal R_D -matrix for $U_q(\mathfrak{sl}_2)$:

$$R_D = S \sum_{n=0}^{\infty} \frac{(-q)^{-n}}{\prod_{j=1}^n (1 - q^{-2j})} [Y_4^{-1}(1 + q^{-1}Y_2^{-1})(1 + q^{-1}Y_6^{-1})]^n \quad (3.106)$$

Operator $S = q^{N_3 N_6 / 2}$ is just a q -shift due to permutation of Wigner droplets. Let us introduce a state vector $|N_a, k_a\rangle$ corresponding to a Wigner droplet associated to a puncture q_a . It is defined by two numbers: k_a from the Lagrangian and N_a - Wigner droplet filling number.

Notice that parts of the R -matrix expression in terms of cluster coordinates Y_i can be recognized as elements of $U_q(\mathfrak{sl}_2)$:

$$E \sim e^{-N_3}(1 + q^{-1}Y_2^{-1}), \quad F \sim e^{N_6}(1 + q^{-1}Y_6^{-1}) \quad (3.107)$$

Thus for two states

$$Y_4^{-1}(1 + q^{-1}Y_2^{-1})(1 + q^{-1}Y_6^{-1}) \sim E \otimes F$$

And our ground state function (3.59) can be thought of as an element of tensor product:

$$\Psi(N_1, \dots, N_n) \sim |N_1, k_1\rangle \otimes \dots \otimes |N_n, k_n\rangle \quad (3.108)$$

Remember we assume that LG fields ϕ_i are *indistinguishable*, hence, say, a state when field ϕ_1 is placed to the critical point v_1 and ϕ_2 is placed to the critical point v_2 is physically identical to a state when ϕ_1 is placed to v_2 and ϕ_2 is placed to v_1 , so indeed the state is defined just by filling numbers of Wigner droplets.

3.4.4 Spin- $\frac{1}{2}$ \mathcal{R} -interface in the model of Wigner droplets

Now we try to adopt eq.(3.103) to the case of the fundamental representations.

As we discussed in the previous section the critical points of the LG model play a role of representation vectors $|N, k\rangle$ meaning that N vacuum slots are occupied near a puncture with parameter k . In particular case of finite dimensional representations N and k are integers, moreover $0 \leq N \leq k$, this implies that number of particles N localized near a puncture with parameter k is integer and not greater than k . This implies a need to reconcile equation for \mathcal{R} -interface (3.103).

Indeed, an elementary mutation (3.89) used here should be modified since the infinite product in (3.89) starting from an edge of Wigner droplet and going towards its opposite edge should be terminated when the opposite edge of the Wigner droplet is reached.

Now consider a part of \mathcal{R} -interface $\Phi_2 \boxtimes \Phi_1$. As we braid two punctures the first mutation Φ_1 causes a shower of solitons going from one Wigner droplet to another (see fig.3.5 and fig.3.2):



The next shower of solitons corresponding to Φ_2 has the following form:



Notice that the solitons corresponding to the most left path in Φ_1 and Φ_2 coincide. Nevertheless, degeneracy of this soliton is expected to be 1. So we just smoothly combine these pictures getting a family of solitons:

$$\Phi_2 \boxtimes \Phi_1 \sim \prod_i (\mathbb{C} \oplus \mathbb{C}[\Psi[\mathfrak{s}_i]]) \quad (3.111)$$

Where \mathfrak{s}_i are following solitons:



Factors in this product are ordered according to counterclockwise order of the corresponding soliton direction. So first appear solitons corresponding to Φ_1 then those corresponding to Φ_2 . Similarly we do for $\Phi_4 \boxtimes \Phi_3$. Eventually, the expression for the \mathcal{R} -interface takes the following form:

$$\mathcal{R} = S \boxtimes \prod_j^{\widehat{}} (\mathbb{C} \oplus \mathbb{C}[\Psi[\tilde{\mathfrak{s}}_j]]) \boxtimes \prod_i^{\widehat{}} (\mathbb{C} \oplus \mathbb{C}[\Psi[\mathfrak{s}_i]]) \quad (3.113)$$

Another important notice is about fermion numbers of these solitons:

$$\boxed{f[\tilde{\mathfrak{s}}] = f[\mathfrak{s}] + 1} \quad (3.114)$$

This contribution comes from the fact that the soliton \mathcal{B}_2 , or equivalently \mathcal{B}_6 , has to have a fermion number 1. Here we argue that this is the case:

$$f[\mathcal{B}_2] = f[\mathcal{B}_6] = 1 \quad (3.115)$$

Indeed we can use the known solution of 2d CFT.

Indeed if composed \mathcal{B}_2 and \mathcal{B}_3 give just a central element that is twice (on two sheets) a monodromy of around the singularity. Thus if we assume that \mathcal{B}_2 and \mathcal{B}_3 have the same homological degree then it is equal to degree of a path around singularity. If we assume that singularity in point p is analogous to singularity of $(2s+1, 1)$ -degenerate CFT field in (3.51) then we know asymptotic behavior of the soliton partition function in the neighbourhood of $z \rightarrow p$ is given by OPE of degenerate fields:

$$\Phi_{(2,1)}(0)\Phi_{(2s+1,1)}(z) \sim \underbrace{z^{\Delta_{(2(s\pm 1)+1,1)} - \Delta_{(2s+1,1)} - \Delta_{(2,1)}}}_{\sim \Xi(z)} \Phi_{(2(s\pm 1)+1,1)}(0) \quad (3.116)$$

Thus for the partition function Z according to (3.50) we have:

$$Z(z) \sim e^{\xi \log(z-p)}, \quad (3.117)$$

$$\xi = \frac{1}{2}(\Delta_{2s} + \Delta_{2s+2,1}) - \Delta_{2s+1,1} - \Delta_{2,1} + 2\alpha_{2s+1,1}\alpha_{2,1} = \frac{1}{2} + \underbrace{b^2}_{\lambda} \frac{2s+1}{2}$$

Where α 's are corresponding Liouville momenta defined as $\Delta(\alpha) = \alpha(Q - \alpha)$. As expected from the asymptotic form (3.28) it has two contributions: the one proportional to λ corresponds to the fields' action, while the second contribution is due to fermion determinant sign. And the loop around puncture p gives us a desired fermion number:

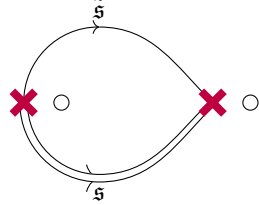
$$f[\mathcal{B}_2] = \frac{1}{\pi i} (\xi|_{b^2 \rightarrow 0}) \oint_p d \log(z-p) = 1 \quad (3.118)$$

Let us consider the simplest case of the fundamental representation. In this case all the puncture parameters $k_a = 1$ and we have one either filled or unoccupied vacuum. In this case eq.(3.113)

simplifies drastically

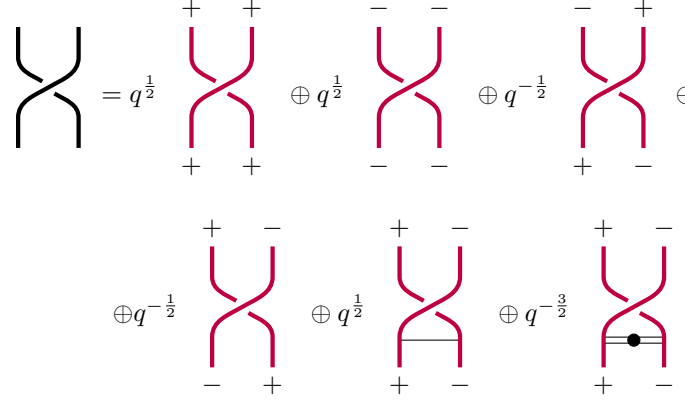
$$\mathcal{R}_\square = S \oplus S \boxtimes \mathbb{C}[\Psi[\tilde{\mathfrak{s}}]] \oplus S \boxtimes \mathbb{C}[\Psi[\mathfrak{s}]] \quad (3.119)$$

Where we have just two non-trivial solitons (we will denote them by single and double line):



$$(3.120)$$

Let us describe this interface pictorially (compare to the vertex model (1.79)):



$$(3.121)$$

Here we imply a correspondence spin projections and states in LG model: $|+\rangle \sim |0, 1\rangle$ and $|-\rangle \sim |1, 1\rangle$. A horizontal line and a double line imply solitons $\tilde{\mathfrak{s}}$ and \mathfrak{s} correspondingly interpolating between Wigner droplets. A black bullet implies that the second soliton carries fermion degree $[+1]$. We will comment on this abbreviation and other elements necessary to construct MSW complex in what follows.

3.4.5 Spin- $\frac{1}{2}$ \mathcal{R} -interface in the model with symmetry breaking

A similar picture can be derived in the LG model with an extra symmetry breaking *à la* [48]:

$$W = \sum_{a,i} k_a \log(q_a - w_i) - 2 \sum_{i < j} \log(w_i - w_j) + c \sum_i w_i \quad (3.122)$$

The case of the fundamental representation corresponds to $k_a = 1$. In this case the vacuum equation reads:

$$\sum_a \frac{1}{w_i - q_a} - \sum_{j \neq i} \frac{2}{w_i - w_j} + c = 0, \quad \forall i \quad (3.123)$$

If the number of punctures q_a is greater or equal to the number of LG fields w_i we can present the following solution in the limit $c \rightarrow \infty$:

$$w_i = q_{a(i)} - \frac{1}{c} + O\left(\frac{1}{c^2}\right) \quad (3.124)$$

where $q_{a(i)}$ is some choice among the punctures. Thus we see that LG fields are accompanying punctures. This model is similar to the one of Wigner droplets, though in this case droplets consist of only **one** LG field. Mutual repulsion between LG particles prevents them from gathering near one puncture.

Similarly to consideration in s.3.4.4 we have two states for strands: $+ -$ puncture is accompanied by one LG particle, $- -$ the puncture is not accompanied by LG particles:

$$\begin{array}{c} + \\ | \\ + \end{array} \sim \begin{array}{c} \times \\ \circ \\ q_a \end{array}, \quad \begin{array}{c} - \\ | \\ - \end{array} \sim \begin{array}{c} \circ \\ q_a \end{array} \quad (3.125)$$

Consider the simplest non-trivial case of two punctures and one LG field (we have used notations $q_1 = x, q_2 = y$):

$$W = \log(x - w) + \log(y - w) + cw \quad (3.126)$$

There are two possible vacua:

$$w_- = x - \frac{1}{c} + O\left(\frac{1}{c^2}\right), \quad w_+ = y - \frac{1}{c} + O\left(\frac{1}{c^2}\right) \quad (3.127)$$

Following techniques of [19] we draw vanishing cycles (all the possible ζ -soliton equation solutions beginning in a concrete vacuum), in this case this is simple since we need to solve a one dimensional differential equation:

$$\text{Im} [\zeta^{-1} \partial_w W(w(s)) \dot{w}(s)] = 0, \quad (3.128)$$

where the dot means a derivative with respect to proper time s . We can write two cycles for each vacuum since in the neighbourhood of the vacuum w_* there are two solutions to equation (3.128):

$$w(s) = \pm \frac{2s}{\sqrt{\zeta^{-1} \partial_w^2 W|_{w_*}}} + O(s^2) \quad (3.129)$$

In our situation vanishing cycles have the following form (we have chosen $\zeta = 1$):

$$w_- \times \overbrace{\circ x}$$

$$w_+ \times \overbrace{\circ y}$$

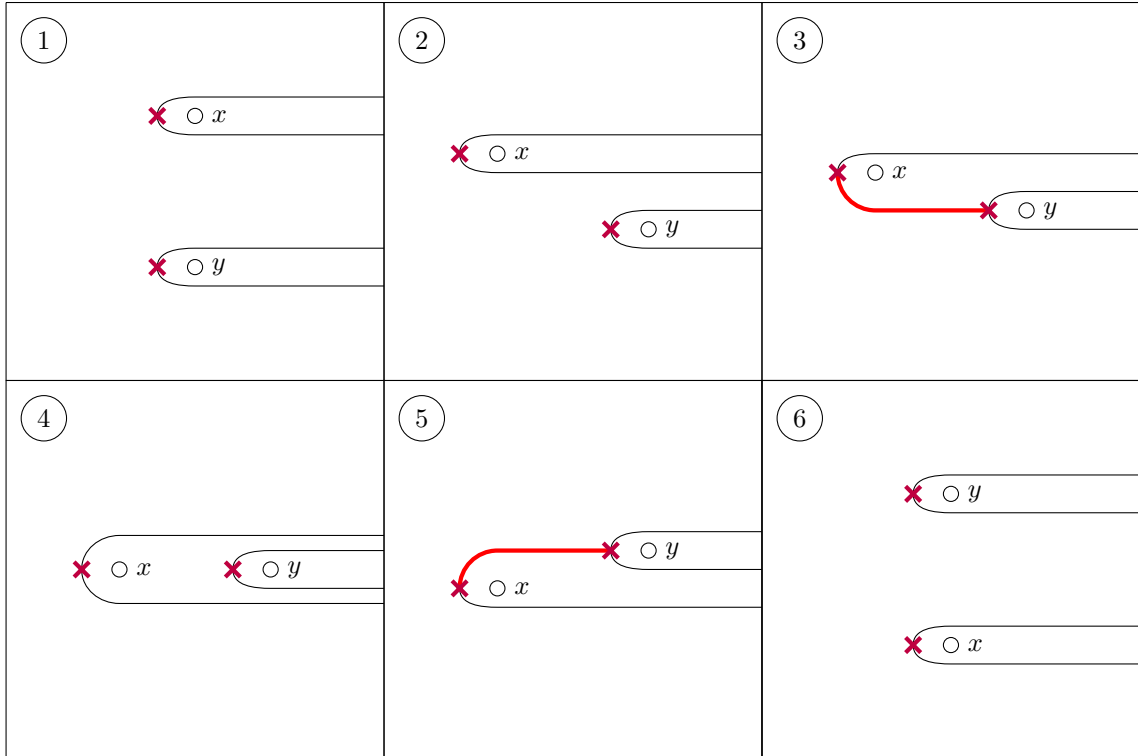


Figure 3.6: Solitons in LG model with symmetry breaking.

As we braid x and y counterclockwise we get a consequent set of “film frames” (see fig.3.6). Solitons appear when either two vanishing cycles intersect or a vanishing cycle emanated from one vacuum merges to another vacuum.

As we see on these figures only two solitons interpolate between $w_- \rightarrow w_+$ (marked by red on the figure). It is not complicated to calculate their contribution to the q -degree and confirm equivalence to (3.121)⁶.

⁶Actually it is not so simple to calculate the corresponding η -invariants to derive corresponding fermion numbers. For example the naive formula $\frac{1}{2\pi i} \int d \log W''$ gives the wrong answer in this case. So we omit here this calculation using results of the previous section.

In the same way we can calculate an inverse \mathcal{R} -interface, or \mathcal{R}^{-1} -interface

$$\begin{aligned}
 \begin{array}{c} \text{---} \\ \diagdown \\ \diagup \\ \text{---} \end{array} &= q^{-\frac{1}{2}} \begin{array}{c} + \quad + \\ \text{---} \\ \diagdown \\ \diagup \\ \text{---} \\ + \quad + \end{array} \oplus q^{-\frac{1}{2}} \begin{array}{c} - \quad - \\ \text{---} \\ \diagdown \\ \diagup \\ \text{---} \\ - \quad - \end{array} \oplus q^{\frac{1}{2}} \begin{array}{c} + \quad - \\ \text{---} \\ \diagdown \\ \diagup \\ \text{---} \\ - \quad + \end{array} \oplus \\
 &\oplus q^{\frac{1}{2}} \begin{array}{c} - \quad + \\ \text{---} \\ \diagdown \\ \diagup \\ \text{---} \\ + \quad - \end{array} \oplus q^{\frac{3}{2}} \begin{array}{c} - \quad + \\ \text{---} \\ \diagdown \\ \diagup \\ \text{---} \\ - \quad + \end{array} \oplus q^{-\frac{1}{2}} \begin{array}{c} - \quad + \\ \text{---} \\ \diagdown \\ \diagup \\ \text{---} \\ - \quad + \end{array} \oplus
 \end{aligned} \tag{3.130}$$

3.4.6 Soliton spectrum of the model with symmetry breaking

Let us define the spectrum of solitons in a simple model with symmetry breaking with two punctures and one dynamical field defined by superpotential (3.126).

Following [47, Sec.18.4.7] we define the target space X as a minimal cover of the configuration space $\text{Conf}(n, \mathcal{C})$ of *indistinguishable* n Landau-Ginzburg fields on the Riemann surface \mathcal{C} with punctures where superpotential W is single-valued. To be specific $X = \widehat{\text{Conf}}(n, \mathcal{C})/H$ where $\widehat{\text{Conf}}(n, \mathcal{C})$ is a universal cover, and H is a subgroup of π_1 given by the kernel of the homomorphism $\oint dW : \pi_1 \rightarrow 2\pi i\mathbb{Z}$. So that $\pi_1(X) = H$.

Solitons in this model are charged with respect to the Abelianization of H . We will denote this charge by h .

The critical points on X , defined by condition $\partial_{w_i} W = 0$, form a \mathbb{Z} -torsor when one takes into account the sheet on which the critical point lies.

On the other hand the soliton equation (1.31) and its boundary conditions are well-defined on the configuration space $\text{Conf}(n, \mathcal{C})$. Generically (if parameters k_a are integer) a soliton solution can be lifted to any sheet of W , though mutual difference between sheet numbers is fixed by the soliton phase ζ , since a change of this difference shifts the soliton central charge by $2\pi i$, and unless $\zeta = \pm i$ shifts ζ .

Nevertheless, there is a specific soliton set $\mathfrak{S}_{\alpha\alpha}(i)$ that do not change a position of a critical point in the configuration space, though it makes a transition between different sheets of W -cover. We call these solutions ‘‘Bloch’’ solitons in analogy to Bloch wave functions spreading in periodic structures like crystals [13].

The homotopy class of a path corresponding to Bloch solitons is simple. It is just a loop (clockwise or counterclockwise) around a puncture (see fig.3.7).

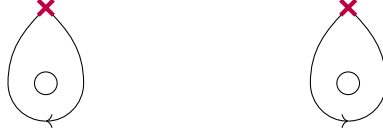


Figure 3.7: Example of Bloch counterclockwise and clockwise solitons.

Independently of the puncture positions q_α these solitons have a central charge $\pm 2\pi i$ (if we set all $k_a = 1$) so they can not form binding points at arbitrary interface phase ζ except a special value $\zeta = \pm i$. In the case $\zeta = \pm i$ to construct a generic classical ground state we will have to consider Bloch waves on the W -cover along similar construction in QCD (see e.g.[89, chap.13.5]). So we have chosen arbitrary phase ζ different from $\pm i$. Generically Bloch solitons are very similar, the only thing distinguishing them from each other is the flavour charge h , or, in other words, we distinguish punctures Bloch solitons are winding around.

Although Bloch solitons do not form binding points they are still present in the spectrum of the theory and they do contribute to the instanton field configurations as boosted soliton trajectories as we will see in what follows.

So, summarizing, the soliton spectrum consists of a \mathbb{Z} -torsor over a finite set of solitons: \mathcal{X} , \mathcal{Y} , \mathcal{B}_x , \mathcal{B}_y and corresponding anti-solitons \mathcal{X}^{-1} , \mathcal{Y}^{-1} , \mathcal{B}_x^{-1} , \mathcal{B}_y^{-1} (see fig.3.8) flowing in the opposite direction.

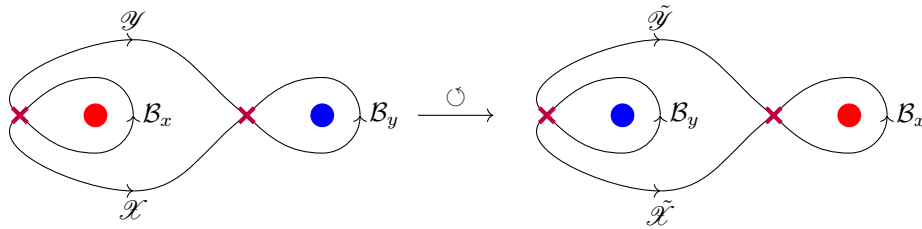


Figure 3.8: Soliton spectrum in the model with symmetry breaking

Suppose we smoothly braid punctures x and y and denote the braiding angle as θ . Notice we can not map homotopically the soliton spectrum at $\theta = 0$ to the soliton spectrum at $\theta = \pi$. Indeed as we tune smoothly θ we get following transition between solitons:

$$\mathcal{Y} \rightarrow \tilde{\mathcal{X}}^{-1}, \quad \mathcal{B}_x \rightarrow \mathcal{B}_x, \quad \mathcal{B}_y \rightarrow \mathcal{B}_y$$

Solitons \mathcal{X} and $\tilde{\mathcal{Y}}^{-1}$ have the same central charge, though they can not be homotopically mapped

to each other since their flavour charges are different:

$$h[\mathcal{X}] = h[\mathcal{Y}] + h[\mathcal{B}_x] \neq h[\mathcal{Y}] + h[\mathcal{B}_y] = h[\tilde{\mathcal{Y}}^{-1}] \quad (3.131)$$

Since there is no homotopy map in the field space connecting two spatial field configurations with different flavour charges we expect the flavour charge h to be conserved in the Yang-Yang-Landau-Ginzburg theory.

So the system undergoes a phase transition crossing a stability wall (see fig.3.9, solitons that remain stable across the wall we marked by solid line, solitons decaying or recombining are marked by a dashed line). On this wall soliton \mathcal{X} decays to \mathcal{Y} and \mathcal{B}_x that go through the wall smoothly, meanwhile soliton $\tilde{\mathcal{Y}}^{-1}$ recombines from \mathcal{Y} and \mathcal{B}_y .

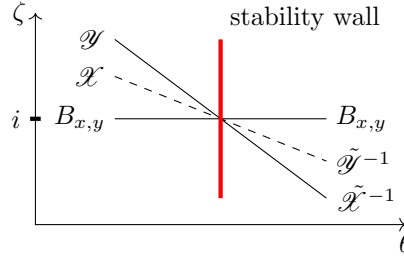


Figure 3.9: Phase transition in the model with symmetry breaking

3.5 Spin- $\frac{1}{2}$ knot(link) (co-)homology

3.5.1 Instantons in Landau-Ginzburg model

First we review a construction of instantons in LG model following [47].

We perform the Wick rotation ($t \rightarrow -i\tau$) and consider field configurations in the Euclidean space-time. A ζ -instanton “self-duality” equation in the LG model (\mathbb{Q}_ζ -fixed point condition) takes the following form:

$$(\partial_x + i\partial_\tau)\phi^i = \frac{i\zeta}{2} g^{i\bar{j}} \frac{\partial \bar{W}}{\partial \bar{\phi}^{\bar{j}}} \quad (3.132)$$

Recall that ζ_0 -soliton is a constant in time field configuration satisfying (3.132) for ζ_0 :

$$\partial_x \varphi_{\zeta_0}^i(x) = \frac{i\zeta_0}{2} g^{i\bar{j}} \frac{\partial \bar{W}}{\partial \bar{\phi}^{\bar{j}}} \Big|_{\phi_i = \varphi_{\zeta_0}^i(x)} \quad (3.133)$$

Consider a μ -boost (rotation) in Euclidean space-time:

$$\begin{pmatrix} x \\ \tau \end{pmatrix} \rightarrow \begin{pmatrix} \cos \mu & \sin \mu \\ -\sin \mu & \cos \mu \end{pmatrix} \begin{pmatrix} x \\ \tau \end{pmatrix} \quad (3.134)$$

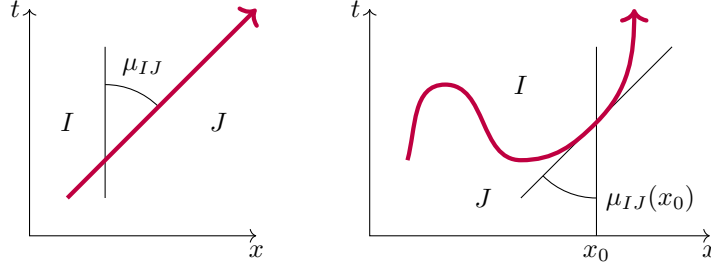


Figure 3.10: Straight and curved instanton trajectories.

A boosted configuration

$$\hat{\phi}^i(x, \tau) := \varphi_{\zeta_0}^i(x \cos \mu + \tau \sin \mu) \quad (3.135)$$

satisfies (3.132) with $\zeta = \zeta_0 e^{i\mu}$. Hence ζ -instantons can be constructed as moving boosted ζ_0 -solitons, the boost amount reads $\mu = \text{Arg} \frac{\zeta}{\zeta_0}$.

Solitons interpolating between I 'th and J 'th vacua can be viewed as a localized field configuration: a domain wall at a collective coordinate X_0 . The phase of the soliton ζ_{IJ} is given by the superpotential difference between I 'th and J 'th vacua:

$$\zeta_{IJ} = \frac{\Delta W_{IJ}}{|\Delta W_{IJ}|} \quad (3.136)$$

Therefore instantons are domain walls in the space-time bent at a certain angle:

$$\mu_{IJ} = -\text{Arg} \frac{\zeta^{-1} \Delta W_{IJ}}{|\Delta W_{IJ}|} \quad (3.137)$$

Or we can write its trajectory explicitly using collective coordinates $X(s)$ and $T(s)$:

$$\frac{dX(s)}{ds} = \frac{\text{Im} [\zeta^{-1} \Delta W_{IJ}]}{|\Delta W_{IJ}|}, \quad \frac{dT(s)}{ds} = \frac{\text{Re} [\zeta^{-1} \Delta W_{IJ}]}{|\Delta W_{IJ}|} \quad (3.138)$$

Where s is a proper time along the trajectory. Since we would like to consider interfaces with the superpotential $W(x)$ depending explicitly on the spatial coordinate x the domain walls are curved:

$$\frac{dX(s)}{ds} = \frac{\text{Im} [\zeta^{-1} \Delta W_{IJ}(X(s))]}{|\Delta W_{IJ}(X(s))|}, \quad \frac{dT(s)}{ds} = \frac{\text{Re} [\zeta^{-1} \Delta W_{IJ}(X(s))]}{|\Delta W_{IJ}(X(s))|} \quad (3.139)$$

These equations give rise to the curved web formalism of [47] to construct instantons in the LG model. See, for example, fig. 3.10.

To construct a curved web one needs also vertices representing soliton scattering processes (see fig.3.11). So we get joints of domain walls separating some fan of vacua $\{I_1, I_2, \dots, I_n\}$.

This process implies a conservation of the central charge. Indeed $Z_{IJ} = W_I - W_J$, thus we get:

$$Z_{I_1 I_2} + Z_{I_2 I_3} + \dots + Z_{I_n I_1} = 0 \quad (3.140)$$

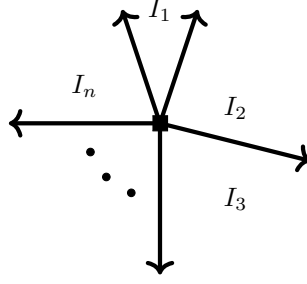


Figure 3.11: Bulk vertices

Calculation of explicit contributions of the vertices is not an easy task. One should explicitly solve the ζ -instanton equation (3.132) with boundary condition associated to the vacua fan $\{I_1, I_2, \dots, I_n\}$. For our purposes we need only to know if certain vertex is non-zero, or correspondingly the instanton process associated to this vertex is allowed. We will comment on the calculation of these vertices in sec.3.5.3.4.

As well we have boundary vertices. These vertices appear as soliton contributions to quasi-classical LG wave-functions forming the MSW complex. An IJ -soliton appears at a specific coordinate x of the interface when $\text{Im} [\zeta^{-1} \Delta W_{IJ}] = 0$. As we see from eq.(3.139) these boundary vertices represent binding points at future and past infinity for the instanton trajectory.

Eventually we will have soliton contribution corresponding to caps and cups, they correspond to binding rays of certain phase ζ constraining boundary conditions at spatial $\pm\infty$.

To contribute to the \mathbb{Q}_ζ -matrix element the instanton solution should carry one zero fermion mode. We can count zero fermion modes using supersymmetry. It implies that we should associate one fermion mode to each modulus of the solution. Indeed suppose we consider a family of solutions to (3.132) $\phi(x, \tau | r_1, \dots, r_n)$ parameterized by moduli r_1, \dots, r_n . To each modulus we can associate a tangent vector $\delta\phi^i$ to solutions of (3.132) in the space of field configurations:

$$(\partial_x + i\partial_\tau)\delta\phi^i = \frac{i\zeta}{2} g^{i\bar{j}} \left(\partial_{\bar{j}\bar{k}}^2 \bar{W} \delta\bar{\phi}^{\bar{k}} - g^{l\bar{j}} \Gamma_{kl}^i \partial_{\bar{j}} \bar{W} \delta\phi^k - g^{i\bar{l}} \Gamma_{\bar{k}\bar{l}}^{\bar{j}} \partial_{\bar{j}} \bar{W} \delta\bar{\phi}^{\bar{k}} \right) \quad (3.141)$$

Combined together with its conjugate counterpart these two equations can be reformulated in the form:

$$\nabla \Psi = 0 \quad (3.142)$$

Where ∇ is the Dirac operator acting on the fermions and $\Psi = (i\zeta^{-\frac{1}{2}} \delta\phi^i, i\zeta^{\frac{1}{2}} \delta\bar{\phi}^{\bar{i}})$. Eventually, we have one-to-one correspondence between fermion zero modes and moduli:

$$\psi_-^i \longleftrightarrow i\zeta^{-\frac{1}{2}} \delta\phi^i, \quad \bar{\psi}_+^{\bar{i}} \longleftrightarrow i\zeta^{\frac{1}{2}} \delta\bar{\phi}^{\bar{i}} \quad (3.143)$$

Consider for simplicity a MSW complex consisting of two quasi-classical states Ψ_1 and Ψ_2 on an interface of degree 0 and 1 correspondingly:

$$\mathbb{M} = \mathbb{C}[\Psi_1^{(0)}] \oplus \mathbb{C}[\Psi_2^{(1)}] \quad (3.144)$$

Now suppose $\Psi_1^{(0)}$ has two solitons at x_1 and x_2 :

$$\Psi_1^{(0)} = \begin{array}{c} \xrightarrow{I} \quad \xrightarrow{J} \quad \xrightarrow{K} \\ \text{---} \quad \text{---} \quad \text{---} \\ \quad \quad \quad \color{green}\blacksquare \quad \color{red}\blacksquare \\ \quad \quad \quad x_1 \quad x_2 \end{array} \xrightarrow{x} \quad (3.145)$$

Similarly we assume $\Psi_2^{(0)}$ has also two solitons at x_3 and x_4 correspondingly:

$$\Psi_2^{(1)} = \begin{array}{c} \xrightarrow{I} \quad \xrightarrow{L} \quad \xrightarrow{K} \\ \text{---} \quad \text{---} \quad \text{---} \\ \quad \quad \quad \color{orange}\blacksquare \quad \color{red}\blacksquare \\ \quad \quad \quad x_3 \quad x_4 \end{array} \xrightarrow{x} \quad (3.146)$$

Then, in principle, we can expect the following instanton configuration:

$$(3.147)$$

Notice that instanton trajectories are approaching boundary binding points asymptotically, though some of the trajectories connecting web to the boundary vertices should be straight, otherwise the instanton configuration has more moduli than 1 and does not contribute to the \mathbb{Q}_ζ -matrix element.

The presented field configuration has exactly one modulus T_0 , so it can be moved forwards and backwards in time. So we conclude

$$\langle \Psi_2^{(1)} | \mathbb{Q}_\zeta | \Psi_1^{(0)} \rangle = \pm 1 \quad (3.148)$$

The concrete sign of this matrix element is determined by the determinant of Dirac operator in the instanton background or by orientation of the form $\Psi_2 \wedge \star \mathbb{Q}_\zeta \Psi_1$ along the steepest descend path ([59] or [47, Appendix F]). We will comment on the sign computation in sec.3.5.2 and sec.3.7.4.

To conclude this subsection let us explicitly calculate an example of a curved web representing instanton in the cubic model of a simpleton (see sec.3.3.2).

Without loss of generality we choose x -dependence of the parameter z to be $z(x) = e^{2\pi i x}$ and the ζ -phase to be 1. The quasi-classical state corresponding to path a (see eq.(2.21)) does not contain solitons, while the state corresponding to a' contains two solitons at phases 0 and $\frac{2\pi}{3}$, or at x -coordinates 0 and $\frac{1}{3}$:

$$\Psi_{s(a)} = \overrightarrow{\hspace{10em} + \hspace{10em}} \quad (3.149)$$

$$\Psi_{s(a')} = \overrightarrow{\hspace{10em} + \hspace{1em} \blacksquare \hspace{1em} - \hspace{1em} \blacksquare \hspace{1em} + \hspace{10em}} \quad (3.150)$$

$0 \qquad \qquad \qquad \frac{1}{3}$

Substitute (3.82) into (3.139). This gives us the following equation for the trajectory:

$$\frac{dX}{ds} = -\sin 3\pi X, \quad \frac{dT}{ds} = \cos 3\pi X \quad (3.151)$$

These equations can be easily solved:

$$T(X) = T_0 - \frac{1}{3\pi} \log \sin 3\pi X \quad (3.152)$$

We depict schematically this trajectory on fig.3.12.

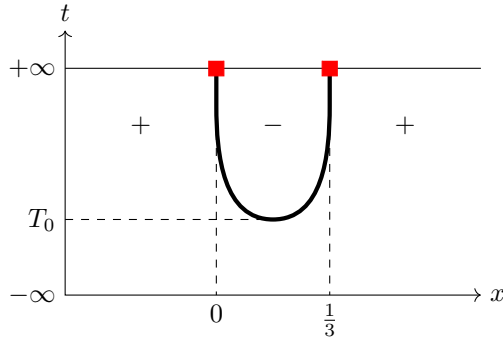


Figure 3.12: Instanton curved web for a simpleton.

As we see the instanton is represented by a domain wall separating $+$ and $-$ vacua and interpolating between two soliton configurations: no solitons in the past infinity, a soliton – anti-soliton configuration (we depicted soliton boundary vertices by red squares) in the future infinity.

This instanton field configuration has one free parameter t_0 that is a one real collective coordinate. Hence in the quantum theory we have **exactly one** fermion zero mode associated to this collective coordinate. This means that the instanton carries fermion number 1 as it is expected.

3.5.2 Why is $\mathbb{Q}_\zeta^2 = 0$?

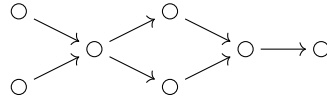
As for now we can define if for two states Ψ_1 and Ψ_2 the matrix element $\langle \Psi_2 | \mathbb{Q}_\zeta | \Psi_1 \rangle$ is zero or non-zero, and generically we can scale non-zero matrix element to be ± 1 .

The concrete sign of this matrix element is given by a relative sign of the top form $\Psi_2 \wedge \star \mathbb{Q}_\zeta \Psi_1$ and the volume form on the field space [59]. Both forms are infinite dimensional, so this complicates the problem of defining the matrix element sign.

Suppose we have a collection of cochain generators. Associate to them nodes of a graph. Two nodes corresponding to generators of degree f ψ and of degree $f + 1$ χ if $\langle \chi | \mathbb{Q}_\zeta | \psi \rangle \neq 0$ we connect by an arrow

$$\begin{array}{ccc} \psi & & \chi \\ \circ & \longrightarrow & \circ \end{array} \quad (3.153)$$

Then we can represent a complex as an oriented graph, say,



First suppose the graph is a tree. Without loss of generality starting from any root we can choose orientation of each form in the nodes in such a way that all the edges correspond to matrix element $+1$.

Though if the graph has loops some edges are constrained to have definite sign by pre-chosen orientation in nodes.

Consider the simplest loop:

$$\begin{array}{ccccc} & & \beta & & \\ & +1 & \nearrow & +1 & \\ \alpha & \circ & & \circ & \gamma \\ & +1 & \searrow & x & \\ & & \delta & & \end{array} \quad (3.154)$$

So we start with a root α , then fix matrix elements along edges going to node β , then γ , and from α to δ , thus orientations in all the nodes are fixed. So matrix element x is automatically determined by this data. The complex reads:

$$\mathbb{M} = \left(0 \rightarrow \mathbb{C}[\alpha] \xrightarrow{\mathbb{Q}_\zeta^{(21)}} \mathbb{C}[\beta] \oplus \mathbb{C}[\delta] \xrightarrow{\mathbb{Q}_\zeta^{(32)}} \mathbb{C}[\gamma] \rightarrow 0 \right) \quad (3.155)$$

The differential reads:

$$\mathbb{Q}_\zeta^{(21)} = \begin{pmatrix} 1 \\ 1 \end{pmatrix}, \quad \mathbb{Q}_\zeta^{(32)} = \begin{pmatrix} 1 & x \end{pmatrix} \quad (3.156)$$

Then condition $\mathbb{Q}_\zeta^2 = \mathbb{Q}_\zeta^{(32)}\mathbb{Q}_\zeta^{(21)} = 1 + x = 0$ implies $x = -1$.

Let us motivate this sign from field theory. We should calculate explicitly how the sign of the form differs for two paths $\alpha \rightarrow \beta \rightarrow \gamma$ and $\alpha \rightarrow \delta \rightarrow \gamma$.

Let us start with approximate ground state in the Landau-Ginzburg theory. We just use an infinite dimensional analog of formula (3.10):

$$|\Psi\rangle = e^{-\sum_n |\kappa_n| \int |\delta\phi_n^i|^2 dx} \left(\prod_{n:\kappa_n < 0} \bar{\psi}_{n,+}^i \right) \left(\prod_{n:\kappa_n > 0} \bar{\psi}_{n,-}^i \right) |0\rangle \quad (3.157)$$

Where $\delta\phi_n^i$ is n -th eigenfunction of the Dirac operator ∇ :

$$\partial_x \delta\phi_n^i - \frac{i\zeta}{2} g^{i\bar{j}} \left(\partial_{\bar{j}k}^2 \bar{W} \delta\bar{\phi}_n^{\bar{k}} - g^{l\bar{j}} \Gamma_{kl}^i \partial_{\bar{j}} \bar{W} \delta\phi_n^k - g^{i\bar{l}} \Gamma_{kl}^{\bar{j}} \partial_{\bar{j}} \bar{W} \delta\bar{\phi}_n^{\bar{k}} \right) = -i\kappa_n \delta\phi_n^i \quad (3.158)$$

Here we used slightly loose notations. Indeed, after some energy level the spectrum becomes continuous. So by a sum over states we imply both a sum over discrete spectrum and an integral over continuous one.

If we considered a quasi-classical state in the free (spatial translationally invariant) Landau-Ginzburg theory as a perturbation to a solitonic solutions there was a modulus corresponding to spatial translations and correspondingly a fermion zero mode. So the ground state is double degenerate. This degeneration disappears in the presence of the interface since the translation invariance is broken and there is no fermion zero mode.

In other words the zero mode gets a correction $\Delta\kappa_0$ to its eigenvalue that is either negative or positive.

We can estimate the correction to the eigenvalue using simple perturbation theory:

$$\Delta\kappa_n = \text{Re} \left[\zeta^{-1} \int dx \frac{\partial^2(W - \tilde{W})}{\partial\phi^i \partial\phi^j} \frac{\delta\phi_n^i}{\|\delta\phi_n^i\|} \frac{\delta\phi_n^j}{\|\delta\phi_n^j\|} \right] \quad (3.159)$$

Where W is a superpotential of an interface and \tilde{W} is a superpotential of a free theory. We can make the difference between these potentials as negligible as possible, thus fermion zero mode eigenvalue correction is non-zero but small, much smaller than a typical eigenvalue order Λ that is of order of a soliton mass.

In this coordinates the supercharges has the following form:

$$\begin{aligned} \mathbb{Q}_\zeta &= \sum_n \int dx \left[ig_{i\bar{j}} \psi_{n,-}^i (|\kappa_n| - \tilde{\kappa}_n) \delta\bar{\phi}_n^{\bar{j}} - i\zeta^{-1} g_{i\bar{j}} \bar{\psi}_{n,+}^{\bar{i}} (|\kappa_n| - \tilde{\kappa}_n) \delta\phi_n^j \right] \\ \bar{\mathbb{Q}}_\zeta &= \sum_n \int dx \left[ig_{i\bar{j}} \bar{\psi}_{n,-}^{\bar{i}} (|\kappa_n| + \tilde{\kappa}_n) \delta\phi_n^j - i\zeta^{-1} g_{i\bar{j}} \psi_{n,+}^i (|\kappa_n| + \tilde{\kappa}_n) \delta\bar{\phi}_n^{\bar{j}} \right] \end{aligned} \quad (3.160)$$

Where $\tilde{\kappa}_n$ is the true n -th eigenvalue differing from κ_n by instanton contributions.

We keep track only of fermion variables, so we suppress all the indices. Fermion zero modes are highly localized on solitons. Indeed, if we assume a soliton to have a form of a kink, approximately Heaviside step function $\theta(x)$, then fermion zero mode wave function is given by $\theta'(x) = \delta(x)$ (see (3.143)). We will denote a mode localized at coordinate x as $\bar{\psi}_\pm(x)$. Solitons corresponding to a single line (3.213) bring in $\bar{\psi}_-(x)$ -modes, while those corresponding to double line bring in $\bar{\psi}_+(x)$ -modes.

So suppose we have a state Ψ with a collection of binding points \mathcal{B} , $\mathcal{B} = \mathcal{B}^- \sqcup \mathcal{B}^+$, where \mathcal{B}^- are binding points for what $\Delta\kappa_0 < 0$, and \mathcal{B}^+ are those with $\Delta\kappa_0 > 0$ correspondingly.

Then we write a form corresponding to the state Ψ as

$$\Psi \sim \prod_{x_b^- \in \mathcal{B}^-} \bar{\psi}_+(x_b^-) \prod_{x_b^+ \in \mathcal{B}^+} \bar{\psi}_-(x_b^+) \wedge \Omega \quad (3.161)$$

where Ω is a form corresponding to higher energy modes.

In these terms the supercharge takes the following form:

$$\mathbb{Q}_\zeta \sim \left(\sum_{i^+ \in \mathcal{R}^{+1}} \bar{\psi}_+(x_{i^+}) + \sum_{i^- \in \mathcal{R}^{-1}} \psi_-(x_{i^-}) \right) \wedge \quad (3.162)$$

Where \mathcal{R}^{+1} is a collection of binding points corresponding to \mathcal{R} -interfaces and \mathcal{R}^{-1} is a collection of binding points corresponding to \mathcal{R}^{-1} -interfaces.

Typical loop situation (3.154) arises when we have a kink-anti-kink ‘‘bubble’’ when kink and anti-kink appear from the vacuum and merge back creating something else. For example, consider two consequently glued \mathcal{R} -interfaces. We have two possibilities: binding point given by a single line trajectory (3.213) bound to the first interface located at x_1 and binding point given by a double line trajectory bound to the second interface and located at x_2 , or vice versa:

$$\beta \sim \bar{\psi}_+(x_2)\bar{\psi}_-(x_1) \wedge \Omega_\beta, \quad \delta \sim \bar{\psi}_+(x_1)\bar{\psi}_-(x_2) \wedge \Omega_\delta \quad (3.163)$$

Suppose there are no binding points on states α and γ :

$$\alpha \sim \Omega_\alpha, \quad \gamma \sim \Omega_\gamma \quad (3.164)$$

Now consider path $\alpha \rightarrow \beta$. First the action of \mathbb{Q}_ζ gives a new mode $\psi_+(x_2)$, then one of the high energy modes ψ_- becomes a low energy mode, but it does not intersect the zero eigen value to preserve the fermion number:

$$\Omega_\alpha \xrightarrow{\mathbb{Q}_\zeta} \bar{\psi}_+(x_2) \wedge \Omega_\alpha \xrightarrow{\text{flow}} \bar{\psi}_+(x_2)\bar{\psi}_-(x_1) \wedge \Omega_\beta \quad (3.165)$$

Now consider path $\beta \rightarrow \gamma$. The action of the supercharge gives a mode $\bar{\psi}_+(x_1)$ and the mode $\bar{\psi}_-(x_1)$ returns back to high energy modes. So we reconstruct the whole path $\alpha \rightarrow \beta \rightarrow \gamma$:

$$\begin{aligned} \Omega_\alpha \xrightarrow{\mathbb{Q}_\zeta} \bar{\psi}_+(x_2) \wedge \Omega_\alpha \xrightarrow{\text{flow}} \bar{\psi}_+(x_2)\bar{\psi}_-(x_1) \wedge \Omega_\beta \xrightarrow{\mathbb{Q}_\zeta} \\ \xrightarrow{\mathbb{Q}_\zeta} \bar{\psi}_+(x_1)\bar{\psi}_+(x_2)\bar{\psi}_-(x_1) \wedge \Omega_\beta \xrightarrow{\text{flow}} \bar{\psi}_+(x_1)\bar{\psi}_+(x_2) \wedge \tilde{\Omega} \end{aligned} \quad (3.166)$$

On the other hand if we move along path $\alpha \rightarrow \delta \rightarrow \gamma$ modes $\bar{\psi}_+(x_1)$ and $\bar{\psi}_+(x_2)$ appear in different order:

$$\begin{aligned} \Omega_\alpha \xrightarrow{\mathbb{Q}_\zeta} \bar{\psi}_+(x_1) \wedge \Omega_\alpha \xrightarrow{\text{flow}} \bar{\psi}_+(x_1)\bar{\psi}_-(x_2) \wedge \Omega_\beta \xrightarrow{\mathbb{Q}_\zeta} \\ \xrightarrow{\mathbb{Q}_\zeta} \bar{\psi}_+(x_2)\bar{\psi}_+(x_1)\bar{\psi}_-(x_2) \wedge \Omega_\beta \xrightarrow{\text{flow}} \bar{\psi}_+(x_2)\bar{\psi}_+(x_1) \wedge \tilde{\Omega} \end{aligned} \quad (3.167)$$

Obviously, two resulting forms differ by the sign:

$$\underbrace{\langle \gamma | \mathbb{Q}_\zeta | \beta \rangle}_{+1} \underbrace{\langle \beta | \mathbb{Q}_\zeta | \alpha \rangle}_{+1} = - \underbrace{\langle \gamma | \mathbb{Q}_\zeta | \delta \rangle}_x \underbrace{\langle \delta | \mathbb{Q}_\zeta | \alpha \rangle}_{+1} \quad (3.168)$$

Or, as we expected $x = -1$.

3.5.3 Homotopy

3.5.3.1 Interface homotopy and complex quasi-isomorphism

In supersymmetric quantum mechanics it is shown that supercharge cohomologies are invariant under homotopic changes of the superpotential and metric on the manifold. Similar is expected in the Landau-Ginzburg theory, so we expect the invariance of the constructed knot cohomology. In this section we will present an explicit check of this invariance.

Following the usual idea (see sec.1.5) this check is made locally in elementary homotopic moves called Reidemeister moves.

So first we will be ensured that invariance can be reduced to local homotopy. This is non-trivial statement, since generically the very cohomology is not local, we can not cut out arbitrary braid from a knot and assume it will be a proper subcomplex.

Afterwards we verify the Reidemeister moves II and III.

To prove isomorphism of cohomological groups we use simple reasoning following [47, sec.10.7].

Consider two chain complexes V and V' endowed with degree 1 differentials Q and Q' . A degree d linear map $U : V \rightarrow V'$ is called chain map if it satisfies

$$Q'U = (-1)^d UQ \quad (3.169)$$

If we have two chain maps $U : V \rightarrow V'$ and $U' : V' \rightarrow V$ and their composition is homotopic to an identity map:

$$\begin{aligned} UU' &= \mathbf{Id} + QT + TQ \\ U'U &= \mathbf{Id} + QT' + T'Q \end{aligned} \tag{3.170}$$

then the following cohomologies are isomorphic:

$$H^\bullet(V, Q) \cong H^\bullet(V', Q') \tag{3.171}$$

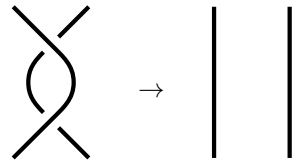
As U and U' we can use homotopy map between different knot diagrams. Speaking plainly under this map the true ground states are mapped to each other, while fake ones merge or appear by pairs as they have non-zero matrix element with the supercharge \mathbb{Q}_ζ .

As it is proposed in [47, sec.10.7] we consider moduli $q_\alpha(x, \sigma)$ depending on the homotopy parameter σ in (3.48) and change homotopically the superpotential with “time” σ as fast as we like, then we get a curved web defined by the instanton equation (3.132) with τ substituted by σ and boundary conditions given by V and V' . Notice that in this time we break the time translation invariance of the equation, the curved web has no moduli, and the map U has degree 0 opposed to the differential.

If we change knot embedding very slowly we can assume that solitons remain in their binding points, so we can construct the web just by following migration of the binding points as we transform the knot diagram. This reasoning allows us to work locally. If we move the knot diagram only inside some part of the knot, only binding points in this part are moving. In what follows we check consequently the Reidemeister moves II and III necessary for claiming that the presented construction gives braid invariants. To construct knot invariants we will introduce braid closures and verify Reidemeister move I afterwards.

3.5.3.2 Reidemeister move II

Consider homotopic Reidemeister move II:



The diagram shows a crossing of two strands on the left, which is transformed via an arrow into two parallel vertical strands on the right. The strands are black lines.

$$\tag{3.172}$$

The l.h.s. gives following contributions to the MSW complex:

$$\begin{aligned}
 \mathbb{M} \left(\begin{array}{c} \text{diagram} \end{array} \right) &= \begin{array}{cccc} \text{diagram} & \text{diagram} & \text{diagram} & \text{diagram} \\ \oplus & \oplus & \oplus & \oplus \end{array} \\
 &\oplus q \left(\begin{array}{cc} \text{diagram} & \text{diagram} \\ \oplus & \oplus \end{array} \right) \oplus q^{-1} \left(\begin{array}{cc} \text{diagram} & \text{diagram} \\ \oplus & \oplus \end{array} \right)
 \end{aligned} \tag{3.173}$$

First four terms do not contain binding points and transform to corresponding contributions from the r.h.s. under homotopy as they are. Remnant terms in two subcomplexes \mathbb{M}_1 and \mathbb{M}_{-1} of q -degrees 1 and -1 correspondingly merge to each other under homotopy. Indeed notice that binding points correspond to solitons that have homologically equivalent paths, so these solitons have the same central charge Z . We can construct $\text{Im}[\zeta^{-1}Z]$ as a function of position x and homotopy “time” σ (see fig.3.13).

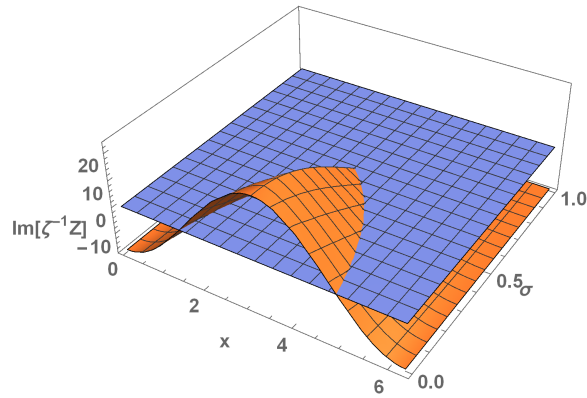


Figure 3.13: Soliton central plot

Horizontal plane on this figure denotes the zero level. Intersection line of the plot with zero level

corresponds to solutions $x_0(\sigma)$ of $\text{Im}[\zeta^{-1}Z(x_0, \sigma)] = 0$, soliton positions as a function of homotopy “time” σ . Thus as we see two binding points are moving towards each other merging.

3.5.3.3 Reidemeister move III

The most intriguing part is homotopic Reidemeister move III:

(3.174)

Both sides contain multiple contributions.

We can divide all the generators of complexes at both sides of this map into groups. Homotopy does not change the boundary conditions of the interfaces. So the homotopy invariance condition for a group of generators mapping boundary state $|a\rangle \otimes |b\rangle \otimes |c\rangle$ to $|a'\rangle \otimes |b'\rangle \otimes |c'\rangle$ as $\mathbf{Htpy}_{a,b,c}^{a',b',c'}$.

We start with \mathbf{Htpy}_{---} :

(3.175)

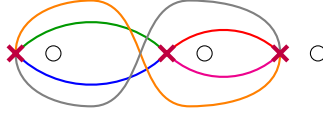
Notice the homotopy map does not change gradings. In this case neither of two sides has binding points, thus the homotopy map is just a literal homotopic map of braids. Other groups \mathbf{Htpy}_{--+} , \mathbf{Htpy}_{-+-} , \mathbf{Htpy}_{-++} , \mathbf{Htpy}_{+--} , \mathbf{Htpy}_{+-+} and \mathbf{Htpy}_{+++} are checked in the same simple fashion.

Now we turn to the next type of groups \mathbf{Htpy}_{-+-} :

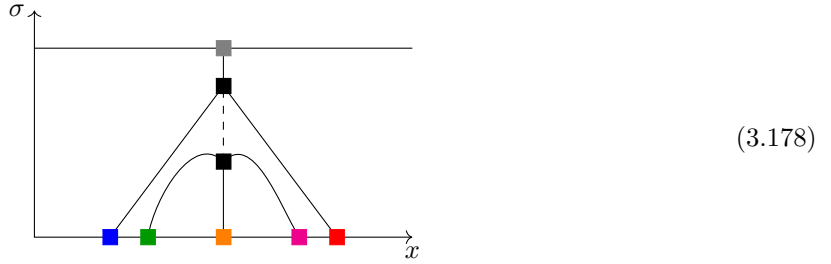
(3.176)

This case can be also checked in a simple way. Notice there is one-to-one map of each q -graded component, the whole top twist goes to the bottom twist under homotopy map, the binding points

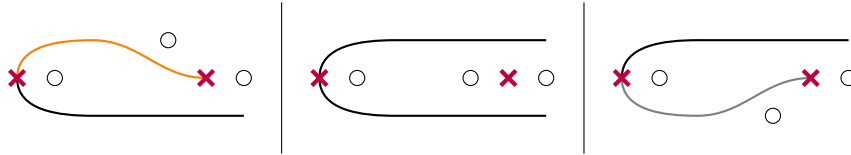
paths in the field space (all the solitons flow from left to right):



From this diagram it is clear that generators containing binding points marked by orange, green and magenta colors are fake and merge through a 3-valent bulk vertex, while a generator containing binding points marked by red and blue is mapped to the generator on r.h.s. We can depict both curved webs corresponding to two these processes on the following diagram:



Notice that solitons marked by orange and gray binding points have **identical** central charges. Thus they give identical trajectories in the curved web formalism. This trajectory is continued by dashed line on the presented diagram. So two black bulk vertices that are lying on this dashed line might be merged into a multi-valent vertex, then maps \mathbb{Q}_ζ and U might be much more complicated. Nevertheless this does not happen since this solitons are not present in the spectrum at the same point of the parameter space, moreover chambers where gray and orange solitons are presented in the spectrum of the theory are separated by another chamber where there are no solitons of this central charge. We can observe this explicitly by constructing steepest descend paths:



In the same way we check \mathbf{Hpty}_{++-} . All the other possible groups are empty so we have demonstrated homotopy invariance of the cohomology under Reidemeister move III.

3.5.3.4 Bulk vertices from wall-crossing formulae

Generically to define a bulk vertex one should solve the instanton equation (3.132) at a certain point in the parameter space q_α and with boundary conditions prescribed by the vacua fan $\{I_1, \dots, I_n\}$:

$$\beta_{I_1, \dots, I_n}[q_\alpha] = \begin{array}{c} \begin{array}{c} \nearrow I_1 \\ \leftarrow I_n \\ \rightarrow I_2 \\ \searrow I_3 \\ \vdots \end{array} \end{array} \quad (3.179)$$

This is a pretty tough problem. Nevertheless, we know a problem of a similar difficulty: to derive an explicit solution of the soliton equation (1.31). And usually in practice an explicit form of the solution is irrelevant, instead we are interested in solution degeneracies. Similarly, in our construction we are interested if a vertex $\beta_{I_1, \dots, I_n}[q_\alpha]$ is zero or non-zero, if a solution to the instanton equation exists or not.

A nice way around to determine soliton degeneracies is so called wall-crossing formulae (as we discussed in chapter 2). We use a contribution of existing soliton solutions to a parallel transport with tt^* -connection. Then homotopy invariance of this parallel transport following from tt^* -connection flatness allows us to relate soliton contributions and, consequently, soliton degeneracies in different areas of the parameter space.

Suppose we have chosen two homotopic paths φ and φ' on the parameter space, consider two MSW complexes $\mathbb{M}(\varphi)$ and $\mathbb{M}(\varphi')$ corresponding to interfaces associated to these paths. Homotopy invariance implies equivalence of Euler characteristics:

$$\chi(\mathbb{M}(\varphi)) = \chi(\mathbb{M}(\varphi')) \quad (3.180)$$

Let us make this statement tautological, assume $\mathbb{M}(\varphi)$ and $\mathbb{M}(\varphi')$ are one-dimensional:

$$\mathbb{M}(\varphi) = (0 \rightarrow \mathbb{C}[\Psi_1] \rightarrow 0), \quad \mathbb{M}(\varphi') = (0 \rightarrow \mathbb{C}[\Psi_2] \rightarrow 0) \quad (3.181)$$

The homotopy should act on this spaces as a non-degenerate linear map U :

$$\langle \Psi_2 | U | \Psi_1 \rangle \neq 0 \quad (3.182)$$

Sometimes we could do even better and reduce U to just one vertex $\beta[q_a]$, thus we conclude $\beta[q_a] \neq 0$.

Let us illustrate this statement with an example.

Consider a superpotential (3.122) with three punctures q_1 , q_2 and q_3 and one LG field w . As before we consider three vacua $w_i^* \sim q_a - \frac{1}{c}$ and fix phase ζ to be 1. Let us draw Lefschetz thimbles

for all vacua and consider two homotopic paths A and B in the space (q_1, q_2, q_3) :

(3.183)

This example illustrates the simplest wall-crossing formula. Indeed we get following MSW complexes for two paths:

$$\mathbb{M}(A) = (\mathbb{C} + \mathbb{C}[\Psi[E_{12}]]) \boxtimes (\mathbb{C} + \mathbb{C}[\Psi[E_{23}]]) \quad (3.184)$$

$$\mathbb{M}(B) = (\mathbb{C} + \mathbb{C}[\Psi[E_{23}]) \boxtimes (\mathbb{C} + \mathbb{C}[\Psi[E_{13}]) \boxtimes (\mathbb{C} + \mathbb{C}[\Psi[E_{12}])$$

Where E_{ij} is a soliton interpolating between vacua i and j . Expanding both sides and comparing two Chan-Paton factors we conclude that two following complexes are quasi-isomorphic:

$$\mathbb{C}[\Psi[E_{12}]] \boxtimes \mathbb{C}[\Psi[E_{23}]] \sim \mathbb{C}[\Psi[E_{13}]] \quad (3.185)$$

Though both this complexes are one-dimensional, so there is U mapping co-chain on the left hand side to co-chain on the right hand side that is saturated by a vertex β_{123} that is non-zero.

On the other hand we also can easily say when β is zero: when a *stability* condition is broken. Indeed solitons forming domain walls of the vacua fan should be solutions to the ζ -soliton equation (1.31). Each IJ -ray outgoing from the bulk vertex has its own phase ζ_0 , if the soliton equation (1.31) fails to have a solution interpolating between I and J vacua at phase ζ_0 the corresponding vertex β is zero. So $\beta[q_\alpha]$ are not constant functions of parameters q_α . Rather, they jump across the stability walls.

Let us make a concluding remark for this subsection. Notice the presented bulk vertex β_{123} is described by a homotopic interpolation between two field configurations: first a soliton brings a LG field to a vacant vacuum near a puncture by some moment x_1 , then we change spatial coordinate x further, at some moment $x_2 > x_1$ appears another soliton that carries this field away. Smoothly shrinking the difference $x_2 - x_1$ to zero we get a homotopic interpolation between a trajectory in the field space where the LG field stays “for a while” in the critical point and a trajectory without delays (see fig.3.14).

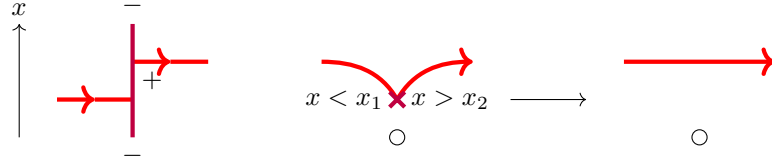


Figure 3.14: Gluing field trajectories I.

Consider an opposite situation: the first soliton makes a vacuum near a puncture unoccupied, then the next soliton fills it in (see fig.3.15). A similar analysis requires the bulk vertex for this process to be non-zero (for instance, a subcomplex of q -degree 2 in $\mathbf{Htpy}_{++-}^{++-}$ (see sec.3.5.3.3 for a definition)), thus there is a 3-valent bulk vertex connecting two trajectories in the field space depicted in fig.3.15. Notice, effectively, two LG fields denoted by red and blue colors turn out to be permuted during this transition, though we think of them as *indistinguishable*, so boundary critical points are equivalent. This 3-valent vertex breaks flavour charge conservation (see sec.3.5.4.1).

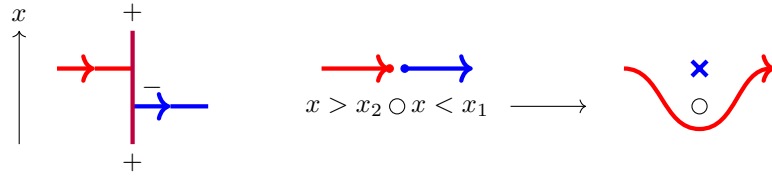


Figure 3.15: Gluing field trajectories II.

3.5.4 Fusing/defusing interfaces

3.5.4.1 Quantum algebra heritage

Fusing/defusing interfaces can be defined as D-branes, i.e. proper boundary conditions for a theory with two punctures.

We will try to approach this problem in an indirect way. Let us start with some generic boundary conditions for a theory with two punctures. We will denote the very interfaces as “black boxes”. We can define what critical points one can as an output of this interface. There are two strands, i.e. two vacant vacua, they are filled or unoccupied (we will denote them as $\mathfrak{V}_{(ij)}$):

$$\cup = \begin{matrix} ++ \\ \blacksquare \\ \mathfrak{V}_{(++)} \end{matrix} \oplus \begin{matrix} +- \\ \blacksquare \\ \mathfrak{V}_{(+-)} \end{matrix} \oplus \begin{matrix} -+ \\ \blacksquare \\ \mathfrak{V}_{(-+)} \end{matrix} \oplus \begin{matrix} -- \\ \blacksquare \\ \mathfrak{V}_{(--)} \end{matrix} \tag{3.186}$$

where we have denoted the defusing interface as a “black box”. A major property of this interface is that it does not change vacuum properties of the empty theory, it behaves as it is not present. For example, in the quantum algebra construction of Jones polynomials analogous expression (q -Clebsch-Gordan coefficient, see sec.1.5) behaves as a trivial representation under action of $U_q(sl_2)$ generators K , E and F . Using co-multiplication formulae one can derive explicitly expressions for corresponding q -Clebsch-Gordan coefficients.

After categorification we lose a naive notion of $U_q(sl_2)$ -generators. Still we can mimic their action by braids:

1. $\Delta(K)$: Total charge of the defusing interface should be 0. This cuts possible boundary conditions at the spatial $+\infty$:

$$\cup = \mathfrak{A}_{(+ -)} \oplus \mathfrak{A}_{(- +)} \tag{3.187}$$

2. $\Delta(E)$, $\Delta(F)$: These generators can be interpreted as following braid – defusing interface relations:

$$\text{Braid 1} = \text{Braid 2} = \text{Braid 3} \tag{3.188}$$

The second condition is similar to *two* copies of one $\Delta(F)$ co-product condition:

$$\text{Configuration 1} \oplus \text{Configuration 2} \sim \emptyset \tag{3.189a}$$

$$\text{Configuration 3} \oplus \text{Configuration 4} \sim \emptyset \tag{3.189b}$$

Indeed the soliton brings the Landau-Ginzburg field to a strand of the defusing interface so it acts as lowering operator F . Although we have two types of solitons (denoted by a single and by a double line).

It turns out that these two conditions are inconsistent with the conservation of the flavour charge discussed in sec.3.4.6. Different flavour charge of soliton configurations implies that they lie in different homology classes of trajectories on the field space, so there is no a smooth field configuration connecting them. This in turns implies that there are no instantons carrying flavour charge, thus the flavour charges of two complex generators homotopic to \emptyset should coincide. Comparing (3.189a) and (3.189b) we get two inconsistent relations for flavour charges of defusing interfaces:

$$h[\mathfrak{V}_{(-+)}] = h[\mathfrak{V}_{(+-)}] + h[\mathcal{X}_1] \quad (3.190a)$$

$$h[\mathfrak{V}_{(-+)}] = h[\mathfrak{V}_{(+-)}] + h[\mathcal{X}_2] \quad (3.190b)$$

where \mathcal{X}_1 and \mathcal{X}_2 are solitons depicted in fig.3.16. This is an apparent *obstacle* in the construction of the fusing/defusing interfaces and therefore knot invariants.

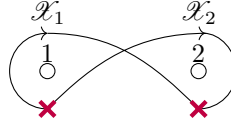


Figure 3.16: Solitons \mathcal{X}_1 and \mathcal{X}_2 .

The obstacle would be eliminated if there were an instanton interpolating between Bloch solitons, and the flavour charge was not conserved.

From now on let us **add** this transition by hand: we posit that there is a finite action process breaking flavour charge conservation. Let us draw consequences of this assumption.

All the states become h -scalars, so all the Bloch solitons are indistinguishable, there are just counterclockwise \mathcal{B} and clockwise \mathcal{B}^{-1} Bloch solitons and it can be put to any puncture with filled vacuum, all these situations are equivalent. Furthermore, we are allowed to eliminate the stability wall in the model with symmetry breaking (see fig.3.9). Soliton \mathcal{X} is smoothly continued by soliton $\tilde{\mathcal{X}}^{-1}$ across the wall.

It is worth mentioning that we have already encountered a case when the h -charge is not conserved (see fig.3.15). We have transition between two trajectories p_1 and p_2 in the field space. The corresponding change of the flavour charge can be calculated in the following way:

$$\Delta h = h(p_2) - h(p_1) = h(p_2 \circ p_1^{-1}) = \frac{1}{2}h(p_2 \circ p_1^{-1} \circ p_2 \circ p_1^{-1}) \quad (3.191)$$

Where \circ denotes concatenation of paths. The path $p_2 \circ p_1^{-1} \circ p_2 \circ p_1^{-1}$ can be easily drawn (see fig.3.17) To see that this path in the field space of two LG fields has non-trivial homotopy class it is enough



Figure 3.17: Path $p_2 \circ p_1^{-1} \circ p_2 \circ p_1^{-1}$

to deform the parameter corresponding to the puncture $k_a \rightarrow 1 + \epsilon_a$, in this case the central charge (2.8) of this path reads $2\pi i \epsilon_a$, and the path having a non-zero central charge is non-contractible.

3.5.4.2 Construction of fusing/defusing interfaces

Having broken flavour symmetry one can propose some model of fusing/defusing interfaces.

We will try to present a model of fusing/defusing interfaces made of \mathcal{R} -interfaces considered already.

In the algebraic sense the twist map (R -matrix) is a map

$$R : \mathcal{A} \otimes \mathcal{A} \rightarrow \mathcal{A} \otimes \mathcal{A} \quad (3.192)$$

where \mathcal{A} is a representation of $U_q(sl_2)$. It splits into “s-channels” according to the spin in the isotopical decomposition of the tensor product of representations $\mathcal{A} \otimes \mathcal{A}$:

$$\begin{aligned} \mathcal{A} \otimes \mathcal{A} &\rightarrow \mathcal{A} \rightarrow \mathcal{A} \otimes \mathcal{A} \\ R_{j_1, j_2}^{j_2, j_1} &= \sum_j C_{j_1, j_2}^j f(j) C_j^{j_2, j_1} \end{aligned} \quad (3.193)$$

where $f(j)$ are certain coefficients (“s-channel amplitudes”) depending only on the spin j of the intermediate representation.

So our strategy is to choose just one channel containing the trivial representation:

$$R_0 = (\mathcal{A} \otimes \mathcal{A} \rightarrow \mathbb{C} \rightarrow \mathcal{A} \otimes \mathcal{A}) \quad (3.194)$$

Then we can apply this artificial interface as fusing(defusing) interface.

Generically we consider a knot (link) diagram consisting of n strands embedded into a n -strand braid. We continue fusing and defusing interfaces to R_0 -interfaces:

$$\cap \rightarrow \begin{array}{c} \cup \\ \cap \end{array}, \quad \cup \rightarrow \begin{array}{c} \cup \\ \cap \end{array} \quad (3.195)$$

Generically to an n -strand braid we associate a linear map $\mathcal{A}^{\oplus n} \rightarrow \mathcal{A}^{\oplus n}$. R_0 -interfaces act as projectors on the space of maps $\mathcal{A}^{\oplus n} \rightarrow \mathcal{A}^{\oplus n}$ giving just a component of the n -strand map being knot

invariant. Similarly, a categorified version will act, we will consider a subspace of the perturbative ground states space of a braid, cohomologies of this subspace will give a knot invariant.

Now we present a proper channel choice without a proof, afterwards we will show that our choice satisfies Reidemeister move I.

As fusing interface we choose fourth and sixth terms of \mathcal{R} -interface (3.212a), as defusing interface we choose third and fifth terms of the inverse \mathcal{R} -interface (3.212b) with proper rescaling:

$$\begin{aligned}
 \cap &= q^{\frac{1}{2}} \begin{array}{c} + \quad - \\ | \quad | \\ \diagdown \quad / \\ | \quad | \\ - \quad + \end{array} \oplus q^{-\frac{1}{2}} \begin{array}{c} + \quad - \\ | \quad | \\ \diagdown \quad / \\ | \quad | \\ + \quad - \end{array} \\
 \cup &= q^{\frac{1}{2}} \begin{array}{c} - \quad + \\ | \quad | \\ \diagup \quad \diagdown \\ | \quad | \\ - \quad + \end{array} \oplus q^{-\frac{1}{2}} \begin{array}{c} + \quad - \\ | \quad | \\ \diagdown \quad / \\ | \quad | \\ - \quad + \end{array}
 \end{aligned} \tag{3.196}$$

Let us show that this construction is invariant under change of the knot diagram by adding or subtracting strands. In particular, we would like to state the following equivalence:

$$| = \cup \tag{3.197}$$

Let us decompose both sides:

$$| = \begin{array}{c} - \\ | \\ - \end{array} \oplus \begin{array}{c} + \\ | \\ + \end{array}, \quad \cup = \begin{array}{c} + \quad + \quad - \\ | \quad | \quad | \\ \diagdown \quad / \quad \diagdown \quad / \\ | \quad | \quad | \\ - \quad + \quad + \end{array} \oplus \begin{array}{c} - \quad + \quad - \\ | \quad | \quad | \\ \diagup \quad \diagdown \quad \diagup \quad \diagdown \\ | \quad | \quad | \\ - \quad + \quad - \end{array} \tag{3.198}$$

First notice that both sides give equivalent number of term with equivalent critical points at spatial boundaries and fermion numbers.

Thus we would like to show that the l.h.s. and r.h.s. give identical contributions to \mathbb{Q}_ζ matrix elements. A typical instanton is represented by a boosted soliton \mathcal{X} moving, say, towards positive x -direction, for example,

$$\begin{array}{c} x \quad - \\ \uparrow | \\ - \\ + \end{array} \xrightarrow{\mathbb{Q}_\zeta} \begin{array}{c} x \quad - \\ \uparrow | \\ + \\ + \end{array} \mathcal{X} \quad \begin{array}{c} \tau \\ \xrightarrow{\mathcal{X}} \\ x \end{array} \tag{3.199}$$

At the r.h.s. we have an analogous process:

(3.200)

Notice that the soliton marked as 2 is the future binding point, so its trajectory is straight vertical line. Thus the process goes through a 4-valent bulk vertex. The coordinate of the 4-valent vertex is defined by x -coordinate of the soliton 2, so this curved sub-web does not have internal moduli, if there is a 1-parametric curved web saturating \mathbb{Q}_c matrix element at the l.h.s. there is analogous curved web at the r.h.s. and vice versa. So the MSW complexes for knots with a straight strand and the strand with a hump are quasi-isomorphic.

In what follows we will use fusing(defusing interfaces) at spatial infinities, so we can simplify their representation by untwisting their diagrams:

$$\cap = q^{\frac{1}{2}} \begin{array}{c} - \quad + \\ | \quad | \\ - \quad + \end{array} \oplus q^{-\frac{1}{2}} \begin{array}{c} - \quad + \\ | \quad | \\ + \quad - \end{array} \quad (3.201)$$

$$\cup = q^{\frac{1}{2}} \begin{array}{c} - \quad + \\ | \quad | \\ + \quad - \end{array} \oplus q^{-\frac{1}{2}} \begin{array}{c} + \quad - \\ | \quad | \\ + \quad - \end{array} \quad (3.202)$$

Solitons that were binding points in the representation (3.196) are boundary conditions for instanton configurations at spatial infinities, binding rays, they define curved web trajectories that go to spatial infinity at certain fixed angle.

An important property of the fusing/defusing interfaces is that it performs an “inversion” of strands, in this way we can relate, for example, \mathcal{R} -interface and \mathcal{R}^{-1} -interface:

$$\begin{array}{c} \diagdown \quad \diagup \\ | \quad | \\ \diagup \quad \diagdown \end{array} = \begin{array}{c} \diagup \quad \diagdown \\ | \quad | \\ \diagdown \quad \diagup \end{array} \quad (3.203)$$

Let us decompose both sides of this equality in diagrams:

$$\begin{aligned}
 LHS = q & \begin{array}{c} \begin{array}{ccc} - & - & + \\ \diagdown & \diagup & | \\ \diagup & \diagdown & | \\ - & + & - \end{array} \\ \oplus q^{-1} & \begin{array}{ccc} + & - & - \\ \diagdown & \diagup & | \\ \diagup & \diagdown & | \\ - & + & - \end{array} \\ \oplus & \begin{array}{ccc} - & + & + \\ \diagdown & \diagup & | \\ \diagup & \diagdown & | \\ + & + & - \end{array} \\ \oplus & \begin{array}{ccc} - & + & + \\ \diagdown & \diagup & | \\ \diagup & \diagdown & | \\ + & + & - \end{array} \end{array}
 \end{aligned} \tag{3.204}$$

$$\begin{aligned}
 \oplus q & \begin{array}{ccc} + & - & + \\ \diagdown & \diagup & | \\ \diagup & \diagdown & | \\ + & + & - \end{array} \\ \oplus q^{-1} & \begin{array}{ccc} + & - & + \\ \diagdown & \diagup & | \\ \diagup & \diagdown & | \\ + & + & - \end{array} \\ \oplus & \begin{array}{ccc} + & + & - \\ \diagdown & \diagup & | \\ \diagup & \diagdown & | \\ + & + & - \end{array}
 \end{aligned}$$

$$\begin{aligned}
 RHS = q & \begin{array}{ccc} - & - & + \\ | & \diagdown & \diagup \\ | & \diagup & \diagdown \\ + & - & - \end{array} \\ \oplus q^{-1} & \begin{array}{ccc} + & - & - \\ | & \diagdown & \diagup \\ | & \diagup & \diagdown \\ + & - & - \end{array} \\ \oplus & \begin{array}{ccc} - & + & + \\ | & \diagdown & \diagup \\ | & \diagup & \diagdown \\ + & - & + \end{array} \\ \oplus & \begin{array}{ccc} - & + & + \\ | & \diagdown & \diagup \\ | & \diagup & \diagdown \\ + & - & + \end{array}
 \end{aligned} \tag{3.205}$$

$$\begin{aligned}
 \oplus q & \begin{array}{ccc} + & - & + \\ | & \diagdown & \diagup \\ | & \diagup & \diagdown \\ + & - & + \end{array} \\ \oplus q^{-1} & \begin{array}{ccc} + & - & + \\ | & \diagdown & \diagup \\ | & \diagup & \diagdown \\ + & - & + \end{array} \\ \oplus & \begin{array}{ccc} + & + & - \\ | & \diagdown & \diagup \\ | & \diagup & \diagdown \\ + & - & + \end{array}
 \end{aligned}$$

Obviously, each term in the left hand side expression is homotopic to the corresponding term in the right hand side expression. The fourth and fifth terms are homotopic through a 3-valent bulk vertex similarly to what we have discussed in sec.3.5.3.3.

3.5.4.3 Reidemeister move I

. Here we consider Reidemeister move I:

$$\begin{array}{c} \diagdown \diagup \\ \diagup \diagdown \end{array} \xrightarrow{U} \begin{array}{c} \diagdown \\ \diagup \end{array} \tag{3.206}$$

The l.h.s. of this move gives the following contribution to MSW complex:

$$\text{MI} \left(\begin{array}{c} \diagdown \diagup \\ \diagup \diagdown \end{array} \right) = q^{-\frac{3}{2}} \left[q^{\frac{1}{2}} \begin{array}{ccc} - & + \\ \diagdown & \diagup \\ \diagup & \diagdown \\ + & - \end{array} \oplus q^{-\frac{1}{2}} \begin{array}{ccc} - & + \\ \diagdown & \diagup \\ \diagup & \diagdown \\ + & - \end{array} \oplus q^{\frac{3}{2}} \left(\begin{array}{ccc} - & + \\ \diagdown & \diagup \\ \diagup & \diagdown \\ + & - \end{array} \oplus \begin{array}{ccc} - & + \\ \diagdown & \diagup \\ \diagup & \diagdown \\ + & - \end{array} \right) \right] \tag{3.207}$$

As we see the map U shifts the q -degree by $-\frac{3}{2}$ and homological degree by $+1$, so we can write

$$\begin{array}{c} \text{Diagram: a crossing with a loop on the top strand} \\ \end{array} = q^{-\frac{3}{2}} t \begin{array}{c} \text{Diagram: a simple arch} \\ \end{array} \tag{3.208}$$

This coefficient is interpreted as a change of framing, since we construct invariants not of the knots rather of thin knotted strips. The framing can be taken into account by an overall monomial pre-factor of the knot polynomial.

To confirm cohomology homotopic invariance we make an untwist of the braid top end and follow the true states mapped to each other and fake states merge by pairs.

When we untwist the braid two first terms in (3.207) are mapped to two corresponding terms in the cap interface (3.212c). The binding point at the top under the instanton equation (3.132) flow runs away to the spatial infinity.

Two complex generators in round brackets correspond to fake ground states and merge during homotopic move. Indeed notice that thin line soliton binding point if moved across the \mathcal{R} -twist becomes thick line soliton binding point. Thus in the last term binding point in the middle merges with boundary binding point at the top and they both flow to spatial infinity.

Naively, there are more Reidemeister type I moves: we can pair \mathcal{R} - or \mathcal{R}^{-1} -interface with cap or cup, so there are four possibilities. Also we can put a loop not on the cap, rather on the vertical strand. Actually, having derived (3.208) we are able to reconstruct all the others through more elementary moves we have encountered before, for example

$$\begin{array}{c} \text{Diagram: a crossing with a loop on the left strand} \\ \end{array} \stackrel{(3.203)}{=} \begin{array}{c} \text{Diagram: a crossing with a loop on the right strand} \\ \end{array} \stackrel{3.208}{=} q^{-\frac{3}{2}} t \begin{array}{c} \text{Diagram: a crossing with a loop on the top strand} \\ \end{array} \stackrel{3.197}{=} q^{-\frac{3}{2}} t \left| \begin{array}{c} \text{Diagram: a crossing with a loop on the top strand} \\ \end{array} \right. \tag{3.209}$$

To conclude this section let us consider one more type of Reidemeister move I relation:

$$\begin{array}{c} \text{Diagram: a crossing with a loop on the top strand} \\ \end{array} = q^{\frac{3}{2}} t^{-1} \begin{array}{c} \text{Diagram: a simple arch} \\ \end{array} \oplus \left(\begin{array}{c} \text{Diagram: a crossing with a loop on the top strand, top-left strand has '-' sign, top-right '+'} \\ \text{Diagram: a crossing with a loop on the top strand, top-left strand has '-' sign, top-right '+'} \end{array} \right) \tag{3.210}$$

The terms in the brackets should merge this relation to satisfy Reidemeister I move, it is easy to notice that the solitons corresponding to binding points in the last term have the same central charge though, but different flavour charge h . They are analogous to solitons \mathcal{X}_1 and \mathcal{X}_2 depicted in fig.3.16, so the fact that in sec.3.5.4.1 we have proposed charge h is unconserved is explicitly applicable in this situation, otherwise terms in the brackets can not merge and the invariance of the construction under Reidemeister I move is broken.

3.6 Summary of rules for MSW knot complex construction

Let us summarize rules to construct MSW complex in the case of the fundamental representation and show how to calculate its Poincare polynomial.

First we associate $\frac{1}{2}$ -spin states ($|+\rangle$ and $|-\rangle$) to filled or vacant vacuum near a puncture:

$$\begin{array}{c} + \\ | \\ + \end{array} \sim \begin{array}{c} \times \\ \circ \\ q_a \end{array}, \quad \begin{array}{c} - \\ | \\ - \end{array} \sim \begin{array}{c} \circ \\ q_a \end{array} \quad (3.211)$$

Now we present \mathcal{R} -interfaces, inverse \mathcal{R} -interfaces, cups and caps (the spatial x -axis is oriented vertically from the bottom to the top):

$$\begin{array}{c} \text{Diagram} \\ = q^{\frac{1}{2}} \text{Diagram} \oplus q^{\frac{1}{2}} \text{Diagram} \oplus q^{-\frac{1}{2}} \text{Diagram} \oplus \\ \oplus q^{-\frac{1}{2}} \text{Diagram} \oplus q^{\frac{1}{2}} \text{Diagram} \oplus q^{-\frac{3}{2}} \text{Diagram} \end{array} \quad (3.212a)$$

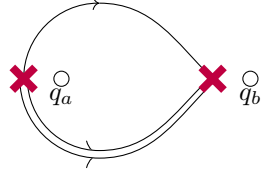
$$\begin{array}{c} \text{Diagram} \\ = q^{-\frac{1}{2}} \text{Diagram} \oplus q^{-\frac{1}{2}} \text{Diagram} \oplus q^{\frac{1}{2}} \text{Diagram} \oplus \\ \oplus q^{\frac{1}{2}} \text{Diagram} \oplus q^{\frac{3}{2}} \text{Diagram} \oplus q^{-\frac{1}{2}} \text{Diagram} \end{array} \quad (3.212b)$$

$$\text{Diagram} = q^{\frac{1}{2}} \text{Diagram} \oplus q^{-\frac{1}{2}} \text{Diagram} \quad (3.212c)$$

$$\cup = q^{\frac{1}{2}} \begin{array}{c} - \quad + \\ | \quad | \\ \text{---} \circ \text{---} \\ | \quad | \\ + \quad - \end{array} \oplus q^{-\frac{1}{2}} \begin{array}{c} + \quad - \\ | \quad | \\ | \quad | \\ | \quad | \\ + \quad - \end{array} \quad (3.212d)$$

In the interface, solitons of the two homotopy types can exist at binding points and these are indicated in equations (3.212a) – (3.212d) by horizontal single or double lines. If the soliton has fermion number f then horizontal lines with black bullet (\bullet) or white bullet (\circ) represent solitons with fermion number $f + 1$ or $f - 1$ respectively. We will not need to know the precise value of f to compute the homology, only relative fermion number matters.

Both soliton homotopy types are flowing from left to right and their trajectories on the ϕ -plane for two punctures q_a and q_b can be depicted as follows:



$$(3.213)$$

We have expanded interfaces on a segment $[x_-, x_+]$ over elementary quasi-classical LG wave functions corresponding to soliton contributions \mathcal{I}_i .

Each \mathcal{I}_i connects two LG ground states at x_- and x_+ . We call them $\partial_-(\mathcal{I})$ and $\partial_+(\mathcal{I})$.

We can **glue** two wave functions \mathcal{I}_1 and \mathcal{I}_2 corresponding to two consequent segments according to a simple rule:

$$\mathcal{I}_1 \boxtimes \mathcal{I}_2 = \begin{cases} \mathcal{I}_{12}, & \text{if } \partial_+(\mathcal{I}_1) = \partial_-(\mathcal{I}_2), \\ \emptyset, & \text{otherwise} \end{cases} \quad (3.214)$$

Moreover, $\partial_-(\mathcal{I}_{12}) = \partial_-(\mathcal{I}_1)$ and $\partial_+(\mathcal{I}_{12}) = \partial_+(\mathcal{I}_2)$.

We construct MSW complex in the following way:

1. Cut knot (link) K into “time” slices as we did in sec.3.4.1. Each slice contains either \mathcal{R} -twist or caps/cups.
2. Substitute interfaces and expand.
3. Glue wave functions with respect to the gluing rule (3.214).

As a result of this procedure we get explicitly all the chains of MSW complex $\mathbb{M}(K)$ corresponding

to the knot K as generated by quasi-classical wave functions Ψ_p ⁷:

$$\mathbb{M}(K) = \bigoplus_p \mathbb{C}[\Psi_p(K)] \quad (3.215)$$

The complex is double graded. We use **qdeg** for q -grading and **tdeg** for homological grading (fermion number). Each generator \mathcal{I} in the complex gives a homotopy class of trajectories in the field space $\phi_i(s)$ and the moduli space $q_a(s)$ we denote $\text{traj}(\mathcal{I})$ and has some amount of black bullets (●) and white bullets (○). Degrees of certain generator are defined as follows:

$$\mathbf{qdeg} \mathcal{I} = \frac{1}{\pi i} \int_{\text{traj}(\mathcal{I})} dW \quad (3.216)$$

$$\mathbf{tdeg} \mathcal{I} = \#(\bullet) - \#(\circ)$$

Let us split the complex into separate subcomplexes according to their q -degree. We write:

$$\mathbb{M}(K) = \bigoplus_{\alpha} q^{\alpha} \mathbb{M}_{\alpha}(K) \quad (3.217)$$

The differential (supercharge \mathbb{Q}_{ζ}) acts inside each component \mathbb{M}_{α} . The corresponding instanton field configuration saturating $\langle \Psi' | \mathbb{Q}_{\zeta} | \Psi \rangle$ is approximately given by curved webs. This is a collection of boosted IJ -soliton trajectories satisfying (3.139) connected by bulk vertices of different valence. A possible way of calculating bulk vertices was presented in sec.3.5.3.4.

Generically solitons trajectories can not intersect stability walls, though we have sacrificed a stability wall where flavour charge of certain solitons jumps (see sec.3.4.6), if across a wall a soliton with flavour charge h_1 becomes unstable while another soliton with a flavour charge h_2 and the same other charges becomes stable we smoothly glue their trajectories across the wall.

The sign of the matrix element $\langle \Psi' | \mathbb{Q}_{\zeta} | \Psi \rangle$ is defined by the relative sign of the top form $\Psi' \wedge \star \mathbb{Q}_{\zeta} \Psi$ with respect to the volume form on the field space. For an example of this calculation see sec.3.5.2.

Having these data we define the cohomology group of subcomplex $\mathbb{M}_{\alpha}(K)$ in a usual way:

$$H^{\bullet}(\mathbb{M}_{\alpha}(K), \mathbb{Q}_{\zeta}) = \text{Ker } \mathbb{Q}_{\zeta} / \text{Im } \mathbb{Q}_{\zeta} \quad (3.218)$$

Thus we define a framed knot invariant:

$$\mathcal{P}(q, t | K) = \sum_{\alpha, i} q^{\alpha} t^i \dim H^i(\mathbb{M}_{\alpha}(K), \mathbb{Q}_{\zeta}) \quad (3.219)$$

⁷ Here as an underlying ring we are using the complex field \mathbb{C} . We should stress that the Morse theory and the Khovanov theory imply naturally an integer structure, so a natural expectation for the underlying ring would be integer numbers \mathbb{Z} . Though we derive our MSW complex from quantum field theory, in particular it resembles a Hilbert space endowed with a conventional complex structure. In this case the complex is insensitive to a possible torsion. *However* the rules stated here make sense over \mathbb{Z} .

And we can define an unframed knot invariant analogously to (1.88).

We conjecture that the Khovanov polynomial is just a simple redefinition of this polynomial:

$$\mathcal{K}(q, t) = \mathcal{P}(qt, t) \tag{3.220}$$

3.7 Examples

3.7.1 Unknot

The unknot is the easiest calculation. Using our rules we get the following MSW complex:

$$\mathbb{M} \left(\bigcirc \right) = q \underbrace{\begin{array}{c} - \quad + \\ \text{---} \text{---} \\ | \quad | \\ \text{---} \text{---} \\ + \quad - \end{array}}_{\mathbb{C}[\Psi_1]} \oplus q^{-1} \underbrace{\begin{array}{c} - \quad + \\ \text{---} \text{---} \\ | \quad | \\ \text{---} \text{---} \\ + \quad - \end{array}}_{\mathbb{C}[\Psi_2]} \tag{3.221}$$

Obviously q -grading splits this complex in two one-dimensional subcomplexes

$$\mathbb{M}_1 = 0 \xrightarrow{\mathbb{Q}\xi} \mathbb{C}[\Psi_1] \xrightarrow{\mathbb{Q}\xi} 0, \quad \mathbb{M}_{-1} = 0 \xrightarrow{\mathbb{Q}\xi} \mathbb{C}[\Psi_2] \xrightarrow{\mathbb{Q}\xi} 0,$$

in each of them the differential acts trivially. Fermion numbers are

$$f(\Psi_1) = f_0 - 1, \quad f(\Psi_2) = f_0 + 1$$

So we conclude:

$$\mathcal{P}(q, t|\text{Unknot}) = \frac{q}{t} + \frac{t}{q} \tag{3.222}$$

Let us add a twist to the unknot and calculate its polynomial again:

$$\mathbb{M} \left(\bigcirc \right) = q^{-\frac{1}{2}} \left(\begin{array}{c} - \quad + \\ \text{---} \text{---} \\ | \quad | \\ \text{---} \text{---} \\ + \quad - \end{array} \oplus \begin{array}{c} - \quad + \\ \text{---} \text{---} \\ | \quad | \\ \text{---} \text{---} \\ + \quad - \end{array} \oplus \begin{array}{c} - \quad + \\ \text{---} \text{---} \\ | \quad | \\ \text{---} \text{---} \\ + \quad - \end{array} \right) \oplus q^{-\frac{5}{2}} \begin{array}{c} - \quad + \\ \text{---} \text{---} \\ | \quad | \\ \text{---} \text{---} \\ + \quad - \end{array} \tag{3.223}$$

Let us denote soliton wave functions as Ψ_1, Ψ_2 and so on correspondingly as they appear in this expansion. Thus we have two subcomplexes:

$$\mathbb{M}_{-\frac{1}{2}} = (0 \rightarrow (\mathbb{C}[\Psi_1] \oplus \mathbb{C}[\Psi_2]) \rightarrow \mathbb{C}[\Psi_3] \rightarrow 0), \quad \mathbb{M}_{-\frac{5}{2}} = (0 \rightarrow \mathbb{C}[\Psi_4] \rightarrow 0) \tag{3.224}$$

Cohomology of the second subcomplex can be easily calculated.

To calculate cohomology of the first complex we need to construct \mathbb{Q}_ζ -map between 0-cochain and 1-cochain. Actually we do this by explicit calculation of the \mathbb{Q}_ζ matrix elements. We will draw explicitly 1-parameter curved web families representing instantons saturating corresponding matrix elements:

$$\langle \Psi_3 | \mathbb{Q}_\zeta | \Psi_1 \rangle = 1 \sim \begin{array}{c} t \uparrow \\ +\infty \\ T_0 \\ -\infty \\ -\infty \quad +\infty \quad x \end{array} \quad , \quad \langle \Psi_3 | \mathbb{Q}_\zeta | \Psi_2 \rangle = 1 \sim \begin{array}{c} t \uparrow \\ +\infty \\ T_0 \\ -\infty \\ -\infty \quad +\infty \quad x \end{array} \quad (3.225)$$

On these pictures the future binding point corresponds to a soliton coming from \mathcal{R} -interface, and rays going to spatial $\pm\infty$ are represented by solitons form cap and cup.

So we can construct explicit \mathbb{Q}_ζ -map between 0-cochain and 1-cochain:

$$\mathbb{Q}_\zeta = \begin{pmatrix} 1 \\ 1 \end{pmatrix} \quad (3.226)$$

And the only nonzero cohomology of the subcomplex reads:

$$H^0(\mathbb{M}_{-\frac{1}{2}}, \mathbb{Q}_\zeta) = \mathbb{C}[\Psi_1 - \Psi_2] \quad (3.227)$$

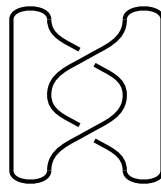
So the knot polynomial

$$\mathcal{P} \left(q, t \mid \bigcirc \right) = q^{-\frac{3}{2}} t \left(\frac{q}{t} + \frac{t}{q} \right) \quad (3.228)$$

differs from $\mathcal{P}(q, t | \text{Unknot})$ only by an overall monomial factor that appears due to change of knot framing⁸.

3.7.2 Hopf link

Let us calculate the link polynomial of a Hopf link



⁸Unframed knot polynomial, an invariant of an oriented knot can be defined by formula (1.88). For the unknot $\hat{\mathcal{P}}(q, t) = qt^{-1} + q^{-1}t$

The calculation gives us four q -subcomplexes:

$$\begin{aligned}
 \mathbb{M}(\text{Hopf}) = & q^{-3} \left(\text{Diagram 1} \right) \oplus q^{-1} \left(\text{Diagram 2} \right) \oplus q^3 \left(\text{Diagram 3} \right) \oplus \\
 & \oplus q \left(\text{Diagram 4} \oplus \text{Diagram 5} \oplus \text{Diagram 6} \right) \oplus \\
 & \left(\text{Diagram 7} \oplus \text{Diagram 8} \right)
 \end{aligned} \tag{3.229}$$

The only non-trivial contribution is \mathbb{M}_1 , we denote generators of this subcomplex $\mathbb{C}[\Psi_i]$ consequently. So we would like to calculate cohomology of the following complex:

$$\mathbb{M}_1 = (0 \rightarrow \mathbb{C}[\Psi_1] \rightarrow \mathbb{C}[\Psi_2] \oplus \mathbb{C}[\Psi_3] \rightarrow \mathbb{C}[\Psi_4] \oplus \mathbb{C}[\Psi_5]) \tag{3.230}$$

As before we find instanton field configurations saturating corresponding supercharge matrix elements.

First we present:

$$\langle \Psi_2 | \mathbb{Q}_\zeta | \Psi_1 \rangle = 1 \sim \begin{array}{c} \tau \\ +\infty \\ T_0 \\ -\infty \\ -\infty \quad +\infty x \end{array} \begin{array}{c} \text{red box} \quad \text{blue box} \\ \text{U-shaped curve} \end{array} \quad (3.231)$$

Here we marked by corresponding colors boundary binding vertices as they appear on the knot diagrams.

The same we have for the other element with permuted vertices:

$$\langle \Psi_3 | \mathbb{Q}_\zeta | \Psi_1 \rangle = 1 \sim \begin{array}{c} \tau \\ +\infty \\ T_0 \\ -\infty \\ -\infty \quad +\infty x \end{array} \begin{array}{c} \text{blue box} \quad \text{red box} \\ \text{U-shaped curve} \end{array} \quad (3.232)$$

Similarly, we construct elements $\langle \Psi_4 | \mathbb{Q}_\zeta | \Psi_2 \rangle, \langle \Psi_5 | \mathbb{Q}_\zeta | \Psi_2 \rangle$:

$$\langle \Psi_4 | \mathbb{Q}_\zeta | \Psi_2 \rangle = \langle \Psi_5 | \mathbb{Q}_\zeta | \Psi_2 \rangle = 1 \sim \begin{array}{c} \tau \\ +\infty \\ T_0 \\ -\infty \\ -\infty \quad +\infty x \end{array} \begin{array}{c} \text{orange ray} \quad \text{green ray} \\ \text{black boxes} \\ \text{red box} \quad \text{blue box} \end{array} \quad (3.233)$$

Here two rays going to spatial infinity correspond solitons coming from caps and cups. Notice that binding points from \mathcal{R} -interface (blue and red boxes on the figure) are future binding points, so vertical trajectories are exactly straight.

Analogous instantons saturate two remnant matrix elements

$$\langle \Psi_4 | \mathbb{Q}_\zeta | \Psi_2 \rangle = \langle \Psi_5 | \mathbb{Q}_\zeta | \Psi_2 \rangle = -1 \sim \begin{array}{c} \tau \\ +\infty \\ T_0 \\ -\infty \\ -\infty \quad +\infty x \end{array} \begin{array}{c} \text{orange ray} \quad \text{green ray} \\ \text{black boxes} \\ \text{blue box} \quad \text{red box} \end{array} \quad (3.234)$$

We have assigned -1 to these elements according to the chosen sign rule discussed in sec.3.5.2.

So, eventually, for the complex

$$\mathbb{M}_1 = \left(0 \longrightarrow \mathbb{C}[\Psi_1] \xrightarrow{\mathbb{Q}_\zeta^{(21)}} \mathbb{C}[\Psi_2] \oplus \mathbb{C}[\Psi_3] \xrightarrow{\mathbb{Q}_\zeta^{(32)}} \mathbb{C}[\Psi_4] \oplus \mathbb{C}[\Psi_5] \longrightarrow 0 \right) \quad (3.235)$$

we have

$$\mathbb{Q}_\zeta^{(21)} = \begin{pmatrix} 1 \\ 1 \end{pmatrix}, \quad \mathbb{Q}_\zeta^{(32)} = \begin{pmatrix} 1 & -1 \\ 1 & -1 \end{pmatrix} \quad (3.236)$$

Obviously, $\mathbb{Q}_\zeta^{(32)}\mathbb{Q}_\zeta^{(21)} = 0$ and we easily calculate cohomology:

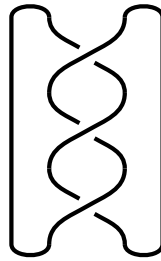
$$H^0(\mathbb{M}_1, \mathbb{Q}_\zeta) = \mathbb{C}[\Psi_4 - \Psi_5] \tag{3.237}$$

The link polynomial of the Hopf link reads:

$$\mathcal{P}(q, t|\text{Hopf}) = q^{-3}t^2 + q^{-1} + q + q^3t^{-2} = \left(\frac{q}{t} + \frac{t}{q}\right) \left(\frac{q^2}{t} + \frac{t}{q^2}\right) \tag{3.238}$$

3.7.3 Trefoil

Now we consider the trefoil knot (knot $\mathbf{3}_1$ according to the Rolfsen knot table)



Applying our strategy we get MSW complex containing five subcomplexes:

$$\mathbb{M}(\mathbf{3}_1) = \bigoplus_{i=-2}^2 q^{2i}\mathbb{M}_{2i} \tag{3.239}$$

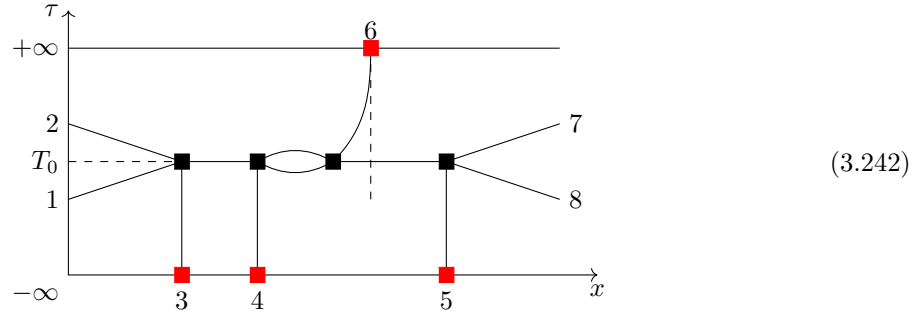
The most intriguing term is

$$\mathbb{M}_{-2} = \left[\begin{array}{c} - \quad + \quad - \quad + \\ \hline - \quad + \quad - \quad + \\ \hline 5 \\ \hline + \quad - \quad + \quad - \\ \hline 4 \\ \hline + \quad - \quad + \quad - \\ \hline 3 \\ \hline - \quad + \quad - \quad + \\ \hline 1 \quad \circ \quad 2 \\ \hline + \quad - \quad + \quad - \end{array} \right] \oplus \left[\begin{array}{c} - \quad + \quad - \quad + \\ \hline 7 \quad \bullet \quad 8 \\ \hline - \quad + \quad - \quad + \\ \hline 6 \\ \hline + \quad - \quad + \quad - \\ \hline + \quad - \quad + \quad - \end{array} \right] \tag{3.240}$$

This subcomplex is two dimensional, one generator has homological degree $[+1]$, the other has homological degree $[+2]$:

$$\mathbb{M}_{-2} = (0 \longrightarrow \mathbb{C}[\Psi_1] \longrightarrow \mathbb{C}[\Psi_2] \longrightarrow 0) \tag{3.241}$$

The matrix element $\langle \Psi_2 | Q_\zeta | \Psi_1 \rangle$ is saturated by the following field configuration:



Here we have marked binding points by corresponding numbers.

Notice here the bulk vertices are 4-valent. The choice of 4-valent vertex is dictated by necessity. Indeed consider a collision point of solitons 1, 2 and 3. For a transition associated to soliton 3 to be possible a vacant vacuum near the second strand from left should be filled and one near the third strand should be unoccupied, this is done exactly by solitons 1 and 2. So neither soliton 1 nor 2 can cross the vertical line of soliton 3 trajectory, otherwise the fan of vacua for such an intersection vertex would be inconsistent. Hence trajectories of solitons 1 and 2 should simultaneously hit trajectory of soliton 3 creating a new soliton.

Thus we have

$$H^\bullet(\mathbb{M}_{-2}, \mathbb{Q}_\zeta) = \emptyset \tag{3.243}$$

Cohomologies of the other subcomplexes can be easily calculated in the fashion of the Hopf link. So, finally, we get

$$\mathcal{P}(q, t | \mathbf{3}_1) = q^{-4}t^3 + 1 + q^2 + q^4t^{-2} \tag{3.244}$$

3.7.4 Figure-eight knot

Now we consider the figure-eight knot (knot $\mathbf{4}_1$ according to the Rolfsen knot table)



Its MSW complex contains six subcomplexes:

$$\mathbb{M}(\mathbf{4}_1) = \bigoplus_{i=0}^5 q^{2i-5} \mathbb{M}_{2i-5} \tag{3.245}$$

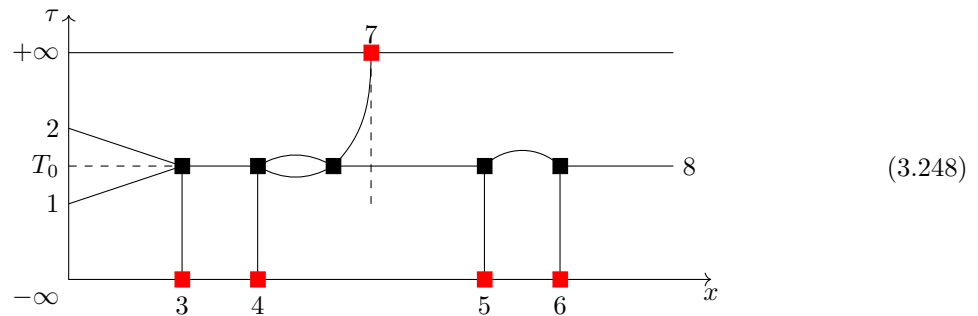
As usual subcomplex \mathbb{M}_{-5} is one dimensional:

$$\mathbb{M}_{-5} = \text{Diagram} \tag{3.246}$$

Now we consider subcomplex \mathbb{M}_{-3} :

$$\mathbb{M}_{-3} = \text{Diagram 1} \oplus \text{Diagram 2} \tag{3.247}$$

It is easy to construct the curved web corresponding to interpolating between these states. We have denoted binding points and boundary rays by numbers as they appear on the expansion diagram:



So we conclude

$$\langle \Psi_2 | Q_\zeta | \Psi_1 \rangle = 1 \tag{3.249}$$

Thus the cohomological group is empty:

$$H^\bullet(\mathbb{M}_{-3}, \mathbb{Q}_\zeta) = \emptyset \tag{3.250}$$

Complex \mathbb{M}_{-1} consists of three co-chains:

$$\mathbb{M}_{-1} = (0 \rightarrow \mathcal{C}^{(-1)} \rightarrow \mathcal{C}^{(0)} \rightarrow \mathcal{C}^{(1)} \rightarrow 0) \tag{3.251}$$

Where

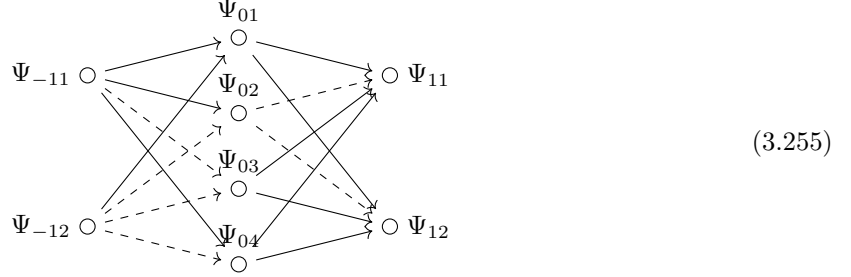
$$\mathcal{C}^{(-1)} = \text{Diagram 1} \oplus \text{Diagram 2} \tag{3.252}$$

$$\mathcal{C}^{(0)} = \text{Diagram 1} \oplus \text{Diagram 2} \oplus \text{Diagram 3} \oplus \text{Diagram 4} \tag{3.253}$$

$$\mathcal{C}^{(1)} = \text{Diagram 1} \oplus \text{Diagram 2} \tag{3.254}$$

We denote corresponding complex generators as Ψ_{ij} where i is homological degree and j is order number of the diagram as they appear in the above expansion.

Then we construct a diagram of \mathbb{Q}_ζ matrix elements (arrows go from degree $[f]$ to degree $[f+1]$, solid arrows correspond to matrix element $+1$, dashed arrows correspond to matrix elements -1):



(3.255)

It is pretty obvious how to construct curved webs corresponding to field configurations saturating all these matrix elements⁹. Instead concrete sign calculation is important, so we concentrate on it. We follow mechanism described in sec.3.5.2. So first we write out all the generators as forms on the field space. For generators of $\mathcal{C}^{(-1)}$ we have:

$$\Psi_{-11} \sim \bar{\psi}_+(x_3)\bar{\psi}_+(x_4) \wedge \Omega_{-11}, \quad \Psi_{-12} \sim \bar{\psi}_+(x_1) \wedge \Omega_{-12} \quad (3.256)$$

For generators of $\mathcal{C}^{(0)}$ we have:

$$\begin{aligned} \Psi_{01} &\sim \bar{\psi}_+(x_2)\bar{\psi}_+(x_3)\bar{\psi}_+(x_4)\bar{\psi}_-(x_1) \wedge \Omega_{01}, & \Psi_{02} &\sim \bar{\psi}_+(x_1)\bar{\psi}_+(x_3)\bar{\psi}_+(x_4)\bar{\psi}_-(x_2) \wedge \Omega_{02}, \\ \Psi_{03} &\sim \bar{\psi}_+(x_1)\bar{\psi}_+(x_2)\bar{\psi}_+(x_4)\bar{\psi}_-(x_3) \wedge \Omega_{03}, & \Psi_{04} &\sim \bar{\psi}_+(x_1)\bar{\psi}_+(x_2)\bar{\psi}_+(x_3)\bar{\psi}_-(x_4) \wedge \Omega_{04} \end{aligned} \quad (3.257)$$

For generators of $\mathcal{C}^{(1)}$ we have:

$$\Psi_{11} \sim \Omega_{11}, \quad \Psi_{12} \sim \bar{\psi}_+(x_1)\bar{\psi}_+(x_2) \wedge \Omega_{12} \quad (3.258)$$

Here by Ω we denoted a bulk of the high energy modes, and we keep an explicit track of nearly zero energy modes. We order them according to the Dirac eigenvalue, so first go $\bar{\psi}_+$ -modes that have negative Dirac operator eigenvalue, then $\bar{\psi}_-$ having positive eigenvalues. We assume that $\bar{\psi}_+$ -modes corresponding to different soliton binding points have nearly equal eigenvalues, though they are localized on the x -axis in the neighbourhood of the binding point, so we order them according to their localization x_i , where i is a number of the \mathcal{R} (\mathcal{R}^{-1})-twist as it appears on the diagram from bottom to top. We expect that the supercharge acts on the left by multiplication:

$$\mathbb{Q}_\zeta \sim (\bar{\psi}_+(x_1) + \bar{\psi}_+(x_2) + \bar{\psi}_-(x_3) + \bar{\psi}_-(x_4)) \wedge \quad (3.259)$$

⁹Though notice that in an instanton saturating matrix element, say, $\langle \Psi_{12} | \mathbb{Q}_\zeta | \Psi_{01} \rangle$ a Bloch boosted soliton appears. For discussion of properties of these solitons see sec.3.4.6.

So, for example, if we calculate an element $\langle \Psi_{11} | \mathbb{Q}_\zeta | \Psi_{-11} \rangle$:

$$\begin{aligned} \bar{\psi}_+(x_3)\bar{\psi}_+(x_4) \wedge \Omega_{-11} \xrightarrow{\mathbb{Q}_\zeta} \bar{\psi}_+(x_2)\bar{\psi}_+(x_3)\bar{\psi}_+(x_4) \wedge \Omega_{-11} \xrightarrow{\text{flow}} \\ \xrightarrow{\text{flow}} \bar{\psi}_+(x_2)\bar{\psi}_+(x_3)\bar{\psi}_+(x_4)\bar{\psi}_-(x_1) \wedge \Omega_{11} \end{aligned} \quad (3.260)$$

Here we first act by the supercharge, so a new form has a degree greater by 1, then a new $\psi_-(x_1)$ comes from the bulk of high energy modes. The bulk form actually changes though we neglect this change assuming that the sign from this change can be absorbed into the definition of the orientation.

Acting in this way, assuming that the supercharge acts on the left and appearing (disappearing) low energy modes coming from (to) the high energy bulk modes should stand on the right, we get diagram (3.255).

Or, explicitly,

$$\mathbb{Q}_\zeta^{(-10)} = \begin{pmatrix} 1 & 1 \\ 1 & -1 \\ -1 & -1 \\ 1 & -1 \end{pmatrix}, \quad \mathbb{Q}_\zeta^{(01)} = \begin{pmatrix} 1 & -1 & 1 & 1 \\ 1 & -1 & 1 & 1 \end{pmatrix} \quad (3.261)$$

And we check easily $\mathbb{Q}_\zeta^{(01)}\mathbb{Q}_\zeta^{(-10)} = 0$. It's easy to calculate cohomology of this complex:

$$H^\bullet(\mathbb{M}_{-1}, \mathbb{Q}_\zeta) = \mathbb{C}[\Psi_{01} + \Psi_{02}] \oplus \mathbb{C}[\Psi_{11} - \Psi_{12}] \quad (3.262)$$

The rest of the knot polynomial can be restored from a symmetry for a figure-eight knot:

$$\mathcal{P}(q, t | \mathbf{4}_1) = \mathcal{P}(q^{-1}, t^{-1} | \mathbf{4}_1) \quad (3.263)$$

The knot polynomial of this knot reads:

$$\mathcal{P}(q, t | \mathbf{4}_1) = q^{-5}t^3 + q^{-1}(1+t) + q(1+t^{-1}) + q^5t^{-3} \quad (3.264)$$

3.8 Further remarks

3.8.1 Cabling and higher spin link (co-)homology

One of the major advantages of field theory approach to knot homology is a natural generalization to higher spins. Indeed, spins are just encoded in parameters k_a in Yang-Yang SLG Lagrangian (3.48), and all our previous logic is applicable.

Though a concrete realization is not so trivial. Indeed, following either an approach using Wigner droplets (sec. 3.4.4), or a model with explicit symmetry breaking (sec. 3.4.5) implies pretty

tough calculations in the generic case. So instead we use a cabling trick (see for example [5]): we construct higher dimensional representations from direct products of the lower dimensional ones. A direct product in the language of Wilson lines usually implies operator product expansion. So we represent a strand of a knot carrying spin J as a collection (a “cable”, so this is the origin of trick’s name) of $2J$ strands carrying spin $\frac{1}{2}$. Though the tensor product of fundamental representations decomposes generically into a mixture of different irreducible representations. So to distill one irreducible representation one should introduce a system of projectors.

An obstacle emerging when we try to categorify the knot homology is we are loosing some natural algebraic structures of quantum algebras, so we did with the q -Clebsch-Gordan coefficients and fusing (defusing) interfaces (see sec. 3.5.4). Though we can expect that a structure corresponding to the specific series of Clebsch-Gordan coefficients $C_{J_1, J_2}^{J_1+J_2}$ should survive categorification. Indeed, in this case we expect a relation between two Yang-Yang-Landau-Ginzburg theories with different number of punctures q_α . However the theory with a puncture q and puncture parameter $k_1 + k_2$ can be represented as a limit of a theory with two punctures q_1 and q_2 with parameters k_1 and k_2 when these two punctures merge.

Thus we expect the higher spin theories are lying naturally on certain boundaries of the parameter space. So we will construct a projector from a product of $2J$ spin- $\frac{1}{2}$ representations to a spin- J representation. Let us start with a classical $U_q(sl_2)$ -algebra story.

R -matrix acts diagonally on the isotypical decomposition, in other words q -clebsch-Gordan coefficients are eigen vectors of the R -matrix:

$$\sum_{j'_1, j'_2} R_{j_1, j_2}^{j'_2, j'_1} C_{j'_2, j'_1}^j = (-1)^{j_1+j_2-j} q^{c_j - c_{j_1} - c_{j_2}} C_{j_1, j_2}^j \tag{3.265}$$

Where $c_j = j(j+1)$ is a classical sl_2 Casimir element of representation of spin j . Or, pictorially, we can rewrite this equation as (see also [66, eq.(4.8)])

$$\begin{array}{c} j \\ | \\ \text{---} \text{---} \\ / \quad \backslash \\ j_1 \quad j_2 \end{array} = (-1)^{j_1+j_2-j} q^{c_j - c_{j_1} - c_{j_2}} \begin{array}{c} j \\ | \\ \text{---} \\ / \quad \backslash \\ j_1 \quad j_2 \end{array} \tag{3.266}$$

Thus for one R -matrix and identity operator can be expanded as

$$\begin{aligned}
 \begin{array}{c} \frac{1}{2} \\ | \\ \frac{1}{2} \end{array} \begin{array}{c} j \\ | \\ j \end{array} &= \begin{array}{c} \frac{1}{2} \quad j \\ \diagdown \quad \diagup \\ \quad j - \frac{1}{2} \\ \diagup \quad \diagdown \\ \frac{1}{2} \quad j \end{array} + \begin{array}{c} \frac{1}{2} \quad j \\ \diagdown \quad \diagup \\ \quad j + \frac{1}{2} \\ \diagup \quad \diagdown \\ \frac{1}{2} \quad j \end{array} \\
 & \tag{3.267} \\
 \begin{array}{c} \frac{1}{2} \quad j \\ \diagdown \quad \diagup \\ j \quad \frac{1}{2} \end{array} &= -q^{-(j+1)} \begin{array}{c} \frac{1}{2} \quad j \\ \diagdown \quad \diagup \\ \quad j - \frac{1}{2} \\ \diagup \quad \diagdown \\ j \quad \frac{1}{2} \end{array} + q^j \begin{array}{c} \frac{1}{2} \quad j \\ \diagdown \quad \diagup \\ \quad j + \frac{1}{2} \\ \diagup \quad \diagdown \\ j \quad \frac{1}{2} \end{array}
 \end{aligned}$$

Combining these two equations we derive easily a recursive equation for the projector to spin j state:

$$P_{j+\frac{1}{2}} = (1 + q^{2j+1})^{-1} \left[\begin{array}{c} \frac{1}{2} \quad j \\ | \quad \vdots \\ \frac{1}{2} \quad j \end{array} + q^{j+1} \begin{array}{c} \frac{1}{2} \quad j \\ \diagdown \quad \diagup \\ j \quad \frac{1}{2} \end{array} \right] \tag{3.268}$$

Here by the dashed line we denoted projector P_j . Or, we can write explicitly few first terms of this recurrent relations:

$$P_1 = (1 + q^2)^{-1} \left[\begin{array}{c} | \quad | \\ | \quad | \end{array} + q^{\frac{3}{2}} \begin{array}{c} \diagdown \quad \diagup \\ \diagup \quad \diagdown \end{array} \right] \tag{3.269}$$

$$P_{\frac{3}{2}} = (1 + q^2)^{-1} (1 + q^3)^{-1} \left[\begin{array}{c} | \quad | \quad | \\ | \quad | \quad | \end{array} + q^{\frac{3}{2}} \begin{array}{c} \diagdown \quad \diagup \\ \diagup \quad \diagdown \end{array} + q^3 \begin{array}{c} \diagdown \quad \diagup \\ \diagup \quad \diagdown \end{array} + q^{\frac{9}{2}} \begin{array}{c} \diagdown \quad \diagup \\ \diagup \quad \diagdown \end{array} \right] \tag{3.270}$$

And so on.

Thus we **conjecture** a categorified analog of the recurrence formula:

$$P_{j+\frac{1}{2}} = \mathcal{B}_1 \left(\begin{array}{c} \frac{1}{2} \quad j \\ | \quad \vdots \\ \frac{1}{2} \quad j \end{array} \right) \oplus \mathcal{B}_{q^{j+1}} \left(\begin{array}{c} \frac{1}{2} \quad j \\ \diagdown \quad \diagup \\ j \quad \frac{1}{2} \end{array} \right) \tag{3.271}$$

where \mathcal{B}_α is an extra Bloch wave factor. Its role is to give a proper q -factor between equivalent terms. So, for example, let us calculate the corresponding fusion and defusion interfaces for spin 1.

For the defusion interface we have:

$$\begin{array}{c} 1 \quad 1 \\ \cup \end{array} = \mathcal{B}_1 \left[\begin{array}{c} \cup \\ \cup \end{array} \right] \oplus \mathcal{B}_{q^{\frac{3}{2}}} \left[\begin{array}{c} \cup \quad \diagdown \\ \cup \quad \diagup \end{array} \right] \tag{3.272}$$

Expanding the first interface we get:

$$\begin{array}{c} \cup \end{array} = q^{-1} \begin{array}{c} + + - - \\ | | | | \\ + + - - \end{array} \oplus \begin{array}{c} + - + - \\ | | \circ | | \\ + + - - \end{array} \oplus \begin{array}{c} - + - + \\ | | \circ | | \\ + + - - \end{array} \oplus q \begin{array}{c} - - + + \\ | | \circ \circ | | \\ + + - - \end{array} \quad (3.273)$$

Expanding the second interface we get:

$$\begin{array}{c} \cup \end{array} = q^{-\frac{1}{2}} \begin{array}{c} + + - - \\ | | | | \\ + - + - \end{array} \oplus q^{-\frac{3}{2}} \begin{array}{c} + - + - \\ | | \text{---} | | \\ + - + - \end{array} \oplus q^{\frac{1}{2}} \begin{array}{c} + - + - \\ | | \circ | | \\ + - + - \end{array} \oplus \\
 \oplus q^{-\frac{1}{2}} \begin{array}{c} - + + - \\ | | | | \\ + - + - \end{array} \oplus q^{-\frac{1}{2}} \begin{array}{c} - + + - \\ | | \circ | | \\ + - + - \end{array} \oplus q^{\frac{3}{2}} \begin{array}{c} - - + + \\ | | \circ \circ | | \\ + - + - \end{array} \quad (3.274)$$

Then we would like to untwist homotopically the second interface, so we permute + and - strands in the bottom of the interface. Notice that the first term in the second interface after this untwist would be identical to the first term in the first interface. Though their q -degrees differ by 2. To get this q -degree shift we add the ‘‘Bloch’’ soliton discussed in sec.3.4.6 to all the terms in the second interface then consider the tensor sum. Notice that after this Bloch soliton addition and untwist the second term in the second interface and the second term in the first interface cancel through the instanton.

Eventually, we get the following expression for the defusion interface in the spin-1 case:

$$\begin{array}{c} \cup \end{array} = q^{-1} \begin{array}{c} + + - - \\ | | | | \\ + + - - \end{array} \oplus q \begin{array}{c} + + - - \\ | | | | \\ + + - - \end{array} \oplus \begin{array}{c} - + - + \\ | | \circ | | \\ + + - - \end{array} \oplus q \begin{array}{c} - + + - \\ | | \circ | | \\ + + - - \end{array} \oplus \\
 \oplus q \begin{array}{c} + - - + \\ | | \circ | | \\ + + - - \end{array} \oplus q^2 \begin{array}{c} + - + - \\ | | \circ | | \\ + + - - \end{array} \oplus q \begin{array}{c} - - + + \\ | | \circ \circ | | \\ + + - - \end{array} \oplus q^3 \begin{array}{c} - - + + \\ | | \circ \circ | | \\ + + - - \end{array} \quad (3.275)$$

Analogously, we get for the fusion interface:

$$\begin{aligned}
 \begin{array}{c} \cup \\ 1 \quad 1 \end{array} &= q \begin{array}{c} \circlearrowleft \\ - \quad - \quad + \quad + \\ \hline | \quad | \quad | \quad | \\ \hline - \quad - \quad + \quad + \end{array} \oplus q^3 \begin{array}{c} - \quad - \quad + \quad + \\ \hline | \quad | \quad | \quad | \\ \hline - \quad - \quad + \quad + \end{array} \oplus \begin{array}{c} \circlearrowright \\ - \quad - \quad + \quad + \\ \hline | \quad | \quad | \quad | \\ \hline - \quad + \quad - \quad + \end{array} \oplus q \begin{array}{c} - \quad - \quad + \quad + \\ \hline | \quad | \quad | \quad | \\ \hline - \quad + \quad + \quad - \end{array} \oplus \\
 &\oplus q \begin{array}{c} - \quad - \quad + \quad + \\ \hline | \quad | \quad | \quad | \\ \hline + \quad - \quad - \quad + \end{array} \oplus q^2 \begin{array}{c} - \quad - \quad + \quad + \\ \hline | \quad | \quad | \quad | \\ \hline + \quad - \quad + \quad - \end{array} \oplus q^{-1} \begin{array}{c} \circlearrowleft \\ - \quad - \quad + \quad + \\ \hline | \quad | \quad | \quad | \\ \hline + \quad + \quad - \quad - \end{array} \oplus q \begin{array}{c} - \quad - \quad + \quad + \\ \hline | \quad | \quad | \quad | \\ \hline + \quad + \quad - \quad - \end{array}
 \end{aligned} \tag{3.276}$$

Here we denoted as \circlearrowleft and \circlearrowright correspondingly clockwise and counterclockwise Bloch solitons.

As spin- j \mathcal{R} -complex we use just a cabled version of the usual \mathcal{R} -complex:

$$\begin{array}{c} j_2 \quad j_1 \\ \diagdown \quad \diagup \\ j_1 \quad j_2 \end{array} \longrightarrow \left\{ \begin{array}{c} \text{Cabled crossing} \\ j_1 \quad j_2 \end{array} \right. \tag{3.277}$$

So we can verify that derived spin-1 fusion (defusion) interfaces satisfy Reidemeister move I:

$$\begin{array}{c} \text{Hourglass crossing} \\ = t^2 q^{-4} \text{ Parallel lines} \end{array} \tag{3.278}$$

In this way we get a construction satisfying two important properties:

1. It gives a knot (link) invariant, since the 2nd and 3rd Reidemeister moves are automatically implemented.
2. The corresponding Euler characteristic gives a knot polynomial proportional to the spin-1 Jones polynomial.

Notice we have not implemented in these expressions a factor $(1 + q^2)^{-1}$ from (3.269). We imply that the Poincaré polynomial constructed for proposed spin-1 knot cohomology factorizes, for example for the unknot we have:

$$\mathcal{P}_{\square}(q, t | \text{Unknot}) = (1 + q^2)^2 [3]_{q/t} \tag{3.279}$$

In a similar way we can construct fusing/defusing interfaces, \mathcal{R} -interfaces and knot K (link) MSW complexes $\mathbb{M}_J(K)$ for arbitrary spin J . Then the corresponding Poincaré polynomial $\mathcal{P}_{[J]}(q, t | K)$ is

almost a link invariant. To get a link invariant we should strip off all the extra factors:

$$\hat{\mathcal{P}}_{[J]}(q, t|K) = \left[\prod_{k=2}^J (1 + q^k) \right]^{1-n_s} (t^J q^{-J(J+1)})^{n_+ - n_-} \mathcal{P}_{[J]}(q, t|K) \quad (3.280)$$

where n_+ and n_- are corresponding numbers of positive and negative intersections as in sec.1.5, and n_s is a number of strands.

3.8.2 On skein relations, knot co-bordisms and equivalence to Khovanov homology

One important expected application of QFT approach to knot homology is a natural construction of knot co-bordisms [99] in terms of certain amplitudes in higher dimensional field theory where knots embeddings impose certain boundary conditions.

To be more specific let us start with a well known skein exact triangle relation [75, 72]. Consider a link L_0 , let us choose any self-intersection in this link. And let us glue in two possible resolutions. In this way we get three links: a link itself and two possible resolutions of chosen self-intersection:

$$\begin{array}{ccc} \begin{array}{c} \diagup \quad \diagdown \\ \diagdown \quad \diagup \\ L_0 \end{array} & , & \begin{array}{c}) \\ L_+ \end{array} \quad \begin{array}{c} (\\ L_- \end{array} \end{array} \quad (3.281)$$

The Khovanov homological group satisfy the exact triangle relation by definition:

$$\dots \rightarrow H(L_0) \rightarrow H(L_+) \rightarrow H(L_-) \rightarrow H(L_0)[1] \rightarrow \dots \quad (3.282)$$

So does the Heegaard Floer homology [82]. It is an interesting question if our construction in terms of Landau-Ginzburg theory admits a simple derivation of this relation.

A usual way to prove such a kind of relations is to start with a construction of chain map satisfying certain properties (see e.g.[72, Lemma 7.1]). Unfortunately, in our construction there is no natural chain map relating MSW complexes of L_0 and L_+ . A naive obstacle for this is that these configurations are not homotopic to each other, so to move between them we should go through boundaries of the parameter space of the YYLG theory when two punctures collide. In what follows we will prove that there is **no local** non-trivial chain map between $\mathbb{M}(L_0)$ and $\mathbb{M}(L_+)$.

A map U of degree d is a chain map if it satisfies

$$U\mathbb{Q}_\zeta = (-1)^d \mathbb{Q}_\zeta U \quad (3.283)$$

So if we manage to present an explicit vector $v \notin \text{Im } U$, s.t. $v \in \text{Im } \mathbb{Q}_\zeta U$, then the chain map condition can not be satisfied.

We expect the chain map U to be local, in other words it should preserve Chan-Paton factors, or classical critical points at the spatial boundaries of the interface. Thus the interface $\mathbb{M}(L_0)$ contains six different subspaces corresponding to six elements in (3.103). Let us enumerate them as they appear in the expression and denote as w_i . Similarly, interface $\mathbb{M}(L_+)$ contains four subspaces:

$$\mathbb{M}(L_+) = \begin{pmatrix} + \\ + \end{pmatrix} \left(\begin{array}{cc} + & - \\ + & - \end{array} \oplus \right) \left(\begin{array}{cc} - & + \\ - & + \end{array} \oplus \right) \left(\begin{array}{cc} - & - \\ - & - \end{array} \oplus \right) \begin{pmatrix} + \\ + \end{pmatrix} \quad (3.284)$$

If we enumerate these subspaces as well according to the order as they appear in the expansion and denote them as v_i . Then the only form the chain map respecting the structure of states the interface is interpolating between could have the following form:

$$U = \begin{pmatrix} a\mathbf{1} & 0 & 0 & 0 & 0 & 0 \\ 0 & b\mathbf{1} & 0 & 0 & 0 & 0 \\ 0 & 0 & 0 & 0 & c\mathbf{1} & d\mathbf{1} \\ 0 & 0 & 0 & 0 & 0 & 0 \end{pmatrix} \quad (3.285)$$

Where a, b, c and d are corresponding complex coefficients. Thus the subspace v_4 has an obvious property $v_4 \notin \text{Im } U$, though we will show it lies in $\text{Im } \mathbb{Q}_\zeta U$. In particular we will demonstrate in concrete examples that there are matrix elements $\langle v_4 | \mathbb{Q}_\zeta | v_i \rangle \neq 0$, where $i = 1, 2, 3$.

Reconsider an example of the twisted unknot (3.223). There is a non-zero matrix element between the first and the third term of $\mathbb{M}_{-\frac{1}{2}}$. So we have an instanton map that just moves the soliton towards positive x -direction:

$$\begin{array}{ccc} \begin{array}{cc} - & + \\ | & | \\ - & + \\ | & | \\ + & - \end{array} & \xrightarrow{\mathbb{Q}_\zeta} & \begin{array}{cc} - & + \\ | & | \\ + & - \\ | & | \\ + & - \end{array} \end{array} \quad (3.286)$$

Then we construct easily two examples by adding a loop

$$v_1 = \begin{array}{ccc} \begin{array}{cc} - & + \\ | & | \\ - & + \\ | & | \\ + & - \end{array} \begin{array}{c} \text{+} \\ \circ \end{array} & \xrightarrow{\mathbb{Q}_\zeta} & \begin{array}{cc} - & + \\ | & | \\ + & - \\ | & | \\ + & - \end{array} \begin{array}{c} \text{+} \\ \circ \end{array} = v_4 \end{array} \quad (3.287)$$

$$v_2 = \begin{array}{c} - \quad + \\ | \quad | \\ \ominus \quad - \quad + \\ | \quad | \\ + \quad - \end{array} \xrightarrow{\mathbb{Q}_\zeta} \begin{array}{c} - \quad + \\ | \quad | \\ \ominus \quad + \quad - \\ | \quad | \\ + \quad - \end{array} = v_4 \quad (3.288)$$

And we have already encountered an example of the matrix element $\langle v_4 | \mathbb{Q}_\zeta | v_3 \rangle$ in (3.240).

Thus we conclude all the coefficients a, \dots, d should be zero, and the map U has to be trivial.

Chapter 4

Discussion and outlook

In the dissertation we have discussed application of interfaces in supersymmetric theories to a study of their IR dynamics. We have applied this technique to $\mathcal{N} = (2, 2)$ supersymmetric two dimensional Landau-Ginzburg theory and $\mathcal{N} = 2$ four dimensional class \mathcal{S} theories. A remarkable property of interfaces in these theories, defects with spatially changing boundary conditions for fields or coupling constants, is they are tightly related to a flat parallel transport on the parameter space of the theory. In particular, they admit a presence of flat connection families

$$\nabla_i(\zeta) = d - \left(\zeta^{-1} \varphi_i dt_i + A + \zeta \varphi_i^\dagger d\bar{t}_i \right)$$

where family parameter ζ is a phase defining the supersymmetry preserved by the interface, and the interface partition function is a flat section of this connection. The flatness condition for this connection can be thought of as a generalization of the Hitchin system to multiple dimensions. A useful way to work with this system is to analytically continue the phase ζ to the punctured complex plane \mathbb{C}^\times and consider a holomorphic limit $\zeta \rightarrow 0$. Then the conventional technique of asymptotic behavior study is applicable.

This asymptotic behavior stores a lot of information about IR dynamics of the theory in question. So, an algebraic equation governing asymptotic behavior, a spectral curve, can be identified with Seiberg-Witten curve. Moreover Stokes coefficients in the representation of the flat section as a sum over asymptotic contributions are not globally well-defined, they jump discontinuously across certain loci in the parameter space. These coefficients and their jumps are identified with BPS indices and wall-crossing phenomena respectively. This procedure allows one to define such IR observables as low energy effective action and indices of BPS excitations in the theory by purely geometrical means.

There is a natural demand for a “refinement” of this construction. Indeed there are physical quantities in the theories in question storing more information about their IR structures that can be

thought of as deformations of BPS indices by some chemical potentials for conserved charges. We have considered two types of such deformations.

First deformation is known as protected spin character (1.20) where we add a chemical potential q for spin and isospin. This type of deformation is expected to be analogous to promotion of algebras of cluster Fock-Goncharov coordinates on the Teichmüller space to quantum coordinates satisfying a Heisenberg algebra relations. We have proposed an abstract way to consider an Abelianization map relating non-Abelian flat parallel transport on Riemann surfaces to Abelian parallel transport on its cover, an analog of asymptotic expansion, and further projection to non-commutative coordinates analogous to Fock-Goncharov coordinates. As a test problem we have considered so called wild wall-crossing in families of theories associated to Kronecker quivers. As a test result we have presented a non-perturbative functional equation encoding protected spin characters and shown that they are in agreement with ones derived by other methods.

Another direction of the deformation program is categorification. This direction is suitable to discuss association with the knot theory. To follow this route braiding should be represented as certain interfaces. It is rather suitable that the quasi-classical description of these interfaces turns out to be quite universal. The classical theory delivers invariants of knots known as hyperbolic volume of the knot complement. q -deformation of the hyperbolic volume, Jones polynomials, is given by averages of Wilson loops in the Chern-Simons theory. The next “refinement” step, a categorification of Jones polynomials was constructed in a combinatorial way by Khovanov. We have presented a way of possible quantum field theory formulation of knot homologies. We have considered braiding as interfaces in Landau-Ginzburg theory and constructed braid invariants as Hilbert spaces of non-perturbative ground states in the theory in the presence of an interface. These Hilbert spaces are bi-graded by q -degree and fermion number and isomorphic to cohomologies of nilpotent supercharge \mathbb{Q}_ζ . So the output is an isomorphism class of bi-graded vector spaces encoded in polynomials of two variables (q, t) that should be compared to Khovanov’s.

The construction of knot invariants includes two more elementary constructions: categorified braid group representation and braid closures through fusing/defusing interfaces. To give a braid invariant the construction should be invariant under Reidemeister moves II and III: consequently placed twist and inverse twist are homotopic to identity and the Yang-Baxter relation. As we have shown these homotopic moves lead to corresponding quasi-isomorphisms of ground state spaces. The construction relies on certain curved web solutions including only 3-valent bulk vertices. These 3-valent bulk vertices can be derived equivalently from conventional soliton wall-crossing formulae for corresponding Euler characteristics.

A naive way to introduce fusion/defusion interfaces leads to contradictory conditions (3.190a) and (3.190b) for their flavour charges. To overcome this problem we have broken flavour charge conservation, fortunately, this way did not lead to obvious pathologies. In this (modified) theory we have used the curved web technique to construct approximate instanton field configurations saturating matrix elements of supercharge Q_ζ . We have proven the resulting construction to satisfy three Reidemeister moves and to be insensitive to homologous changes of number of strands in the braid representation. Resulting knot polynomials are shown to coincide with Khovanov's in explicit examples. Regretably, we were unable to find a general construction of a quasi-isomorphism of our knot homology complex with that of Khovanov. The present construction lacks the combinatorial elegance of Khovanov's. To calculate a field configuration saturating supercharge matrix elements one is required to solve auxiliary problems: construct curved web and define sign of the matrix element determined by a form on the field space. Surely, this complicates any explicit calculation. We hope the present QFT-inspired knot cohomology we have presented can be further reduced to a more elegant combinatorial calculation scheme.

It is a natural question if the introduced modification breaking flavour charge conservation is really physical. Development in this direction might require some completing of the initial theory or lifting of the Yang-Yang super Landau-Ginzburg theory to original 5d SYM as it was proposed in [48, 47]. We leave this direction for further investigation.

To construct fusing/defusing interfaces we used already constructed \mathcal{R} -interfaces, we have considered Hilbert spaces of interfaces corresponding to knots (links) as certain subspaces of Hilbert spaces corresponding to braids. Generically one expects the fusing/defusing interfaces to be certain boundary conditions (D-branes) in the Landau-Ginzburg model [59, 60, 47]. An explicit relation between these two approaches remains to be studied, moreover this might shed some light on the necessity to introduce explicit flavour charge conservation breaking or even allow one to avoid it.

Some approaches to categorification knot polynomials start with categorification of quantum algebras (see e.g.[15, 16, 63, 85]). In sec.3.5.4.1 we have proposed how the co-multiplication structure could be implemented in the braid group representation, and therefore it has a categorified analog in our setup. It might be fruitful to continue this analogy to implement other quantum algebra structures and compare to approaches proposed in mathematical literature.

One of the advantages of the QFT approach is an expected simple generalization to categorified version of colored Jones polynomials: expectation values of Wilson loops in higher spin representations. We have proposed a cabling model: a knot (link) is represented by cable of strands in the fundamental representations, higher spin representations appear in an isotypic decomposition of

such cables.

More effort is needed to construct the analogous cohomology for higher rank groups and compare it to Khovanov-Rozansky categorification of HOMFLY polynomials and superpolynomials. Indeed Witten's five dimensional SYM setup [99] easily allows for such a generalizations, though there is still more to be done to reduce explicitly this setup to simple theories analogous to [48]. We leave this direction for future investigation.

Known approaches to superpolynomials indicate a crucial difference between them and Khovanov-Rozansky polynomials, in particular, coefficients of superpolynomials are not necessarily integer, therefore not dimensions of some vector spaces. This suggests a parallel way of generalization directly related to (q, t) -deformation of conformal field theories and five-dimensional Yang-Mills theories. Differential equations defining flat parallel transport on the parameter space should be promoted to *difference* equations [102], though a spectral curve formalism can be applied, the spectral curve should be substituted by a spectral curve of a relativistic integrable system [79] (see also [1] and references therein), still we can expect some generalization of the Abelianization map to be valid in this case. We leave this direction for future investigation.

Appendix A

Sign rule in Stokes coefficients

First, let us remind how the sign rule (2.22) is realized in the quantum mechanics. Consider a classical application of the WKB method to the 1d Schrödinger equation for a particle with a normalized mass $\frac{1}{2}$ in an external potential $U(x)$:

$$\left[-\hbar^2 \frac{d^2}{dx^2} + U(x) \right] \psi(x) = 0 \quad (\text{A.1})$$

To derive WKB asymptotic expansion one uses a substitution transforming the Schrödinger equation into a Riccati equation:

$$\psi(x) = e^{\hbar^{-1} \int^x J(x') dx'}, \quad J(x)^2 + \hbar J'(x) - U(x) = 0 \quad (\text{A.2})$$

and explicit representation ρ of the path algebra reads:

$$\rho[\mathcal{Y}_a] = e^{\hbar^{-1} \int_a J(x') dx'} \quad (\text{A.3})$$

In this representation we have

$$\rho[\mathcal{Y}_a] + \rho[\mathcal{Y}_{a'}] = \rho[\mathcal{Y}_a] + \underbrace{e^{\hbar^{-1} \int_{a'}^{a'} J(x) dx}}_{\xi} \rho[\mathcal{Y}_a] = (1 + \xi) \rho[\mathcal{Y}_a] \quad (\text{A.4})$$

One would like to define eikonal $J(x)$ as a series expansion:

$$J(x) = J^{(0)}(x) + \hbar J^{(1)}(x) + \dots \quad (\text{A.5})$$

In the neighbourhood of the branching point p we have $J^{(0)}(x) \sim \alpha \sqrt{x-p}$, while $J^{(1)}(x) = \frac{1}{2} \frac{d}{dx} \log J^{(0)}(x)$, higher order contributions do have no log-singularity.

Then

$$\xi = \exp \left[\hbar^{-1} \oint_{a'a^{-1}} J^{(0)}(x) dx + \oint_{a'a^{-1}} J^{(1)}(x) dx + \dots \right] = e^{\pi i} = -1 \quad (\text{A.6})$$

Thus constraint (2.22) is fulfilled explicitly in this representation. Notice in this example the representation admits homotopy invariance rather than just regular homotopy invariance, in this case the “bubble” in a' can be contracted and does not contribute.

Now consider a representation where the regular homotopy is important. This representation is directly related to the tt^* -connection (3.47), indeed, as we have mentioned it can be reformulated as a null-vector equation in CFT:

$$\left[b^{-2} \partial_z^2 - \hat{T}(z) \right] \Xi(z) = 0 \quad (\text{A.7})$$

Similarly, we can expect that the partition function can be derived through the action of the current operator (see [20, 49]):

$$\Xi(z) = \mathcal{P} e^{b \int^z \hat{J}(z') dz'} \Xi(0) \quad (\text{A.8})$$

Though the Riccati equation differs from (A.2) in one coefficient ($Q = b + b^{-1}$) due to quantum corrections:

$$\hat{T}(z) =: \hat{J}^2(z) + Q \hat{J}'(z) \quad (\text{A.9})$$

From this definition it is clear that the current operator is branched over the base curve \mathcal{C} and the commutation relation reads:

$$\left[\oint_{\gamma} \hat{J}(z) dz, \oint_{\gamma'} \hat{J}(z') dz' \right] = 2\pi i \langle \gamma, \gamma' \rangle \quad (\text{A.10})$$

Where $\langle \star, \star \rangle$ is the intersection pairing on the cycles on the branched cover Σ . As it was proposed in [52] a nice representation for the path algebra is given on the closed paths with the help of the writhe ($\text{wr } a$, a signed sum over self-intersections, see [52] for details and peculiarities, $q = e^{\pi i b^2}$):

$$\rho[\mathcal{Y}_a] = q^{\text{wr } a} e^{b \oint_a \hat{J}(z) dz} \quad (\text{A.11})$$

Thus considering the constraint (2.22) in this representation we get:

$$\rho[\mathcal{Y}_a] + \rho[\mathcal{Y}_{a'}] = \left(1 + \underbrace{q^{\text{wr } a' - \text{wr } a}}_{q^{-1}} \underbrace{e^{b \oint_{a'} \hat{J}(z) dz}}_{\xi} \right) \rho[\mathcal{Y}_a] \quad (\text{A.12})$$

The “bubble” gives an extra self-intersection so the writhe term gives a multiplier q^{-1} , on the other hand due to quantum corrections the ξ is not just -1 since coefficient in the quantum Riccati equation differs from the exponential multiplier in the representation formula, so we expect:

$$\hat{J}(z) = \hat{J}^{(0)}(z) + \frac{Q}{2} \frac{d}{dz} \log \hat{J}^{(0)}(z) + \dots \quad (\text{A.13})$$

We expect a square root singularity from $\hat{J}^{(0)} \sim \hat{\alpha}\sqrt{z-p}$ in the neighbourhood of a branching point p , thus

$$\xi = e^{bQ\pi i} = -q \tag{A.14}$$

And again in this representation the constraint (2.22) is fulfilled.

Appendix B

Solitons in \mathbb{CP}^∞ model

Another interesting model with a homogeneous-like superpotential that does not belong to the class (3.46) is for \mathbb{CP}^{N-1} model [60]:

$$W(X, \lambda) = \sum_k X_k + \frac{\lambda}{\prod_{k=1}^{N-1} X_k} \quad (\text{B.1})$$

This model has a \mathbb{Z}_N -symmetry:

$$X_k \rightarrow X_k e^{\frac{2\pi i}{N}}, \quad W \rightarrow W e^{\frac{2\pi i}{N}} \quad (\text{B.2})$$

So the vacuum states labelled by $a = 1, \dots, N$ break this symmetry:

$$X_k^{(a)} = \lambda^{\frac{1}{N}} e^{\frac{2\pi i a}{N}}, \quad W^{(a)} = N \lambda^{\frac{1}{N}} e^{\frac{2\pi i a}{N}} \quad (\text{B.3})$$

To perform our mean field analysis, we also would like to deform the potential by adding to it a Coulomb probe, meanwhile this deformation should be small, so the resulting potential reads

$$\tilde{W}(X|z, \lambda) = \frac{N}{\alpha} \left(\sum_k X_k + \frac{\lambda}{\prod_{k=1}^{N-1} X_k} \right) - \sum_{k=1}^{N-1} \log(z - X_k) \quad (\text{B.4})$$

As always the partition function is given by an integral over some Lefschetz thimbles

$$\Psi(z, \lambda) = \left[\int DX \right] e^{\zeta \tilde{W}(X|z, \lambda)} \quad (\text{B.5})$$

The Ward identities have the same form as usual (for arbitrary function $f(x)$)

$$\left\langle \sum_i f'(X_i) + \zeta \sum_i \partial_{X_i} \tilde{W}(X) f(X_i) \right\rangle = 0 \quad (\text{B.6})$$

Choosing $f(x) = (z - x)^{-1}$ we get

$$\left\langle \sum_i \frac{1 + \zeta}{(z - X_i)^2} + \zeta \frac{N}{\alpha} \sum_i \frac{1}{z - X_i} \left(1 - \frac{\lambda}{\prod X_i} \right) \right\rangle = 0 \quad (\text{B.7})$$

where we denoted $\Pi = \prod_{k=1}^{N-1} X_k$.

Thus we have

$$\zeta^{-1} \partial_z^2 \Psi - \frac{N}{\alpha} \partial_z \Psi - \frac{\zeta N \lambda}{\alpha} \left\langle \sum_i \frac{\Pi^{-1} X_i^{-1}}{z - X_i} \right\rangle \Psi = 0 \quad (\text{B.8})$$

The latter term we decompose as

$$\left\langle \sum_i \frac{\Pi^{-1} X_i^{-1}}{z - X_i} \right\rangle = \frac{1}{z} \left\langle \sum_i \Pi^{-1} X_i^{-1} \right\rangle + \frac{1}{z} \left\langle \sum_i \frac{\Pi^{-1}}{z - X_i} \right\rangle \quad (\text{B.9})$$

Using the Ward identity for $f(x) = 1$ we get the following relation between correlators:

$$\frac{N(N-1)}{\alpha} - \frac{N}{\alpha} \lambda \left\langle \Pi^{-1} \sum_i X_i^{-1} \right\rangle - \left\langle \sum_i \frac{1}{X_i - z} \right\rangle = 0 \quad (\text{B.10})$$

Combining all together we get the following equation:

$$\left[\zeta^{-1} \partial_z^2 - \frac{N}{\alpha} \partial_z - \frac{1}{z} \partial_z + \zeta^{-1} \frac{\lambda}{z} \partial_z \partial_\lambda - \frac{\zeta N(N-1)}{z \alpha} \right] \Psi = 0 \quad (\text{B.11})$$

In the limit $N \rightarrow \infty$ the parameterization of vacua by $2\pi a/N$, $a = 1, \dots, N$ reduces to an arbitrary phase $\vartheta \in [0, 2\pi)$. Thus we expect the following asymptotic behavior of the partition function

$$\Psi(z, \lambda) \sim e^{\zeta \frac{N^2}{\alpha} \lambda^{\frac{1}{N}} e^{i\vartheta} + N \zeta \mathbf{W}(z, \lambda)} \quad (\text{B.12})$$

In the limit $N \rightarrow \infty$ the differential equation gives the following equation for the spectral cover:

$$(\partial_z \mathbf{W})^2 - \alpha^{-1} \left(1 - \frac{e^{i\vartheta}}{z} \right) \partial_z \mathbf{W} - \frac{\alpha^{-1}}{z} = 0 \quad (\text{B.13})$$

This curve does not give good predictions for the pure \mathbb{CP}^∞ unless $\alpha \ll 1$.

Indeed the potential difference of two neighbourhood vacua a and $a + 1$ may be estimated as

$$\Delta W \sim \frac{N}{\alpha} e^{i\vartheta} \quad (\text{B.14})$$

And this term is compatible with the Coulomb probe interaction. If we choose

$$d\mathbf{W} = \alpha^{-1} \left(1 - \frac{e^{i\vartheta}}{z} \right) dz + p dz \quad (\text{B.15})$$

Then the spectral curve is

$$p^2 = \frac{1}{4\alpha^2} \frac{(z - e^{i\vartheta} + \alpha)(z - e^{i\vartheta} - \alpha)}{z^2}, \quad \alpha \ll 1 \quad (\text{B.16})$$

As we see there are two nearly coinciding branching points $p_0^{(\pm)} = e^{i\vartheta} \pm \alpha$. They are located exactly where the average field giving minimum to the potential is.

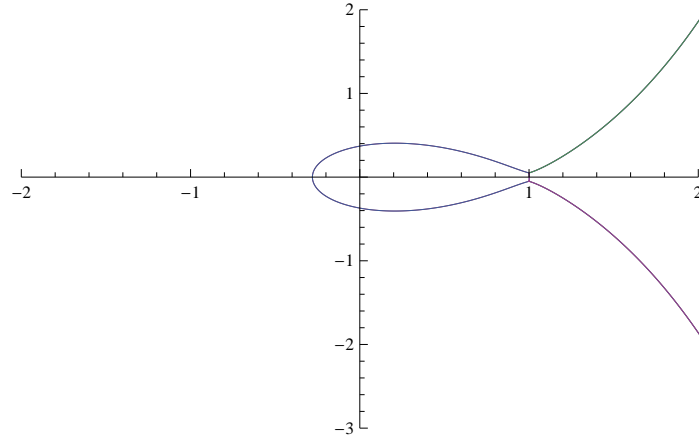


Figure B.1: \mathbb{CP}^∞ critical network

The spectral network technique gives just one critical graph: a looped "fish" (see fig.B.1). The loop implies that there is actually infinite tower of solitons:

$$(1 - Y)^{-1} = \sum_{k=0}^{\infty} Y^k \quad (\text{B.17})$$

where $Y = \exp(\zeta N \oint d\mathbf{W})$. These solitons are labelled by an index k , with the following data:

$$\mu_k = 1 \quad (\text{B.18})$$

$$\Delta W_k = 2\pi i N k e^{i\vartheta} \quad (\text{B.19})$$

$$\text{Arg } \zeta_k^{(\text{crit})} = \vartheta + \frac{\pi}{2} \quad (\text{B.20})$$

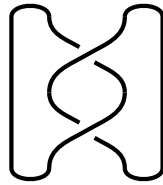
These data coincide with known results.

Appendix C

Homology calculus in Khovanov theory

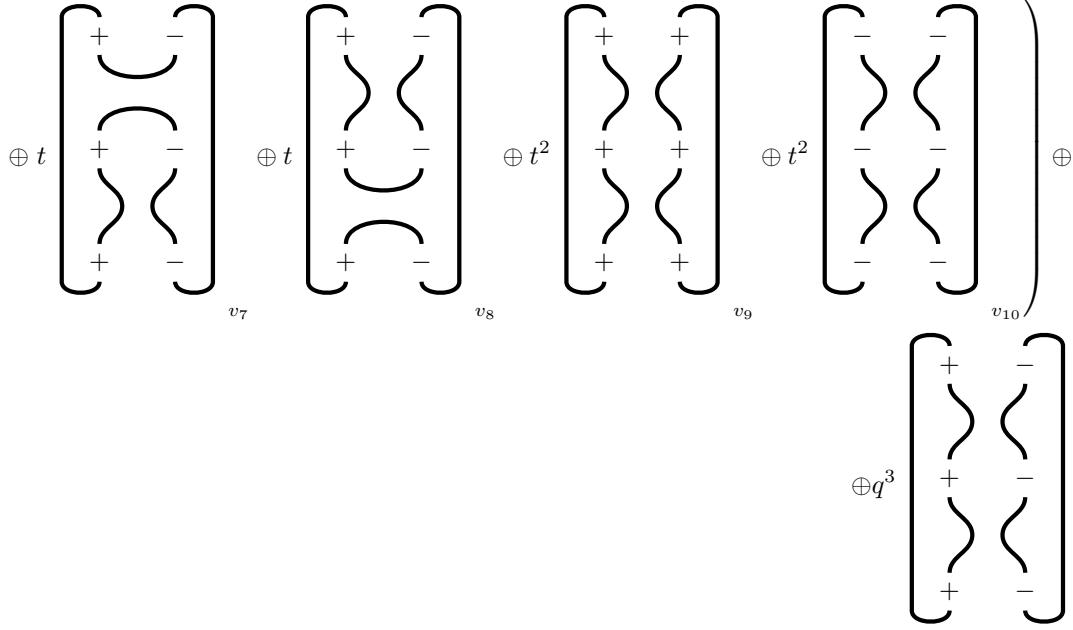
C.1 Hopf link

The Hopf link can be represented by the following link diagram:



Thus for the link complex we have the following expansion:

$$\begin{aligned}
 \langle \text{Hopf} \rangle = & q^{-3}t^4 \left(\begin{array}{c} - \quad + \\ \text{---} \\ + \quad - \\ \text{---} \\ - \quad + \end{array} \right) \oplus q^{-1} \left(t^2 \left(\begin{array}{c} + \quad - \\ \text{---} \\ + \quad - \\ \text{---} \\ + \quad - \end{array} \right)_{v_1} \oplus t^2 \left(\begin{array}{c} - \quad + \\ \text{---} \\ - \quad + \\ \text{---} \\ - \quad + \end{array} \right)_{v_2} \oplus \right. \\
 & \left. \oplus t^3 \left(\begin{array}{c} - \quad + \\ \text{---} \\ - \quad + \\ \text{---} \\ - \quad + \end{array} \right)_{v_3} \oplus t^3 \left(\begin{array}{c} - \quad + \\ \text{---} \\ - \quad + \\ \text{---} \\ - \quad + \end{array} \right)_{v_4} \oplus t^4 \left(\begin{array}{c} - \quad + \\ \text{---} \\ - \quad + \\ \text{---} \\ - \quad + \end{array} \right)_{v_5} \right) \oplus q \left(\begin{array}{c} + \quad - \\ \text{---} \\ - \quad + \\ \text{---} \\ + \quad - \end{array} \right)_{v_6} \oplus
 \end{aligned}$$



Fugacity t indicates the homology degree of the corresponding 1d vector space in the complex.

Clearly, spaces with q -degree -3 and 3 are one dimensional. To find homologies for spaces of q -degree -1 and +1 we label all the 1d spaces by v_i . And we can define matrix elements $\langle v_i|d|v_j\rangle$, where d is our differential, following rules (1.76) and (1.77). These matrix elements are either -1, or 0, or 1, we denote non-zero elements by arrows indicating the action of the differential, if the matrix element is +1 the arrow is solid, if -1 one is dashed¹. For q -degree -1 we have the following picture and just one non-zero homology group:

$$\begin{array}{ccc}
 v_1 & \longrightarrow & v_3 \\
 \oplus & \begin{array}{c} \nearrow \\ \searrow \end{array} & \oplus \\
 v_2 & \longrightarrow & v_4
 \end{array}
 \begin{array}{c}
 \longrightarrow \\
 \dashrightarrow \\
 \dashrightarrow
 \end{array}
 v_5, \quad H_{2,-1} = \text{Span}(e_1 - e_2)
 \tag{C.1}$$

Where by e_i we mean a basis vector of the corresponding 1d vector space v_i .

Similarly for q -degree +1 we find:

$$\begin{array}{ccc}
 & & v_7 \longrightarrow v_9 \\
 & \begin{array}{c} \nearrow \\ \searrow \end{array} & \oplus \\
 v_6 & \longrightarrow & v_8 \dashrightarrow v_{10}
 \end{array}, \quad H_{2,1} = \text{Span}(e_9 - e_{10})
 \tag{C.2}$$

Thus finally we have:

$$\mathcal{P}_{\square}(q, t|\text{Hopf}) = q^{-3}t^4 + q^{-1}t^2 + qt^2 + q^3
 \tag{C.3}$$

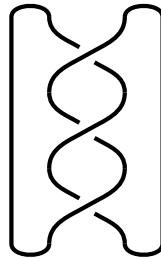
¹ To define what sign we should use we follow a natural physical rule: an ordering of fermionic actions of the differential. Suppose we have chosen any enumeration of all the knot diagram intersections. So at each n -th step we have acted on vertices i_1, i_2 and so on up to i_n . Now we can assume that the 1d vector space corresponding to a concrete diagram corresponds to an ordered tuple $\psi_n = (i_1, \dots, i_n)$, where $i_j < i_{j+1}$. On $n + 1$ -th step we get a new action on i_{n+1} -th vertex. This gives a wave function $\psi_{n+1} = (i_1, \dots, i_n, i_{n+1})$ that is not ordered. So the sign of differential matrix element is defined by the sign of permutation ψ_{n+1} .

It should be compared to the Khovanov polynomial for the trefoil:

$$\mathcal{H}_{\square}(q, t|\text{Hopf}) = \frac{t}{q^3} (q^2 + 1) (q^4 t^2 + 1) \tag{C.4}$$

C.2 Trefoil

The trefoil knot can be represented by the following knot diagram:



First we will consider a particular term in the q -expansion and discuss peculiarities of its calculation.

This term reads

$$\begin{aligned}
 & \left[q^{\frac{1}{2}} \langle \text{Trefoil} \rangle \right]_{q^{-2}} = \\
 & = t^3 \left(\begin{array}{c} \left(\begin{array}{c} \text{Diagram } e_1 \\ \text{Diagram } e_2 \\ \text{Diagram } e_3 \end{array} \right) \oplus \\ \oplus t^4 \left(\begin{array}{c} \text{Diagram } f_1 \\ \text{Diagram } f_2 \\ \text{Diagram } f_3 \end{array} \right) \end{array} \right) \tag{C.5}
 \end{aligned}$$

So we have the following picture of the differential action:

$$\begin{array}{c}
 e_1 \\
 \oplus \\
 e_2 \\
 \oplus \\
 e_3
 \end{array}
 \begin{array}{c}
 \nearrow \\
 \rightarrow \\
 \searrow \\
 \rightarrow \\
 \rightarrow
 \end{array}
 \begin{array}{c}
 f_1 \\
 \oplus \\
 f_2 \\
 \oplus \\
 f_3
 \end{array}
 , \quad
 d = \begin{pmatrix} 0 & 1 & 1 \\ 1 & 1 & 0 \\ 1 & 0 & 1 \end{pmatrix}
 , \quad
 \text{rk } d = 3, \quad
 H_{\star, -2}^{(\text{correct})} = \emptyset
 \tag{C.6}$$

Now let us discuss some peculiarities of this calculation.

Technically the vertex model (1.81) and our soliton model (3.212a) differ by two following terms:

$$q^{\frac{1}{2}} \begin{array}{c} - \\ \curvearrowright \\ - \end{array} \begin{array}{c} + \\ \curvearrowleft \\ + \end{array} \oplus q^{\frac{1}{2}} t^{-1} \begin{array}{c} - \\ \cup \\ - \end{array} \begin{array}{c} + \\ \cap \\ + \end{array}
 \tag{C.7}$$

These two terms have the same q -degree and differ by 1 t -degree, so if any diagram decomposition contains a vector space with the first vertex, say v_1 , there is always a vector space, say v_2 , with just this vertex replaced by the second one, and we can claim $\langle v_2 | d | v_1 \rangle = 1$, and in the classical limit ($t = -1$) these contributions always cancel. We could expect that these terms can be cancelled on the level of the \mathcal{R} -complex, but they **can not**. And this example illustrates this peculiarity explicitly. Indeed, suppose we omitted terms (C.7) in the \mathcal{R} -complex, then we should drop terms e_i and f_i for $i = 2, 3$, then we are left with just two terms e_1 and f_1 , moreover, $\langle e_1 | d | f_1 \rangle = 0$. Thus we would get a wrong result for the homology group:

$$H_{\star, -2}^{(\text{wrong})} = t^3 e_1 \oplus t^4 f_1
 \tag{C.8}$$

So indeed both the complexes as vector spaces and the action of the differential are different in Khovanov homology and QFT cohomology we have constructed despite the resulting Poincaré polynomials are equal in examples we have calculated.

Let us present a calculation of one more term:

$$\left[q^{\frac{1}{2}} \langle \text{Trefoil} \rangle \right]_{q^2} = t^{-1} \left(\begin{array}{c} \left[\begin{array}{c} + \\ \cup \\ - \\ \cup \\ + \end{array} \right]_{e_1} \oplus \left[\begin{array}{c} \left[\begin{array}{c} + \\ \cup \\ - \\ \cup \\ + \end{array} \right] \oplus \left[\begin{array}{c} + \\ \cap \\ - \\ \cap \\ + \end{array} \right] \end{array} \right]_{f_1} \tag{C.9}$$

So we can compose the following chain complex:

$$0 \xrightarrow{d_{-2}} \mathcal{C}_{-1} \xrightarrow{d_{-1}} \mathcal{C}_0 \xrightarrow{d_0} \mathcal{C}_1 \xrightarrow{d_1} \mathcal{C}_2 \xrightarrow{d_2} 0 \quad (\text{C.12})$$

With

$$d_{-1} = \begin{pmatrix} 1 \\ 1 \\ 1 \end{pmatrix}, \quad d_0 = \begin{pmatrix} -1 & 0 & 1 \\ -1 & 1 & 0 \\ 0 & 1 & -1 \end{pmatrix}, \quad d_1 = \begin{pmatrix} 1 & -1 & 1 \\ 1 & -1 & 1 \end{pmatrix} \quad (\text{C.13})$$

Obviously, $d_{i+1}d_i = 0$ and it is simple to calculate the homology of this chain complex:

$$H_{\star,2} = t^2(g_1 - g_2) \quad (\text{C.14})$$

Remaining terms can be calculated in a similar fashion giving the following knot polynomial:

$$\mathcal{P}_{\square}(q, t|\text{Trefoil}) = t^5 q^{-4} + 0 q^{-2} + t^2 + q^2 t^2 + q^4 \quad (\text{C.15})$$

It should be compared to the Khovanov polynomial:

$$\mathcal{K}_{\square}(q, t|\text{Trefoil}) = \mathcal{K}_{\square}(q, t, t|\text{Trefoil}) = \frac{t}{q^4} (1 + q^4 t + q^6 t^3 + q^8 t^3) \quad (\text{C.16})$$

Appendix D

Simplified tt^* -equations

In this Appendix we provide some details on derivation of tt^* -equations in a simplified version of the superpotential

$$W = -\sum_i \log(z - \phi_i) + 2 \sum_{i < j} \log(\phi_i - \phi_j) + \sum_i V(\phi_i, q_a) \quad (\text{D.1})$$

The Ward identity reads in this case

$$\left\langle -\sum_i \frac{1}{(z - \phi^i)^2} + \beta\zeta \sum_i \frac{1}{(z - \phi^i)} \left(-\frac{1}{\phi^i - z} + 2 \sum_{i \neq j} \frac{1}{\phi^i - \phi^j} + V'(\phi^i, q_a) \right) \right\rangle = 0 \quad (\text{D.2})$$

Now we use simple identities

$$2 \sum_i \frac{1}{z - \phi^i} \sum_{j \neq i} \frac{1}{\phi^i - \phi^j} = \sum_{i \neq j} \frac{1}{(z - \phi^i)(z - \phi^j)} \quad (\text{D.3})$$

the term containing z reduces to

$$\left[\oint_{\gamma_i} d\phi^i \right] e^{\beta\zeta W(\phi^i, q_a)} \left(\beta\zeta \left(\sum_i \frac{1}{z - \phi^i} \right)^2 - \sum_i \frac{1}{(z - \phi^i)^2} \right) = \frac{1}{\beta\zeta} \partial_z^2 \left[\oint_{\gamma_i} d\phi^i \right] e^{\beta\zeta W(\phi^i, q_a)} \quad (\text{D.4})$$

In a similar way one can deal with with the potential term. First we can divide it in two parts

$$\left\langle \sum_i \beta\zeta \frac{V'(\phi^i, q_a) - V'(z, q_a) + V'(z, q_a)}{z - \phi^i} \right\rangle = \beta\zeta \left\langle \sum_i \frac{V'(\phi^i, q_a) - V'(z, q_a)}{z - \phi^i} \right\rangle - V'(z, q_a) \partial_z \langle 1 \rangle \quad (\text{D.5})$$

And the term in brackets is indeed in the chiral ring of operators $\mathbb{C}[\phi^i]/\langle \partial_i W = 0 \rangle$ in the LG model, at least for a polynomial model. One can produce expectation values of chiral operators via the following relation

$$\beta\zeta \langle \partial_{q_a} V \rangle = \partial_{q_a} \langle 1 \rangle \quad (\text{D.6})$$

If the ring of chiral operators is finite and there is enough amount of moduli q_a then operators ∂_{q_a} form a basis in this ring. Thus our operator can be decomposed in this basis

$$\beta\zeta \left\langle \sum_i \frac{V'(\phi^i, q_a) - V'(z, q_a)}{z - \phi^i} \right\rangle = \sum_a D^a(z, q) \partial_{q_a} \langle 1 \rangle \quad (\text{D.7})$$

Thus our partition function $Z(z, q)$ is a solution to the following differential equation

$$\left[\frac{1}{\beta\zeta} \partial_z^2 - V'(z) \partial_z + \sum_a D^a(z, q) \partial_{q_a} \right] Z(z, q) = 0 \quad (\text{D.8})$$

We can calculate the coefficients D^a in the case of Yang-Yang model

$$V(p, q) = - \sum_a k_a \log(p - q_a) \quad (\text{D.9})$$

Indeed

$$\begin{aligned} \beta\zeta \left\langle \sum_i \frac{V'(\phi^i, q_a) - V'(z, q_a)}{z - \phi^i} \right\rangle &= \beta\zeta \left\langle \sum_i \frac{1}{z - \phi^i} \left(- \sum_a \frac{k_a}{\phi^i - q_a} + \sum_a \frac{k_a}{z - q_a} \right) \right\rangle = \\ &= -\beta\zeta \left\langle \sum_{i,a} \frac{k_a}{(z - q_a)(\phi^i - q_a)} \right\rangle = - \sum_a \frac{1}{z - q_a} \partial_{q_a} \langle 1 \rangle \end{aligned} \quad (\text{D.10})$$

Appendix E

Spectral curve for

Knizhnik-Zamolodchikov connection

Here we derive a spectral curve describing asymptotic behavior of Wilson loop operators in $SU(2)$ Chern-Simons theory on a manifold $\mathbb{CP}^1 \times I$. Suppose a single time slice, a Riemann sphere is intersected by n strands carrying spins J_i of a link in points q_i , $i = 1, \dots, n$. Wave functions Ψ in the Chern-Simons theory are identified with conformal blocks in WZW model and satisfy the Knizhnik-Zamolodchikov equation:

$$\left(\partial_{q_i} + \frac{1}{\kappa + 2} \sum_{j \neq i} \frac{T_i^a \otimes T_j^a}{q_i - q_j} \right) \Psi = 0 \quad (\text{E.1})$$

We would like to consider as operators in this setup Wilson loops lying in the time slice, so technically we add a new strand position z in the fundamental representation and consider monodromies of the wave function with respect to braiding z with other strands assumed to stay fixed. A new strand modifies the Knizhnik-Zamolodchikov equations:

$$\left(\partial_{q_i} + \frac{1}{\kappa + 2} \sum_{j \neq i} \frac{T_i^a \otimes T_j^a}{q_i - q_j} + \frac{1}{\kappa + 2} \frac{\sigma^a \otimes T_i^a}{q_i - z} \right) \Psi = 0 \quad (\text{E.2a})$$

$$\left(\partial_z + \sum_i \frac{1}{\kappa + 2} \frac{\sigma^a \otimes T_i^a}{z - q_i} \right) \Psi = 0 \quad (\text{E.2b})$$

We take the ∂_z -derivative of eq.(E.2b) and substitute term proportional to $\partial_z \Psi$ again through eq.(E.2b), the resulting expression reads:

$$\partial_z^2 \Psi - \frac{1}{\kappa + 2} \sum_i \frac{\sigma^a \otimes T_i^a}{(z - q_i)^2} \Psi - \frac{1}{(\kappa + 2)^2} \left(\sum_i \frac{\sigma^a \otimes T_i^a}{z - q_i} \right)^2 \Psi = 0 \quad (\text{E.3})$$

The connection square in the third term can be decomposed as

$$\left(\sum_i \frac{\sigma^a \otimes T_i^a}{z - q_i} \right)^2 = \sum_i \frac{(T_i^a)^2}{(z - q_i)^2} + \sum_i \frac{1}{z - q_i} \sum_{j \neq i} \frac{T_i^a \otimes T_j^a}{q_i - q_j} \quad (\text{E.4})$$

The first term in this expansion gives the second Casimir elements of corresponding representations $(T_i^a)^2 = c_2(J_i)$, the second term can be substituted from (E.2a). Summarizing all the substitutions we arrive to the following equation:

$$\left[\partial_z^2 - \frac{\kappa + 3}{(\kappa + 2)^2} \sum_i \frac{\sigma^a \otimes T_i^a}{(z - q_i)^2} - \frac{1}{(\kappa + 2)^2} \sum_i \frac{c_2(J_i)}{(z - q_i)^2} + \frac{1}{\kappa + 2} \sum_i \frac{\partial_{q_i}}{z - q_i} \right] \Psi = 0 \quad (\text{E.5})$$

In the limit $J_i \sim \frac{h_i}{2g}$, $g \rightarrow 0$ different terms in this equation have different behavior, in particular, $\partial_z^2 \sim g^{-2}$, $T_i^a \sim g^{-1}$, $c_2(J_i) \sim g^{-2}$, $\partial_{q_i} \sim g^{-2}$, so we expect the following asymptotic from the wave function $\Psi \sim e^{-\frac{(\kappa+2)^{-1}}{g^2} \mathbf{F}(q_i) - \frac{(\kappa+2)^{-1}}{g} \int^z d\mathbf{W}}$, in the limit $g \rightarrow 0$ this equation reduces to an algebraic equation:

$$d\mathbf{W}^2 = \sum_i \left(\frac{h_i^2}{(z - q_i)} + \frac{\partial_{q_i} \mathbf{F}}{(z - q_i)} \right) dz^2 \quad (\text{E.6})$$

References

- [1] M. Aganagic, N. Haouzi, and S. Shakirov, “ A_n -Triality,” [arXiv:1403.3657 \[hep-th\]](#).
- [2] M. Aganagic and S. Shakirov, “Refined Chern-Simons Theory and Knot Homology,” *Proc. Symp. Pure Math.* **85** (2012) 3–32, [arXiv:1202.2489 \[hep-th\]](#).
- [3] L. F. Alday and Y. Tachikawa, “Affine $SL(2)$ conformal blocks from 4d gauge theories,” *Lett. Math. Phys.* **94** (2010) 87–114, [arXiv:1005.4469 \[hep-th\]](#).
- [4] L. Alvarez-Gaume and S. F. Hassan, “Introduction to S duality in N=2 supersymmetric gauge theories: A Pedagogical review of the work of Seiberg and Witten,” *Fortsch. Phys.* **45** (1997) 159–236, [arXiv:hep-th/9701069 \[hep-th\]](#).
- [5] A. Anokhina and A. Morozov, “Cabling procedure for the colored HOMFLY polynomials,” *Teor. Mat. Fiz.* **178** (2014) 3–68, [arXiv:1307.2216 \[hep-th\]](#).
- [6] S. Arthamonov and S. Shakirov, “Refined Chern-Simons Theory in Genus Two,” [arXiv:1504.02620 \[hep-th\]](#).
- [7] M. F. Atiyah, V. K. Patodi, and I. Singer, “Spectral asymmetry and Riemannian geometry. I,” in *Mathematical Proceedings of the Cambridge Philosophical Society*, vol. 77, pp. 43–69, Cambridge Univ Press. 1975.
- [8] D. Bar-Natan, “On Khovanov’s categorification of the Jones polynomial,” *Algebr. Geom. Topol.* **2** (Jan., 2002) 337–370, [arXiv:math/0201043](#).
- [9] G. Barnich, F. Brandt, and M. Henneaux, “Local BRST cohomology in gauge theories,” *Phys. Rept.* **338** (2000) 439–569, [arXiv:hep-th/0002245 \[hep-th\]](#).
- [10] A. A. Belavin, A. M. Polyakov, and A. B. Zamolodchikov, “Infinite Conformal Symmetry in Two-Dimensional Quantum Field Theory,” *Nucl. Phys.* **B241** (1984) 333–380.
- [11] A. Bilal, “Duality in N=2 SUSY SU(2) Yang-Mills theory: A Pedagogical introduction to the work of Seiberg and Witten,” in *Quantum fields and quantum space time. Proceedings, NATO Advanced Study Institute, Cargese, France, July 22-August 3, 1996*, pp. 21–43. 1997. [arXiv:hep-th/9601007 \[hep-th\]](#). [87(1997)].
- [12] A. Bilal, “Introduction to supersymmetry,” [arXiv:hep-th/0101055 \[hep-th\]](#).
- [13] F. Bloch, “Über die Quantenmechanik der Elektronen in Kristallgittern,” *Zeitschrift für Physik* **52** (1929) 555–600.

- [14] A. G. Bytsko and J. Teschner, “R operator, coproduct and Haar measure for the modular double of $U(q)(sl(2, \mathbb{R}))$,” *Commun. Math. Phys.* **240** (2003) 171–196, [arXiv:math/0208191 \[math-qa\]](#).
- [15] S. Cautis and J. Kamnitzer, “Knot homology via derived categories of coherent sheaves, I: The $sl(2)$ -case,” *Duke Math. J.* **142** no. 3, (2008) 511–588.
- [16] S. Cautis and J. Kamnitzer, “Knot homology via derived categories of coherent sheaves II, $sl(m)$ case,” *Inventiones mathematicae* **174** no. 1, (2008) 165–232.
- [17] S. Cecotti, D. Gaiotto, and C. Vafa, “ tt^* geometry in 3 and 4 dimensions,” *JHEP* **05** (2014) 055, [arXiv:1312.1008 \[hep-th\]](#).
- [18] S. Cecotti and C. Vafa, “Topological antitopological fusion,” *Nucl. Phys.* **B367** (1991) 359–461.
- [19] S. Cecotti and C. Vafa, “On classification of $N=2$ supersymmetric theories,” *Commun. Math. Phys.* **158** (1993) 569–644, [arXiv:hep-th/9211097 \[hep-th\]](#).
- [20] L. Chekhov, B. Eynard, and S. Ribault, “Seiberg-Witten equations and non-commutative spectral curves in Liouville theory,” *J. Math. Phys.* **54** (2013) 022306, [arXiv:1209.3984 \[hep-th\]](#).
- [21] S.-S. Chern and J. Simons, “Characteristic forms and geometric invariants,” *Annals of Mathematics* (1974) 48–69.
- [22] W.-Y. Chuang, D.-E. Diaconescu, J. Manschot, G. W. Moore, and Y. Soibelman, “Geometric engineering of (framed) BPS states,” [arXiv:1301.3065 \[hep-th\]](#).
- [23] F. Denef, “Quantum quivers and Hall / hole halos,” *JHEP* **10** (2002) 023, [arXiv:hep-th/0206072 \[hep-th\]](#).
- [24] R. Dijkgraaf and C. Vafa, “A Perturbative window into nonperturbative physics,” [arXiv:hep-th/0208048 \[hep-th\]](#).
- [25] R. Dijkgraaf and C. Vafa, “Matrix models, topological strings, and supersymmetric gauge theories,” *Nucl. Phys.* **B644** (2002) 3–20, [arXiv:hep-th/0206255 \[hep-th\]](#).
- [26] R. Dijkgraaf and C. Vafa, “On geometry and matrix models,” *Nucl. Phys.* **B644** (2002) 21–39, [arXiv:hep-th/0207106 \[hep-th\]](#).
- [27] T. Dimofte, S. Gukov, J. Lenells, and D. Zagier, “Exact Results for Perturbative Chern-Simons Theory with Complex Gauge Group,” *Commun. Num. Theor. Phys.* **3** (2009) 363–443, [arXiv:0903.2472 \[hep-th\]](#).
- [28] P. A. M. Dirac, “Quantised singularities in the electromagnetic field,” in *Proceedings of the Royal Society of London A: Mathematical, Physical and Engineering Sciences*, vol. 133, pp. 60–72, The Royal Society. 1931.
- [29] V. Dolotin and A. Morozov, “Introduction to Khovanov Homologies. I. Unreduced Jones superpolynomial,” *JHEP* **01** (2013) 065, [arXiv:1208.4994 \[hep-th\]](#).

- [30] J.-M. Drezet, “Cohomologie des variétés de modules de hauteur nulle,” *Math. Ann.* **281** no. 1, (1988) 43–85.
- [31] N. M. Dunfield, S. Gukov, and J. Rasmussen, “The Superpolynomial for knot homologies,” [arXiv:math/0505662 \[math.GT\]](#).
- [32] P. Elyutin, V. Krivchenkov, and N. Bogolyubov, *Quantum mechanics with tasks (in Russian)*. FIZMATLIT, 2001.
- [33] L. D. Faddeev and R. M. Kashaev, “Quantum Dilogarithm,” *Mod. Phys. Lett.* **A9** (1994) 427–434, [arXiv:hep-th/9310070 \[hep-th\]](#).
- [34] V. Fock and A. Goncharov, “Moduli spaces of local systems and higher Teichmüller theory,” *Publications Mathématiques de l’IHÉS* **103** (2006) 1–211.
- [35] P. Francesco, P. Mathieu, and D. Sénéchal, *Conformal field theory*. Springer Science & Business Media, 2012.
- [36] P. Freyd, D. Yetter, J. Hoste, W. B. R. Lickorish, K. Millett, and A. Ocneanu, “A new polynomial invariant of knots and links,” *Bull. Amer. Math. Soc.* **12** (1985) 239–246.
- [37] M. Gabella, “Quantum Holonomies from Spectral Networks and Framed BPS States,” [arXiv:1603.05258 \[hep-th\]](#).
- [38] D. Gaiotto, “N=2 dualities,” *JHEP* **08** (2012) 034, [arXiv:0904.2715 \[hep-th\]](#).
- [39] D. Gaiotto, “Surface Operators in N = 2 4d Gauge Theories,” *JHEP* **11** (2012) 090, [arXiv:0911.1316 \[hep-th\]](#).
- [40] D. Gaiotto, “Open Verlinde line operators,” [arXiv:1404.0332 \[hep-th\]](#).
- [41] D. Gaiotto, G. W. Moore, and A. Neitzke, “Wall-crossing, Hitchin Systems, and the WKB Approximation,” [arXiv:0907.3987 \[hep-th\]](#).
- [42] D. Gaiotto, G. W. Moore, and A. Neitzke, “Four-dimensional wall-crossing via three-dimensional field theory,” *Commun. Math. Phys.* **299** (2010) 163–224, [arXiv:0807.4723 \[hep-th\]](#).
- [43] D. Gaiotto, G. W. Moore, and A. Neitzke, “Wall-Crossing in Coupled 2d-4d Systems,” *JHEP* **12** (2012) 082, [arXiv:1103.2598 \[hep-th\]](#).
- [44] D. Gaiotto, G. W. Moore, and A. Neitzke, “Framed BPS States,” *Adv. Theor. Math. Phys.* **17** no. 2, (2013) 241–397, [arXiv:1006.0146 \[hep-th\]](#).
- [45] D. Gaiotto, G. W. Moore, and A. Neitzke, “Spectral networks,” *Annales Henri Poincaré* **14** (2013) 1643–1731, [arXiv:1204.4824 \[hep-th\]](#).
- [46] D. Gaiotto, G. W. Moore, and A. Neitzke, “Spectral Networks and Snakes,” *Annales Henri Poincaré* **15** (2014) 61–141, [arXiv:1209.0866 \[hep-th\]](#).

- [47] D. Gaiotto, G. W. Moore, and E. Witten, “Algebra of the Infrared: String Field Theoretic Structures in Massive $\mathcal{N} = (2, 2)$ Field Theory In Two Dimensions,” [arXiv:1506.04087](#) [[hep-th](#)].
- [48] D. Gaiotto and E. Witten, “Knot Invariants from Four-Dimensional Gauge Theory,” *Adv. Theor. Math. Phys.* **16** no. 3, (2012) 935–1086, [arXiv:1106.4789](#) [[hep-th](#)].
- [49] D. Galakhov, A. Mironov, and A. Morozov, “S-Duality and Modular Transformation as a non-perturbative deformation of the ordinary pq-duality,” *JHEP* **06** (2014) 050, [arXiv:1311.7069](#) [[hep-th](#)].
- [50] D. Galakhov, A. Mironov, and A. Morozov, “Wall Crossing Invariants: from quantum mechanics to knots,” *J. Exp. Theor. Phys.* **120** no. 3, (2015) 549–577, [arXiv:1410.8482](#) [[hep-th](#)]. [*Zh. Eksp. Teor. Fiz.*147,623(2015)].
- [51] D. Galakhov, P. Longhi, T. Mainiero, G. W. Moore, and A. Neitzke, “Wild Wall Crossing and BPS Giants,” *JHEP* **11** (2013) 046, [arXiv:1305.5454](#) [[hep-th](#)].
- [52] D. Galakhov, P. Longhi, and G. W. Moore, “Spectral Networks with Spin,” *Commun. Math. Phys.* **340** no. 1, (2015) 171–232, [arXiv:1408.0207](#) [[hep-th](#)].
- [53] P. Gavrylenko and A. Marshakov, “Exact conformal blocks for the W-algebras, twist fields and isomonodromic deformations,” [arXiv:1507.08794](#) [[hep-th](#)].
- [54] P. Griffiths and J. Harris, *Principles of algebraic geometry*. John Wiley & Sons, 2014.
- [55] M. Gross and R. Pandharipande, “Quivers, curves, and the tropical vertex,” [arXiv:0909.5153](#).
- [56] S. Gukov and E. Witten, “Gauge Theory, Ramification, And The Geometric Langlands Program,” [arXiv:hep-th/0612073](#) [[hep-th](#)].
- [57] K. Hikami and R. Inoue, “Braiding operator via quantum cluster algebra,” *J. of Phys. A* **47** (2014) 474006, [arXiv:1404.2009](#).
- [58] K. Hikami, “Hyperbolic structure arising from a knot invariant,” *Int. J. Mod. Phys. A* **16** no. 19, (2001) 3309–3333.
- [59] K. Hori, S. Katz, A. Klemm, R. Pandharipande, R. Thomas, C. Vafa, R. Vakil, and E. Zaslow, *Mirror symmetry*, vol. 1 of *Clay mathematics monographs*. AMS, Providence, USA, 2003.
- [60] K. Hori, A. Iqbal, and C. Vafa, “D-branes and mirror symmetry,” [arXiv:hep-th/0005247](#) [[hep-th](#)].
- [61] Y. Ito, T. Okuda, and M. Taki, “Line operators on $S^1 \times \mathbb{R}^3$ and quantization of the Hitchin moduli space,” *JHEP* **04** (2012) 010, [arXiv:1111.4221](#) [[hep-th](#)].
- [62] M. Khovanov, “A categorification of the Jones polynomial,” *Duke Math. J.* **101** (2000) 359–426, [arXiv:math/9908171](#).

- [63] M. Khovanov, “Hopfological algebra and categorification at a root of unity: the first steps,” [arXiv:math/0509083](#).
- [64] M. Khovanov and L. Rozansky, “Matrix factorizations and link homology,” [arXiv:math/0401268](#).
- [65] M. Khovanov and L. Rozansky, “Matrix factorizations and link homology II,” *Geometry & Topology* **12** no. 3, (2008) 1387–1425, [arXiv:math/0505056](#).
- [66] A. N. Kirillov and N. Y. Reshetikhin, “Representations of the algebra $U_q(sl(2))$, q -orthogonal polynomials and invariants of links,” in *Infinite Dimensional Lie Algebras and Groups*, pp. 285–339. World Sci. Publishing, Teaneck, NJ, 1988.
- [67] A. Klemm, W. Lerche, P. Mayr, C. Vafa, and N. P. Warner, “Selfdual strings and N=2 supersymmetric field theory,” *Nucl. Phys. B* **477** (1996) 746–766, [arXiv:hep-th/9604034 \[hep-th\]](#).
- [68] A. Klimyk and K. Schmüdgen, *Quantum groups and their representations*. Springer Science & Business Media, 2012.
- [69] V. G. Knizhnik and A. B. Zamolodchikov, “Current algebra and Wess-Zumino model in two dimensions,” *Nucl. Phys. B* **247** no. 1, (1984) 83–103.
- [70] M. Kontsevich and Y. Soibelman, “Stability structures, motivic Donaldson-Thomas invariants and cluster transformations,” [arXiv:0811.2435 \[math.AG\]](#).
- [71] M. Kontsevich and Y. Soibelman, “Motivic Donaldson-Thomas invariants: Summary of results,” [arXiv:0910.4315 \[math.AG\]](#).
- [72] P. B. Kronheimer and T. S. Mrowka, “Khovanov homology is an unknot-detector,” [arXiv:1005.4346](#).
- [73] R. J. Lawrence, “Homological representations of the Hecke algebra,” *Commun. in Math. Phys.* **135** no. 1, (1990) 141–191.
- [74] P. Longhi and C. Y. Park, “ADE Spectral Networks,” [arXiv:1601.02633 \[hep-th\]](#).
- [75] C. Manolescu, “An unoriented skein exact triangle for knot Floer homology,” *Math. Res. Lett.* **14** no. 5, (2007) 839852.
- [76] J. Manschot, B. Pioline, and A. Sen, “Wall Crossing from Boltzmann Black Hole Halos,” *JHEP* **07** (2011) 059, [arXiv:1011.1258 \[hep-th\]](#).
- [77] G. Moore and N. Seiberg, *Physics, Geometry and Topology*, ch. Lectures on RCFT, pp. 263–361. Springer US, Boston, MA, 1990. http://dx.doi.org/10.1007/978-1-4615-3802-8_8.
- [78] A. Morozov and S. Shakirov, “The matrix model version of AGT conjecture and CIV-DV prepotential,” *JHEP* **08** (2010) 066, [arXiv:1004.2917 \[hep-th\]](#).
- [79] N. Nekrasov, “Five dimensional gauge theories and relativistic integrable systems,” *Nucl. Phys. B* **531** (1998) 323–344, [arXiv:hep-th/9609219 \[hep-th\]](#).

- [80] N. A. Nekrasov, “Seiberg-Witten prepotential from instanton counting,” *Adv. Theor. Math. Phys.* **7** no. 5, (2003) 831–864, [arXiv:hep-th/0206161](#) [[hep-th](#)].
- [81] K. Ohta and Y. Sasai, “Exact Results in Quiver Quantum Mechanics and BPS Bound State Counting,” *JHEP* **11** (2014) 123, [arXiv:1408.0582](#) [[hep-th](#)].
- [82] P. Ozsvath and Z. Szabo, “On the Heegaard Floer homology of branched double-covers,” [arXiv:math/0309170](#).
- [83] B. Ponsot and J. Teschner, “Liouville bootstrap via harmonic analysis on a noncompact quantum group,” [arXiv:hep-th/9911110](#) [[hep-th](#)].
- [84] B. Ponsot and J. Teschner, “Clebsch-Gordan and Racah-Wigner coefficients for a continuous series of representations of $U(\mathfrak{q}(\mathfrak{sl}(2, \mathbb{R})))$,” *Commun. Math. Phys.* **224** (2001) 613–655, [arXiv:math/0007097](#) [[math-qa](#)].
- [85] Y. Qi and J. Sussan, “Categorification at prime roots of unity and hopfological finiteness,” [arXiv:1509.00438](#).
- [86] K. Reidemeister, “Elementare Begründung der Knotentheorie,” in *Abhandlungen aus dem Mathematischen Seminar der Universität Hamburg*, vol. 5, pp. 24–32, Springer. 1927.
- [87] M. Reineke, “The use of geometric and quantum group techniques for wild quivers,” *Representations of finite dimensional algebras and related topics in Lie theory and geometry* **40** (2004) 365–390.
- [88] M. Reineke, “Moduli of representations of quivers,” [arXiv:0802.2147](#).
- [89] V. A. Rubakov, *Classical theory of gauge fields*. Princeton, USA: Univ. Pr., 2002.
- [90] N. Seiberg and E. Witten, “Electric - magnetic duality, monopole condensation, and confinement in $N=2$ supersymmetric Yang-Mills theory,” *Nucl. Phys.* **B426** (1994) 19–52, [arXiv:hep-th/9407087](#) [[hep-th](#)]. [Erratum: *Nucl. Phys.*B430,485(1994)].
- [91] N. Seiberg and E. Witten, “Monopoles, duality and chiral symmetry breaking in $N=2$ supersymmetric QCD,” *Nucl. Phys.* **B431** (1994) 484–550, [arXiv:hep-th/9408099](#) [[hep-th](#)].
- [92] A. Strominger, “Open p-branes,” *Phys. Lett.* **B383** (1996) 44–47, [arXiv:hep-th/9512059](#) [[hep-th](#)].
- [93] A. Tsuchiya and Y. Kanie, “Vertex Operators in Conformal Field Theory on \mathbb{P}^1 and Monodromy Representations of Braid Group,” *Adv. Stud. Pure Math.* **16** (1988) 297–372.
- [94] T. Weist, “Localization in quiver moduli spaces,” [arXiv:0903.5442](#).
- [95] J. Wess and B. Zumino, “Supergauge transformations in four dimensions,” *Nucl. Phys. B* **70** no. 1, (1974) 39–50.
- [96] E. Witten, “Supersymmetry and Morse theory,” *J. Diff. Geom.* **17** no. 4, (1982) 661–692.

- [97] E. Witten, “Quantum field theory and the Jones polynomial,” *Comm. Math. Phys.* **121** no. 3, (1989) 351–399.
- [98] E. Witten, “Solutions of four-dimensional field theories via M theory,” *Nucl. Phys.* **B500** (1997) 3–42, [arXiv:hep-th/9703166](#) [hep-th].
- [99] E. Witten, “Fivebranes and Knots,” [arXiv:1101.3216](#) [hep-th].
- [100] E. Witten, “Two Lectures On The Jones Polynomial And Khovanov Homology,” [arXiv:1401.6996](#) [math.GT].
- [101] A. B. Zamolodchikov and A. B. Zamolodchikov, *Conformal field theory and critical phenomena in two-dimensional systems (in Russian)*. MCCME, 2009.
- [102] Y. Zenkevich, “Quantum spectral curve for (q,t)-matrix model,” [arXiv:1507.00519](#) [hep-th].